UNIVERSITÀ
DI PAVIA

Translational Medicine PhD programme

XXXVII cycle

Department of Molecular Medicine – University of Pavia

Unit of General Biology and Medical Genetics

An innovative and effective NGS-based protocol for GBA1 gene analysis in Parkinson disease.

Supervisor:

Professor *Enza Maria Valente*

Co-supervisor:

Doctor *Micol Avenali*

Chair of the course:

Professor *Roberto Bottinelli*

PhD thesis by

Giada Cuconato

Academic Year 2023/2024

Table of contents

..... 1

List of Abbreviations 4

Introduction 7

1. Parkinson's disease (PD) 7

Epidemiology 7

Motor symptoms 9

Non-motor symptoms 10

2. Pathogenesis 11

3. Neuropathology 14

Neuronal death 14

Lewy bodies 15

Pathological staging 16

4. Diagnosis 18

5. Treatment 20

Other drugs 20

Advanced therapies 21

6. Genetic architecture of PD 22

Autosomal dominant-PD 26

Autosomal recessive-PD 28

7. *GBA1* gene 32

GBA1 gene and glucocerebrosidase (GCase) 32

GBA1 gene variants and complex alleles 33

Effect of *GBA1* variants on GCase activity 35

GBA1 variant classification and nomenclature 35

7.1 GBA1 gene and PD 36

Pathogenetic mechanism of *GBA1* variants in *GBA1-PD* patients 36

GBA1-PD clinical phenotype 38

Advanced therapy: Deep brain stimulation in GBA1-PD patients 39

7.3 Several strategies for molecular analysis of *GBA1*: from Sanger sequencing to NGS-based approaches 39

Aim of the study 41

Materials and methods 42

1. Subjects 42

2. DNA extraction 43

Quantitative and Qualitative Evaluation of DNA 43

3. LONG-NEXT protocol: targeted-NGS of the *GBA1* gene 43

Long-range PCR 43

Nextera XT library preparation workflow 45
Optimized bioinformatic data analysis 51
4. Sanger Sequencing and short-read NGS for *GBA1* analysis 51
Conventional Sanger sequencing 51
Short-read NGS 52
5. Glucocerebrosidase activity assay 55
PBMCs extraction 55
GCase assay 56
BCA assay 56
Statistical analysis 57
Results *58*
1. Optimization phase 58
Sanger sequencing versus LONG-NEXT (n=6) 60
Conventional sr-NGS versus LONG-NEXT (n=7) 62
2. Validation phase 66
3. Multicentric Italian PD cohort genetic screening 69
4. Glucocerebrosidase activity measurement in a PD cohort 74
Discussion *78*
Conclusions *83*
Bibliography *84*
List of papers published during the PhD *107*
List of congress abstract *109*
Websites *110*

List of Abbreviations

ADO	Allele Dropout
AJ	Ashkenazi Jewish
ALS	Autophagy–Lysosomal System
ANS	Autonomic Nervous System
CNS	Central Nervous System
CSF	Cerebro Spinal Fluid
CTR	C-terminal region
DAT	Dopamine Transporter
DBS	Deep Brain Stimulation
ER	Endoplasmic Reticulum
ERAD	ER-associated degradation
GCase	GlucoCerebrosidase
GD	Gaucher Disease
GP	Globus Pallidum
GSH	Glutathione
GWAS	Genome-Wide Association Studies
LBD	Lewy Bodies Dementia
LBs	Lewy Bodies
MAO	Monoamine Oxidase
MDS	Movement Disorders Society
MiRNAs	microRNAs
MRI	Magnetic Resonance
NAC	Non-Amyloid Component
NGS	Next-generation-sequencing
NO	Nitrogen Oxide
NOS	Nitrogen Oxide Species
OMM	Outer Mitochondrial Membrane
OR	Odd Ratio
PD	Parkinson's Disease
PRS	Polygenic Risk Scores
REM	Rapid Eye Movements
RBD	REM Sleep Behaviour Disorder
ROS	Reactive Oxygen Species
SNpc	Substantia Nigra pars compacta
SPECT	Single-Photon Emission Computed Tomography
UPS	Ubiquitin–Proteasome System
WES	Whole-Exome Sequencing
WGS	Whole-Genome Sequencing

Abstract

Variants in the *GBA1* gene represent the most common genetic risk factor for Parkinson's disease (PD). Overall, 8–12% of PD patients carry a heterozygous *GBA1* variant, although prevalence varies considerably across populations. Large-scale sequencing of *GBA1* remains challenging with conventional diagnostic methods—namely Sanger sequencing and standard short-read next-generation sequencing (sr-NGS)—due to the high sequence homology between *GBA1* and its pseudogene *GBA1LP*, which often results in false-positive and false-negative findings. This complexity underscores the need for a reliable, accurate, and rapid alternative for *GBA1* analysis, a requirement that is particularly relevant for the implementation of genotype-based personalized therapies, such as deep brain stimulation (DBS) in *GBA1*-PD patients.

In this work, we designed, optimized, and validated LONG-NEXT, an innovative NGS-based protocol aimed at streamlining large-scale *GBA1* sequencing. The approach employs a single long-range PCR amplicon (6.5 kb) encompassing the entire *GBA1* gene as a template for short-read sequencing library preparation, combined with a dedicated bioinformatic pipeline that masks the *GBA1LP* sequence in the reference genome. The protocol was first tested on selected cases with suspected genotyping errors from conventional methods (n = 13) and subsequently validated on two cohorts previously screened either by Sanger sequencing (n = 101) or standard sr-NGS (n = 294).

In the optimization phase, reanalysis with LONG-NEXT revealed three sr-NGS false positives caused by pseudogene read mismapping, four Sanger false homozygotes due to PCR-related allele dropout, and six false negatives shared by both techniques, attributable to pseudogene misalignment or allele dropout. Validation identified one additional Sanger false homozygote and one sr-NGS false negative.

Within the framework of a study involving a large multicentric Italian PD cohort (PARKNET Study Group), investigating the prognostic impact of *GBA1* variants on long-term motor and non-motor outcomes in PD patients who had undergone DBS surgery, I employed LONG-NEXT as genetic screening method for PD patients recruited at the IRCCS Mondino Foundation (n=137). We identified 41 *GBA1* variant carriers and 96 wild-type PD patients. Among the positive patients, 17 are carriers of severe variants (41%), 2 of complex allele (5%), 8 of mild variants (20%), 8 of risk variants (20%) and 6 of unknown variants (15%).

In addition, glucocerebrosidase (GCase) enzymatic activity was assessed in a subgroup of 30 PD patients (15 *GBA1*-PD, 15 non*GBA1*-PD), revealing significantly reduced activity in *GBA1*-PD, consistent with previous literature.

The LONG-NEXT protocol proved to be a robust, rapid, cost-effective, and accessible strategy for precise *GBA1* genotyping, enabling targeted therapeutic approaches. Our findings confirm that *GBA1*-PD patients derive motor benefit from DBS, while their accelerated cognitive decline appears to reflect the natural history of the disease rather than an effect of the surgical intervention. Future work will expand GCase activity profiling and investigate additional blood-based biomarkers—such as substrate accumulation (e.g., glucosylceramide and glucosylsphingosine) and other lipid metabolism–related markers (e.g., ceramide, sphingomyelin, sphingosine)—using advanced mass spectrometry, with the aim of defining a distinct biochemical signature for *GBA1*-PD.

Introduction

1. Parkinson's disease (PD)

Parkinson's disease (PD) was first described as a neurological syndrome by James Parkinson in 1817 in his Essay on the Shaking Palsy. In the mid-1800s, the French neurologist Jean-Martin Charcot refined and expanded this description, distinguishing PD from multiple sclerosis and other tremor-related disorders—later classified as parkinsonian syndromes—and introducing, for the first time, the term maladie de Parkinson [1].

PD is the second most common neurodegenerative disorder after Alzheimer's disease and the most prevalent movement disorder. From a pathological standpoint, PD is characterized by the progressive loss of dopaminergic neurons in the substantia nigra pars compacta (SNpc) and by the accumulation of misfolded α-synuclein within intracytoplasmic inclusions known as Lewy bodies (LBs) [2]. Clinically, PD manifests primarily as a movement disorder, with motor symptoms such as bradykinesia, resting tremor, rigidity, and disturbances of gait and posture. However, non-motor symptoms—including depression, dementia, sleep disturbances, hyposmia, and constipation—are also common and often precede the onset of classical motor signs [3].

Epidemiology

PD is an age-related condition, affecting approximately 1% of individuals over the age of 60, with prevalence increasing to 5% by age 85 [4]. Nevertheless, PD is not restricted to the elderly: about 25% of affected individuals are younger than 65, and 5–10% develop the disease before age 50 [5]. PD occurs in all ethnic groups, with no substantial global differences in prevalence, although higher incidence rates are reported in industrialized regions such as North America, Europe, and Australia, alongside a rapid increase in newly diagnosed cases in China [6], [7].

Epidemiological and clinical sex-related differences are evident: PD affects men roughly twice as often as women, with women typically exhibiting a later age at onset [5]. Nonetheless, women have

been reported to show higher mortality rates, faster disease progression, greater risk of dyskinesia, motor and non-motor fluctuations, urinary symptoms, and depression [8], [9]. Men, conversely, present a higher risk of cognitive decline [9]. This sexual dimorphism may reflect differences in exposure to environmental risk factors (e.g., smoking, head trauma, pesticide use), as well as the influence of biological variables (e.g., sex chromosome–linked genes, hormonal effects, pregnancy) and sociocultural factors (e.g., education, occupation) [10].

While age remains the most important risk factor for PD, several environmental exposures have also been implicated, including pesticides, prior head injury, rural living, β-blocker use, agricultural occupations, and consumption of well water. Conversely, tobacco use, coffee consumption, and moderate alcohol intake have been controversially associated with a reduced risk of PD [11], [12].

The role of genetics in PD etiology became clear following the discovery of *SNCA* mutations [13]. Since then, multiple genetic loci have been linked to PD susceptibility [14]. Approximately 15–25% of patients report a family history of PD, with an increased risk among first-degree relatives [11]. Genome-wide association studies (GWAS) have estimated that up to 36% of the overall disease risk is attributable to common genetic variation [15]. It is now recognized that 5–15% of PD cases are caused by monogenic forms, while the remainder likely result from multifactorial interactions between environmental and genetic factors.

Symptoms

As noted above, PD is characterized by both motor and non-motor manifestations, reflecting a complex and heterogeneous clinical picture (Figure 1). The four cardinal motor features are often summarized using the acronym TRAP: **T**remor at rest, **R**igidity, **A**kinesia (or bradykinesia), and **P**ostural instability [16]. Additional motor signs, such as flexed posture and freezing episodes, also fall within the parkinsonian spectrum. Non-motor symptoms include autonomic dysfunction, cognitive and neuropsychiatric disturbances, sensory impairments, and sleep abnormalities. Several of these non-motor features—such as olfactory dysfunction, constipation, depression, excessive

daytime sleepiness, and Rapid Eye Movement (REM) sleep behaviour disorder—frequently occur during the prodromal phase and can aid in the early identification of PD before the onset of motor signs [2]. Long-term complications of dopaminergic therapy, including both motor and non-motor fluctuations, dyskinesia, and psychosis, further contribute to patient disability [17].

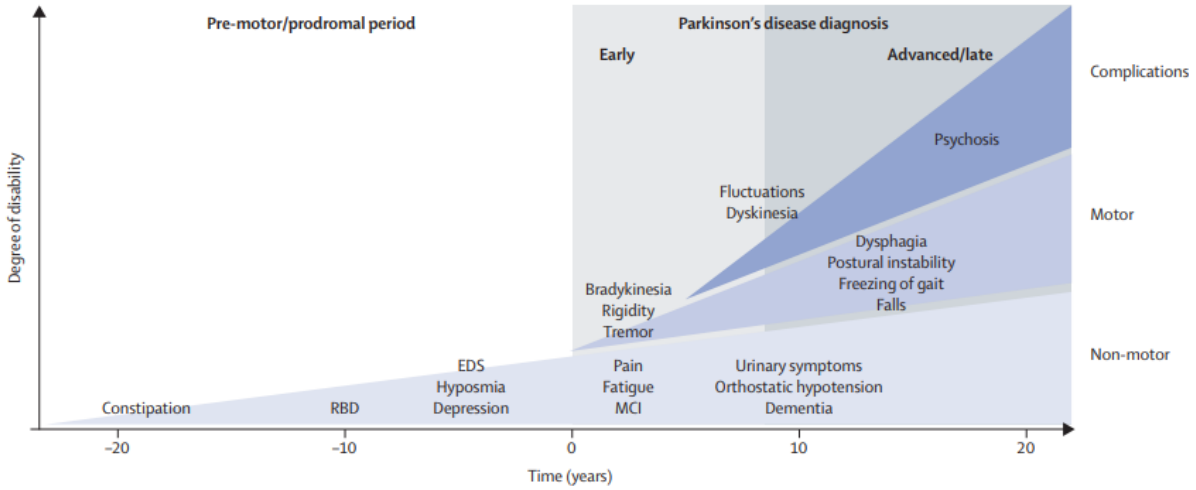

Fig. 1. *Time course of clinical symptoms in PD [2]*

Motor symptoms

Tremor. Clinically, tremor is defined as an involuntary, rhythmic, alternating movement affecting one or more body parts. It occurs in 50–70% of PD patients, although 15% never develop it [16], [18]. Rest tremor (4–6 Hz) is the typical parkinsonian tremor, occurring while the body segment is maintained at rest, fully supported against gravity and may disappear or subside with action [19].

Bradykinesia. Bradykinesia refers to slowness or paucity of movement. It is closely related to *akinesia* (absence of spontaneous movements, such as freezing) and *hypokinesia* (reduced amplitude of movement, e.g., micrographia). Bradykinesia results from impaired basal ganglia output, which normally facilitates the cortical mechanisms required to initiate and execute movement [20]. Recent evidence also implicates cerebellar dysfunction in its pathophysiology [21].

Rigidity. Rigidity is defined as a continuous and uniform increase in muscle tone felt as constant resistance to passive movement. Two types of parkinsonian rigidity are recognized and may coexist:

the “lead pipe” rigidity, where rigidity is uniform throughout the entire range of movement, in both extension and flexion, with a severe progression with advanced disease, and “cogwheel” rigidity, characterized by regularly interrupted hypertonicity at 4 to 6 Hz frequency, often associated with tremor and early onset of PD [22]. Although its exact mechanisms remain unclear, rigidity is thought to involve distributed brain networks rather than direct dopaminergic deficit alone [23].

Postural instability. Postural deformities are frequent in late-stage PD and atypical parkinsonism. These include camptocormia (marked forward flexion of the spine), antecollis (forward flexion of head and neck), Pisa syndrome, and scoliosis. Their pathophysiology is likely multifactorial [24], [25].

Non-motor symptoms

Autonomic nervous system (ANS) dysfunction. ANS impairment affects 70–80% of PD patients [26], resulting from LB aggregation and degeneration in key autonomic regulatory centers (e.g., dorsal vagal nucleus, nucleus ambiguus). Symptoms include sexual dysfunction, dysphagia, gastrointestinal and urinary disturbances, and cardiovascular dysregulation such as orthostatic hypotension [26].

Sleep disturbance. Sleep disorders often appear early in PD [27] and arise from degeneration of central sleep-regulating structures and thalamocortical pathways. They include REM sleep behaviour disorder (RBD) and excessive daytime sleepiness, affecting approximately 33% and 50% of patients, respectively [28], [29].

Neuropsychiatric disturbances. Cognitive and neuropsychiatric non-motor symptoms of PD range from anxiety state, apathy, depression to progressive cognitive impairment and dementia [30]. Depression, occurring in 10–45% of patients, is a major determinant of quality of life and may be linked to serotoninergic, noradrenergic, and dopaminergic deficits. As disease advances, up to 40% of patients experience hallucinations, delusions, or psychosis, the latter often linked to dopaminergic therapy [31] [32] and, in some cases, genetic susceptibility [33].

Sensory symptoms. Olfactory dysfunction is a common symptom in PD, as 90% of patients show hyposmia in the prodromal phase of the disease, representing a potential marker of PD diagnosis [34]. The pathological basis of hyposmia could be the early degeneration of extranigral neurons in the olfactory bulb and anterior olfactory nucleus, confirming the alpha-synuclein pathology spreading suggested by Braak and colleagues [35]. Pain is another common problem in PD affecting almost half patients and can be either primary or secondary to motor dysfunction. Primary pain may be related to motor fluctuations or early morning dystonia, while secondary pain could be due to musculoskeletal pain [36].

2. Pathogenesis

PD is a neurodegenerative disease involving a complex interplay of environmental and genetic factors. Several molecular pathways are involved into PD pathogenesis, including protein aggregation, failure of intracellular clearance pathways, mitochondrial damage, oxidative stress, excitotoxicity, neuroinflammation, and genetic mutations.

α-Synuclein aggregates. α-Synuclein (α-syn) is a presynaptic neuronal protein expressed in both the central and peripheral nervous systems as well as in blood cells and various peripheral tissues [37]. Under physiological conditions, α-syn exists predominantly as a monomer, with a smaller fraction forming α-helical tetramers in healthy neurons [38]. Misfolding of α-syn monomers can lead to protofibril formation and eventually to insoluble fibrils, which are neurotoxic and a hallmark of PD pathology. Genetic evidence supports its role, as duplications, triplications, and missense mutations in *SNCA* have been linked to rare familial forms of PD. Age-related decline in α-syn clearance mechanisms may also promote accumulation [39]. Aggregated α-syn impairs protein degradation, disrupts mitochondrial and endoplasmic reticulum function, alters ion homeostasis through pore formation, and exerts synaptotoxic effects via dysregulation of SNARE complex activity [40][41]. Furthermore, α-syn fibrils may propagate in a “prion-like” fashion, spreading pathology between neurons through exosomes or unconventional secretion pathways [42] [43], [44].

Dysfunctional intracellular clearance mechanism. Cellular quality control relies on the ubiquitin–proteasome system (UPS) and the autophagy–lysosomal system (ALS), which degrade misfolded proteins and damaged organelles [45]. Impairment of these systems can lead to α-syn accumulation, mitochondrial dysfunction, and oxidative stress (Figure 2) [46].

Mutations in *PRKN*, *UCH-L1*, and *SNCA* can disrupt UPS function, while defects in autophagy and mitophagy—linked to *PINK1*, *LRRK2*, *DJ-1*, *VPS35*, and *GBA1*—have been demonstrated in PD-affected brain regions [47] [48] [49].

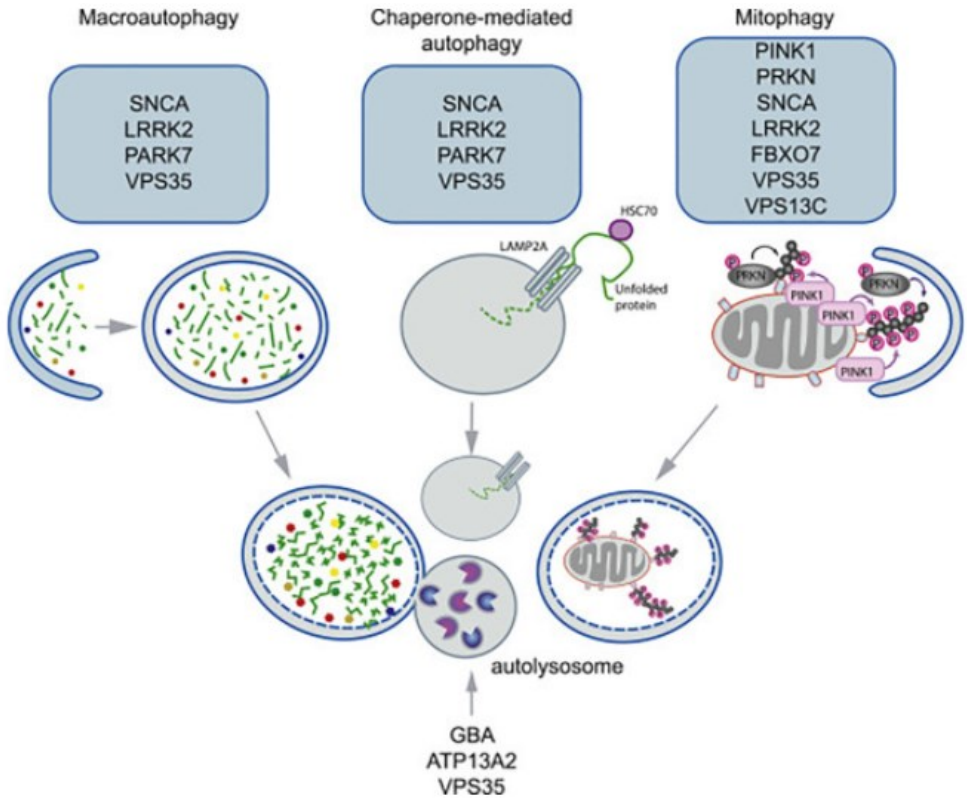

***Fig. 2**. Genes involved in mitophagy, macroautophagy and chaperone-mediated autophagy.*

Mitochondrial dysfunction and ROS production.

Mitochondrial stress resulting from increased reactive oxygen species (ROS) production another mechanism proposed for nigrostriatal degeneration in PD [50]. Production of ROS not only depends on complex I, but other ROS sources include monoamine oxidase (MAO), NADPH oxidase (NOX) and other flavo-enzymes along with nitrogen oxide (NO), which is abundant in the brain due to the

presence of nitrogen oxide species (NOS) [51]. Other potential mechanism for ROS production results from dopamine metabolism, low glutathione (GSH), high levels of iron and calcium in the SNpc, high concentrations of polyunsaturated fatty acids, which under oxidative stress conditions result in lipid peroxidation and the generation of toxic products [51]. Regardless of the source, oxidative stress can induce mitochondrial DNA mutations, damage the respiratory chain, alter membrane permeability, Ca2+ homeostasis and mitochondrial defense systems and dynamics [52].

The role of mitochondria in PD pathogenesis became clear after the discovery of some monogenic form of PD. Indeed, most PD-related genes (i.e., *SNCA, LRRK2*, *PRNK* and *PINK1, DJ-1*) encode for proteins directly associated with mitochondrial functioning [53]. Furthermore, recent studies have demonstrated accumulation of deletions, mutations, and rearrangements of mt-DNA (mitochondrial-DNA) in both animal models of PD and in idiopathic PD patients [54]. Moreover, specific mitochondrial haplogroups seem to be associated with either a lower or higher risk of developing PD [55].

Excitotoxicity. Excitotoxicity is the pathological process through which neurons are damaged and killed after excessive stimulation of glutamatergic receptors by glutamate. Glutamate-mediated neurotoxicity is not responsible for the initial insult and neuronal loss in the SNpc, but is a secondary effect of dopaminergic neurons susceptibility, due to bioenergetic alteration, mitochondrial impairment, inefficient antioxidant defenses and altered proteolytic machinery. Thus, dopaminergic neurons represent the perfect background for the activation of Ca^{2+}-mediated excitotoxic phenomena and death progression [56]. Due to the altered glutamatergic system within basal ganglia of PD patients, toxicity results from an overload of glutamate in the synaptic cleft that over-activates its ionotropic AMPA and NMDA receptors, triggering a massive influx of Ca^{2+}, which in turn results in an increased oxidative burden and apoptosis activation [57].Furthermore, neuroinflammation and activated microglia, which play a major role in the progression of SNpc neurodegeneration, also contribute to glutamate release and potentiate glutamate receptor-mediated responses (in particular NMDARs), thereby leading to the exacerbation of excitotoxic phenomena [58].

Neuroinflammation. Neuroinflammation plays a key role in PD progression. Chronic inflammatory processes are largely recognized as major drivers of pathogenetic mechanisms underlying neurodegeneration. Different conditions in PD, such as α-syn misfolding, polymorphisms in immune-related genes and mitochondrial dysfunction, have been suggested as trigger of inflammation. Both glia cells (e.g. astrocytes, microglia and oligodendrocytes) and peripheral circulating myeloid cells have a role in the persistent neuroinflammatory activation. After neuronal damage, glia cells are activated and recruited, via cytokines and chemokines, other myeloid cells, leading to an amplification of the immune response. Furthermore, SNpc DA neurons itself may release inflammatory mediators, under specific cellular conditions. These self-supporting responses create a vicious loop that further enhances inflammatory signaling, aggravating neuronal degeneration [59].

3. Neuropathology

The cardinal neuropathological features of PD are the dopaminergic cell loss within SNpc in association with the formation of Lewy bodies (LBs) in remaining neurons.

Neuronal death

The degeneration of the dopaminergic nigrostriatal pathway originates in the SNpc, with consequent dopamine depletion (Fig. 3). The loss tends to be greater in the ventrolateral layer, followed by the medial ventral and the dorsal layer, leading to a decrease in motor output [60]. Degeneration in other areas, such as locus ceruleus (where cell loss may exceed that seen in SNpc), dorsal raphe nuclei, nucleus basalis of Meynert and postganglionic sympathetic neurons are also observed, likely contributing to many of the non-motor symptoms of PD [35]. Clinically, motor manifestation of PD becomes evident when 50% to 80% of DA neurons are loss, with a consequent decrease of dopamine in the striatum of about 80% [61].

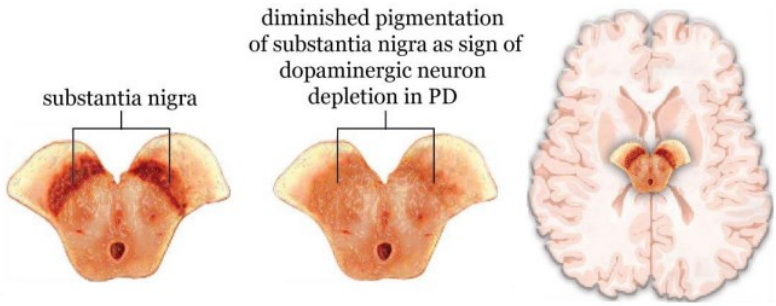

Fig.3. *Midbrain section which highlights differences between the substantia nigra in a normal brain and the substantia nigra in a brain from a PD.*

Lewy bodies

A century ago, Friederich H. Lewy observed peculiar inclusions in the dorsal vagal nucleus and in the nucleus basalis of Meynert in patients with PD. These inclusions were subsequently named in his honor by Tretiakoff who confirmed their presence in the *Substantia Nigra*. LBs are 5-25 μm round, intracytoplasmic, eosinophilic inclusion bodies formed by a fibrillar accumulation of misfolded and aggregated α-syn forming the core, surrounded by ubiquitin and TorsinA, easily seen by light microscopy in hematoxylin-eosin-stained sections [62], [63], [64]. However, recent studies have indicated that nonfibrillar α-syn is cytotoxic and that fibrillar aggregates of α-syn forming LBs may represent a cytoprotective mechanism in PD. LBs consist of a heterogeneous mix of more than 90 molecules, including PD-linked gene products (α-syn, DJ-1, LRRK2, parkin, and PINK-1), mitochondria-related proteins, and molecules implicated in the UPS, autophagy, and aggresome formation [65]. LBs are widely distributed in the central nervous system, including the olfactory bulb, hypothalamus, posterior pituitary, nucleus basalis of Meynert, substantia nigra, locus ceruleus, dorsal raphe nucleus, dorsal vagal nucleus, cerebellum, and spinal cord [66]. These inclusions are also found in the peripheral autonomic nervous system, for this reason the widespread distribution of LBs pathology may correspond to a multisystemic disorder characterized by a variety of motor and non-motor symptoms [67]. LBs are considered a marker of neurodegeneration, and they could even play

a causative role in neuronal loss, but it has become evident that the pathology of the disease cannot be reduced to this histological feature [2].

Pathological staging

Lewy pathology has been hypothesized to progress in a specific pattern over the course of PD. Braak and colleagues have proposed a staging process, made by six steps, with neurodegeneration starting in the peripheral nervous system and progressively affecting the central nervous system in a caudal-to-rostral direction within the brain [35] (Table 1). The Braak model seems to explain the clinical course of PD for the temporal and spatial progression proposed. In detail, stages 1 and 2 could correspond with onset of premotor symptoms; stage 3 corresponds with the onset of motor features, due to nigrostriatal dopamine depletion; stages 4–6 would explain the non-motor symptoms of advanced disease, such us declining intellectual faculties and impaired cognition.

Stage 1	**Column1**
N = 21; medulla oblongata	Lesions in the dorsal IX/X motor nucleus and/or intermediate reticular zone
Stage 2	
N = 13; medulla oblongata and pontine tegmentum	Pathology of stage 1 plus lesions in caudal raphe nuclei, gigantocellular reticular nucleus, and coeruleus–subcoeruleus complex
Stage 3	
N = 24; midbrain	Pathology of stage 2 plus midbrain lesions, in particular in the pars compacta of the substantia nigra
Stage 4	
N = 24; basal prosencephalon and mesocortex	Pathology of stage 3 plus prosencephalic lesions. Cortical involvement is confined to the temporal mesocortex (transentorhinal region) and allocortex (CA2-plexus). The neocortex is unaffected
Stage 5	
N = 17; neocortex	Pathology of stage 4 plus lesions in high order sensory association areas of the neocortex and prefrontal neocortex
Stage 6	
N = 11; neocortex	Pathology of stage 5 plus lesions in first order sensory association areas of the neocortex and premotor areas, occasionally mild changes in primary sensory areas and the primary motor field

Table 1. *Braak staging of Lewy pathology in PD [35]*

4. Diagnosis

Currently, PD diagnosis is based on the latest clinical criteria developed by *International Parkinson and Movement Disorders Society* (MDS) (MDS-PD Criteria) [68]. These criteria emerged from the work of the MDS task force for the definition of PD, a group of recognized international experts [68]. In detail, the diagnosis of PD is based on three criteria: 1) recognition of bradykinesia and at least one of the following symptoms: rigidity, rest tremor, or postural instability not caused by primary visual, cerebellar, vestibular, or proprioceptive dysfunction; 2) absence of exclusion criteria for PD, which are based on the analysis of signs that may suggest the presence of a distinct syndrome, such as Lewy bodies dementia (LBD) and ET, as well as the presence of other NDs; 3) the individuation of at least three other supporting features, such as the unilateral onset, an excellent response (70–100%) to levodopa, rest tremor, and a clinical course of 10 years or more. Sensitivity of these criteria can be as high as 90% [69]. Determination of PD as the cause of parkinsonism relies on three categories of diagnostic features: absolute exclusion criteria, red flags, and supportive criteria. The golden standard to have a definitive diagnosis of PD is the neuropathological assessment, via confirmation of nigrostriatal neurodegeneration in post-mortem autopsy brain and the presence of Lewy bodies in the remaining neurons.

A great variety of biomarkers for PD diagnosis are currently under investigation. These biomarkers can be classified as clinical, imaging, biochemical (CSF and serum) and genetic. Candidate imaging markers include magnetic resonance (MRI), dopamine transporter (DAT) single-photon emission computed tomography (SPECT) and 18F-DOPA L-6-[18F] fluoro-3,4-dihydroxyphenylalanine positron emission tomography (18F-DOPA PET). Biochemical biomarkers are analyzed mainly in cerebrospinal fluid (CSF) and include α-syn, glial fibrillary acidic protein (an intermediate filament obtained after astrocytes destruction - GFAP), beta-amyloid 1-42, tau and p-tau. A recent method for alpha-synuclein CSF analysis, called α-syn seed amplification assays (SAAs), has been used as an alternative to traditional CSF analysis, examining the seed capacity of this protein. However, good

serum biomarkers still have to be identified,. Potential serum biomarkers that have been investigated are extracellular vesicles containing α-syn (EV-α-syn), general inflammatory markers, microRNAs (MiRNAs) and other small, non-coding RNAs (smnRNAs) found in plasma's exosomes [70].

With the advent of NGS, several genetic biomarkers for PD diagnosis are now under investigation. Relatives of PD patients, affected by monogenic forms of the disease, can undergo genetic testing, but due to the low penetrance of several PD genes, a genetic diagnosis is usually not definitive for many asymptomatic carriers [2].

Strategies to develop new biomarkers for the diagnosis of PD are critically needed, especially to enable diagnosis in the prodromal phase of the disease before the onset of motor symptoms, to prevent neurodegeneration and disease progression. High-throughput technologies intended for clinical applications in combination with computational systems biology approaches and bioinformatics analyses will support this purpose in future studies.

5. Treatment

The pharmacological treatment for PD is merely symptomatic and is based on overcoming the dopaminergic deficit in the brain by administration of its precursor, the 3,4-hydroxyphenylalanine (L-DOPA), which decreases PD motor deficit. Normally, the therapy is complemented by the addition of Carbidopa or Benserazide, a peripheral dopa decarboxylase inhibitor, that prolongs the therapeutic benefits of levodopa, blocking the metabolism in the periphery, limiting peripheral side effect such as dyskinesia, nausea and vomiting, and increasing central nervous system bioavailability [71]. Moreover, as the disease progresses, patients are less responsive to dopaminergic medication and require higher and more frequent doses of dopaminergic drugs, which can lead to motor complications such as wearing off (when the drug concentration is below the therapeutic threshold) and peak dose dyskinesias (when the concentration exceeds the critical threshold) [72].

Other drugs

To prevent levodopa-induced complications it is recommend to use dopaminergic agonists in the initial phase of dopaminergic therapy [73]. Dopamine agonists (pramipexole, ropinirole, and rotigotine) exert their pharmacologic effect by directly activating dopaminergic receptors, bypassing the presynaptic synthesis of dopamine. Serious adverse effects include hallucinations, dopaminergic dysregulation syndrome, and impulse control disorder (ICD), which can manifest as pathological gambling, hyperphagia, hypersexuality, or compulsive shopping and affect about 15% of individuals taking dopamine agonists [74]. MAO-B and catechol-O-methyltransferase (COMT) inhibitors, on the other hand, act by preventing dopamine degradation in the central nervous system (CNS) and are administered in combination with levodopa or dopamine agonists; used as monotherapy, in fact, they are often ineffective.

In addition, nondopaminergic drugs, such as the anticholinergics and amantadine (NMDA receptor blocker), may also be useful in early phases of anti-PD therapy. Drugs, such as trihexyphenidyl or benzatropine, are particularly useful in younger patients who are primarily bothered by tremor. Yet

anticholinergic side effects such as dry mouth and urinary symptoms limited their use [75]. Antipsychotic treatment is used for a variety of psychiatric disturbances, particularly psychosis with agitation, delusions, paranoid beliefs and hallucinations experienced by PD patients [32]. As the estimated prevalence of depression is around 40% in PD, tricyclic antidepressants and selective serotonin reuptake inhibitors (SSRIs) have been recommended [76], [77].

Advanced therapies

Over the past 20 years, several advanced therapeutic strategies have been developed, the most popular being Deep Brain Stimulation (DBS) and continuous intrajejunal infusion of levodopa-carbidopa intestinal gel.

DBS surgery is based on delivers of electrical impulses to a targeted areas of brain in particular subthalamic nucleus, the globus pallidus internus, or the ventral intermediate nucleus of the thalamus [78]. DBSs of subthalamic nucleus is effective for all major motor symptoms of PD, such as tremor, bradykinesia, rigidity, and problems of balance. The thalamic target is sometimes selected for patients with tremor symptoms [78].

Future promising therapeutic approaches consist in neuroprotective drugs, like neurturin (NTN) [79] and the glial cell-line-derived neurotrophic factor (GDNF) [80] These neurotrophic factors have been reported to enhance the survival of midbrain dopaminergic neurons in vitro and to rescue degenerating neurons in vivo. Gene therapy models, immunotherapy, and stem cell therapy represent future hopes for PD treatments [2]. A major relevance goes to tailored treatments for genetic forms of PD; for PD patient carrying *GBA1* variants, Ambroxol, a known antitussive drug, was shown to increase glucocerebrosidase (GCase) activity while exerting the opposite effect on α-syn levels. Due to positive results, this drug is now studied in several clinical trials [81].

6. Genetic architecture of PD

Historically, PD was considered a sporadic disorder in which environmental factors and age were the main risk factors. It is only in the last three decades that PD genetics has made significant progress, showing the relevance of its impact on PD pathogenesis [82]. PD cases are more represented by sporadic forms (idiopathic PD), although a positive family history for PD is found in approximately 15% of patients, and 5–10% follow a classical Mendelian inheritance pattern [83]. However, the formal distinction between hereditary/familial and sporadic PD needs to be reevaluated as it represents an oversimplification. Genetic contributors to PD encompass a continuum of variants with different effects and frequency, ranging from rare high penetrance DNA variants, which typically are associated with monogenic PD forms, to common variants each exerting a small increase in lifetime risk of disease found in sporadic cases [84]. In between, there are intermediate situations with variants that are relatively common and exert intermediate risk, such as those in the *GBA1* and *LRRK2* genes (Figure 4).

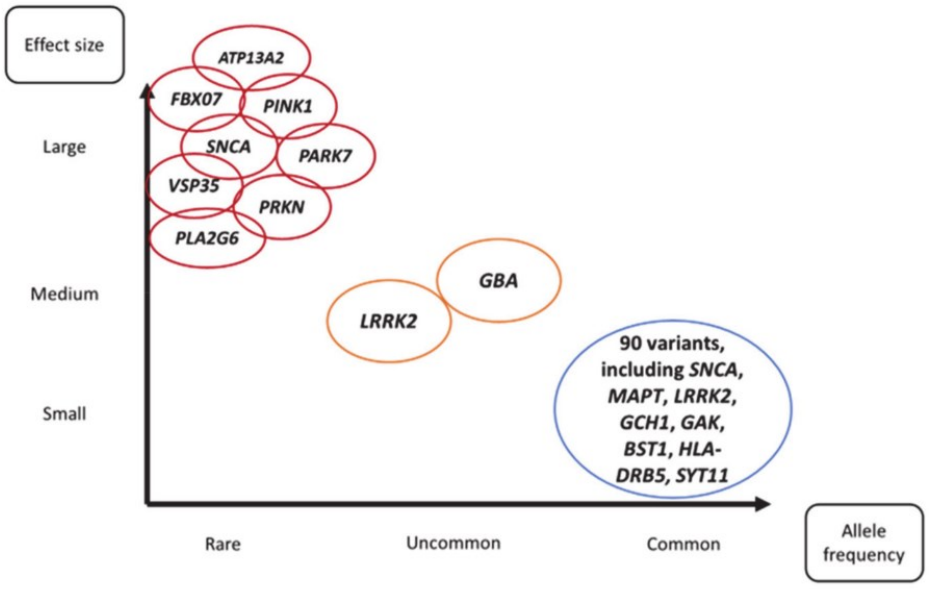

Fig.4 *Genetic contributors to PD grouped according to allele frequency and associated risk [85].*

Classically, linkage analysis has been useful to identify rare genetic variants, while more recently, PD-associated genes have been identified by means of high throughput sequencing technologies; the list of most common PD-genes is shown below (Table 2) [86]. Variants in α-syn (*SNCA)*, leucine-rich repeat kinase 2 (*LRRK2*) and vacuolar sorting protein 35 (*VPS35*) genes are examples of genes responsible for autosomal dominant PD forms, while variants in the PARK2 gene encoding the E3 ubiquitin-protein ligase Parkin *(PRKN*), PTEN-induced kinase 1 *(PINK1*) and deglycase (*DJ-1*) are associated to autosomal recessive PD form. The relevance of many other genes, such as *LRP10*, *TMEM2*30, and *DNAJC13,* is debated, or still pending replication and functional validation studies [87], [88], [89], [90].

The genetic contribution of common variants for sporadic PD was first described in 2009 through a genome wide association study (GWAS) [91]. To date, nearly 90 genetic risk loci have been identified the many numerous GWASs carried out on larger cohorts of patients and controls from distinct populations [15], [92]. Interestingly, common risk variants occur in some genes already identified as Mendelian disease genes, such as *SNCA*, *LRRK2* or *MAPT* (microtubule-associated gene tau), highlighting common pathogenic mechanisms between idiopathic and genetic PD. Individual GWAS loci confer relatively small amounts of disease risk; however, the development of polygenic risk scores (PRS) allows to calculate a global genetic risk score by summing the cumulative genetic risk [15].

Gene	Mutation	Note	Year	Mechanism	Inheritance	Frequency	GWAS	Families	Functional	Negative	Reference
SNCA	Missense or multiplication	Often with dementia	1997, 2003	Gain of function or overexpression	Dominant	Very rare	Yes	++	++	+	Polymeropoulos MH et al., Science, 1997
PRKN	Missense or loss of function	Often early onset	1998	Loss of function	Recessive	Rare	No	++	++	+	Kitada T et al., Nature, 1998
UCHL1	Missense	--	1998	Loss of function?	Dominant	Unclear	No	–	+	--	Leroy E et al., Nature, 1998
PARK7	Missense	Often early onset	2003	Loss of function	Recessive	Very rare	No	++	++	+	Bonifati V et al., Science, 2003
LRRK2	Missense	--	2004	Gain of function	Dominant	Common	Yes	++	++	+	Zimprich A et al., Neuron, 2004
PINK1	Missense or loss of function	Often early onset	2004	Loss of function	Recessive	Rare	No	++	++	+	Valente EM et al., Science, 2004
POLG	Missense or loss of function	Atypical PD	2004	Loss of function?	Dominant	Rare	No	++	+	+	Luoma P et al., Lancet Neurology, 2004
HTRA2	Missense	--	2005	Unclear	Dominant	Unclear	No	–	+	--	Strauss KM et al., Human Molecular Genetics, 2005
ATP13A2	Missense or loss of function	Atypical PD	2006	Loss of function	Recessive	Very rare	No	++	++	+	Ramirez A et al., Nature Genetics, 2006
FBXO7	Missense	Often early onset	2008	Loss of function	Recessive	Very rare	No	++	++	+	Shojaee S et al., AJHG, 2008
GIGYF2	Missense	--	2008	Unclear	Dominant	Unclear	No	+	+	--	Lautier C et al., AJHG, 2008
GBA	Missense or loss of function	--	2009	Likely loss of function	Dominant	Common	Yes	++	++	+	Sidransky E et al., NEJM, 2009
PLA2G6	Missense or loss of function	Often early onset	2009	Loss of function	Recessive	Rare	No	++	++	+	Morgan NV et al., Nature Genetics, 2006/2009
EIF4G1	Missense	--	2011	Unclear	Dominant	Unclear	No	–	+	--	Chartier-Harlin MC et al., AJHG, 2011
VPS35	Missense	--	2011	Loss of function	Dominant	Very rare	No	++	+	+	Vilarino-Guell C et al., AJHG, 2011
DNAJC6	Missense or loss of function	Often early onset	2012	Loss of function	Recessive	Very rare	No	++	+	+	Edvardson S et al., AJHG, 2012
SYNJ1	Missense or loss of function	Often atypical PD	2013	Loss of function	Recessive	Very rare	No	++	+	+	Quadri M et al., Human Molecular Genetics, 2013

DNAJC13	Missense	Same family as TMEM230	2014	Unclear	Dominant	Unclear	No	+	+	–	Vilariño-Güell C et al., AJHG, 2014
TMEM230	Missense	Same family as DNAJC13	2016	Loss of function?	Dominant	Unclear	No	–	+	–	Deng HX et al., Nature Genetics, 2016
VPS13C	Missense or loss of function	--	2016	Loss of function	Recessive	Rare	Yes	++	+	+	Lesage S et al., AJHG, 2016
LRP10	Missense or loss of function	--	2018	Loss of function?	Dominant	Unclear	No	–	+	--	Quadri M et al., Acta Neuropathologica, 2018

Table 2. *Genetic cause of PD [14]*

Autosomal dominant-PD

SNCA

Gene. SNCA is located on chromosome 4q22 (PARK1/4 loci), contains 6 exons, and spans about 117 kb.

Protein. *SNCA* encodes for α-syn, composed of an amphipathic N-terminal region, binding both lipid membranes and presynaptic vesicles; a hydrophobic central core (the non-amyloid component (NAC)); and a negatively charged C-terminal portion. α-syn is highly expressed in the brain and localizes predominantly to presynaptic terminals of neurons. α-syn is the major component of LBs, and this discovery identified a link between the genetic and pathological hallmark of PD [93]. Genetic alterations in *SNCA* result in protein misfolding, leading to fibrils aggregates; α-syn fibrillar aggregates are a major component of Lewy body inclusions also in other neurodegenerative synucleinopathies.

Genetics. The first missense variant (c.209G>A) identified in the α-syn gene (*SNCA*) causes an amino acid substitution (p.A53T) [13]. This substitution falls into α-helix of the mutant α-syn protein, disrupting it and extending a β-sheet structure. β-sheet structures are thought to be implicated in protein aggregation, leading to the formation of LBs [94]. Other missense *SNCA* variants have been then discovered including p.A30P, p.E46K and p.G51D [95], [96], [97] Duplications and triplications (CNVs) of *SNCA* can also cause PD with evidence for a 'dosage effect', where greater expression of α-syn m-RNA leads to more severe clinical features [98]. GWASs approach also revealed common genetics variants in *SNCA* gene. The two most relevant, with an odd ratio (OR) higher than 1, seems to modify gene expression. The clinical phenotype of PD patients with *SNCA* variants (including CNVs) has specific characteristics. The cardinal signs of parkinsonism are present, but most patients also develop severe autonomic dysfunction, behavioral changes, and cognitive decline. At first, levodopa improves PD symptoms, but in advanced disease there is often marked rigidity that cannot be alleviated with levodopa, dementia and cortical myoclonus.

LRRK2

Gene. The leucine-rich repeat kinase 2 gene (*LRKK2)* is located on chromosome 12q12 (PARK8 locus) and comprises 51 exons.

Protein. *LRRK2* gene codifies for a large protein with 5 functional domains: an N-terminal leucine-rich repeat (LRR) domain, a Ras of complex protein (Roc) domain, a C-terminal of Roc (COR) domain, a mitogen-activated protein kinase kinase kinase (MAPKKK) domain, and a C-terminal WD40 repeat domain. It has been implicated in regulation of autophagy, mitochondrial function, and microtubule stability.

Genetics. A few pathogenic variants in *LRRK2* have been linked to AD-PD, including p.G2019S, p.R1441C/G/H, p.Y1699C, p.I2020T and p.N1437H. Among them, p.G2019S is especially frequent in PD patients and explains between 5% and 13% of familial and 1-5% of sporadic PD [99], [100]. The frequency is higher in selected populations, reaching 13% in Ashkenazi Jewish (AJ) and more than 30% in Arab-Berber populations [101]. p.G2019S falls within the kinase domain, and results in increased kinase activity and thus leading to a gain of function. With these variants leading to increase kinase activity the possibility of pharmacological inhibition represents a possible therapeutic strategy [102]. Patient carriers of the p.G2019S variant have a clinical phenotype similar to the idiopathic PD, with average onset at age 60 and nearly complete penetrance by age 80. The p.R1441 'hotspot' amino acid codon residue (G/H/C) in the complex Ras protein domain is the second most common site of pathogenic *LRRK2* variants after p.G2019S, with most carriers developing symptoms by the age of 75 years. Overall, *LRRK2* mutation carriers are generally similar to patients with late onset idiopathic PD and present with the usual typical clinical features [101].

VPS35

Gene. *VPS35* gene maps on chromosome 16q11.2 (PARK17 locus) spanning 29.6 kb.

Protein. VPS35 encodes for a vacuolar protein of the multimeric retromer complex (CSC), critical for endosome-trans-Golgi trafficking and the recycling of membrane-associated proteins, important in neuronal transport in dendrites and neuronal cells.

Genetics. Through WES in 2011 a missense variant in the *VPS35* gene (p.D620N) was identified in Swiss and Austrian families [103]. The pattern of inheritance was autosomal dominant, with incomplete penetrance. The frequency of this variant is rare, accounting for about 1.3% of familial parkinsonism and 0.3% of sporadic PD [103]. In vitro cellular models demonstrated that p.D620N variant disrupts endosomal transport leading to abnormal accumulation of α-syn and reactive oxygen species (ROS). Moreover, the p.D620N substitution falls into the binding site between VPS35 and VPS29, another subunit of the retromer complex, interfering with the correct formation or folding of the retromer's cargo recognition complex. VPS35 is involved in recycling the cation independent mannose-6-phosphate receptor (CIMPR), involved in the transport of the lysosomal hydrolase cathepsin D from the TGN (trans-Golgi network) to the endosome. Cathepsin D is involved in the degradation of α-syn, so a retromer dysfunction may be related to the accumulation of α-syn [104], [105].

Autosomal recessive-PD

PRKN (PARK2)

Gene. *PRKN (parkin/PARK2*) gene is placed on chromosome 6q25 (PARK2 locus), spans more than 500 kb and has 12 exons.

Protein. *PRKN* encodes a protein of 465 amino acids composed of an amino-terminal ubiquitin-like domain, a central linker region, and a carboxy-terminal RING domain. Parkin is a E3 ubiquitin ligase involved in the ubiquitin proteasomal degradation system and in maintaining mitochondrial structure, regulating their biogenesis and mitophagy. Abrogation of E3 ligase activity leads to accumulation of toxic protein aggregates [106] Additionally, Parkin is recruited on the surface of damaged or dysfunctional mitochondria and activated by PTEN-induced putative kinase 1 (PINK1), resulting in

the ubiquitination of outer mitochondrial membrane (OMM) proteins and their subsequent proteasomal degradation, and subsequent mitochondrial removal via the autophagy-lysosomal pathway [107]. Under homeostatic conditions, Parkin also modulates mitochondrial biogenesis through the degradation of PARIS, a repressor of mitochondria biogenesis. Loss of Parkin function allows PARIS to accumulate and repress mitochondrial biogenesis [108].

Genetics. Variants in *PRKN* were reported to cause the majority of autosomal recessive early onset PD cases [109]. *PRKN* variants include chromosome rearrangements, CNVs, deletions and duplications of exons, as well as single nucleotide variants that cause missense, nonsense, and splice site variants. Of these, missense variants are the most frequently reported in PD patients and, because they do not impact on protein expression, they may represent potential targets for therapies that enhance Parkin activity [110]. Homozygous and heterozygous variants in this gene are responsible for almost 50% familiar and up to 20% of sporadic early onset PD. Clinical phenotype of PRKN-related PD is characterized by younger age of onset (average 31 years) and unusual symptoms, such as dystonia at onset, hyperreflexia, and early treatment-related complications.

PINK1

Gene. *PINK1* (PTEN-induced kinase 1) gene is located on chromosome 1p36.12 (PARK6 locus) and it has 8 exons spanning about 1.8 kb.

Protein. PINK1 encodes a serine/threonine kinase with a N-terminal mitochondrial targeting sequence followed by a putative transmembrane domain and a C-terminal region (CTR). This CTR is highly conserved and was proven to play a crucial role in the interaction with Beclin 1 [111] and in the autophosphorylation of PINK1 [112]. PINK1 has an eclectic role and seems to be involved in several pathways, including mitochondrial and calcium homeostasis, protection against misfolded protein damage, autophagy/mitophagy and endoplasmic reticulum-mitochondria crosstalk [113], [114]. Upon mitochondrial depolarization or damage, PINK1 accumulates on the OMM, “flagging” the damaged organelle for degradation [115] and undergoes autophosphorylation, a step necessary for its complete activation [112]. Eventually, PINK1 recruits and ubiquitinates Parkin, which in turn

will ubiquitinate mitochondrial proteins of the OMM [116]. PINK1 can induce the autophagic degradation of damaged mitochondria independently from Parkin [117]. Moreover, PINK1 promotes basal and starvation-induced autophagy beyond mitophagy, by its interaction with Beclin1. This is crucial for the formation of omegasomes, the precursors of autophagosomes that will engulf damaged cellular structures primed for degradation [111]. Besides that, several studies showed that PINK1 is an anti-apoptotic protein. and is also involved in regulating the biogenesis of mitochondrial components. PINK1 deficiency leads to an excessive increase of intramitochondrial Ca^{2+}, which is known to inhibit oxidative phosphorylation, activate the intrinsic apoptosis pathway and increase production of ROS.

Genetics. Its association with early-onset PD was discovered in 2004 studying two large Italian and one Spanish families with early onset ARPD [118]. The Spanish family carried a G→A transition in exon 4, resulting in an amino acid substitution (p.G309D) from a glycine to an aspartic acid in position 309, at a highly conserved position in the putative kinase domain, while Italian families carried the same G→A transitions in exon 7, which resulted in a p.W437X substitution from a tryptophan residue to a stop codon, truncating the last 145 amino acids encoding the C terminus of the kinase domain. To date, over 40 variants in *PINK1* gene were identified, comprising missense, nonsense, insertions, deletions, and single or multiple exon CNVs, leading to a loss of function in most cases. Homozygous and compound heterozygous mutations in *PINK1* are the second most frequent causes of AR early-onset parkinsonism ranging from 1 to 15% of familiar and 1-4% of sporadic early-onset PD cases [83]. The prevalence of heterozygous rare variants, including both sporadic and familial cases of all onset ages, ranged between 0.3 and 4.2% in different studies [119]. Some studies have suggested a potential role for heterozygous *PINK1* variants in influencing PD risk in offspring of biallelic mutation carriers or families with a seemingly autosomal dominant pattern of inheritance, for the PINK1 p.G411S variant [120]. This potential effect is supported by functional evidence showing that the PINK1 p.G411S variant interferes with the protective functions of PINK1-mediated mitochondrial quality control. Additionally, PINK1 p.G411S heterozygous carriers present a

significant reduction in kinase activity [121]. From a neuropathological point of view, if compared to idiopathic PD, this type of PD is sporadic-like, with loss of dopaminergic neurons and presence of LBs, a good response to levodopa, and rapid development of dyskinesias.

DJ-1

Gene. *DJ-1* is located on chromosome 1p36 (PARK7 locus) and contains 8 exons; the first 2 exons (1A and 1B) are noncoding and alternatively spliced.

Protein. DJ-1 is a homo dimeric 189 amino acid protein with antioxidant and transcription modulation properties. DJ-1 deficiency leads to altered mitochondrial morphology, defects in mitophagy and increase in ROS production. In oxidative stress conditions DJ-1 translocate to mitochondria, where it is found in the matrix and intermembrane space, and later to the nucleus, providing neuroprotection [122], [123]. DJ-1 levels rise in response to oxidative stress caused by dopamine and, to suppress the consequent ROS accumulation, gets oxidized and acts as ROS scavenger [124]. Moreover, under physiological condition DJ-1 can directly inhibit the early aggregation steps of α-Syn by acting as a redox-dependent molecular chaperone. Moreover, DJ-1 deficiency causes a decrease in LAMP-2A expression, the receptor required for α-syn degradation through chaperon mediated autophagy (CMA) [125].

Genetics. DJ-1 gene is the third gene associated with an autosomal recessive form of PD. This association was done in the 2002, when homozygous variants were detected in a Dutch and in an Italian family affected by PD and not present in unaffected individuals [126].

The first variants found where a 14kb deletion spanning exons 1-5 in the Dutch family and a homozygous missense variant, within exon 7 which leads to a substitution from leucine into proline in position 166 (p.L166P), in the Italian family [126]. Variants in this gene explain 1-2% of the PD with an early onset (24-40 years) [127] PD associated with *DJ-1* is significantly less common than PRKN- or PINK1-PD, and only 33 mutation carriers have been described. Clinical and neuroimaging features are similar to the other two recessive PD syndromes. Atypical features have been noted in 29% of patients. Dystonia is particularly common (73%) in DJ-1 mutation carriers, as well as postural

tremor (67%) and psychotic signs (73%). Patients have been described as having depression, suggesting that psychiatric features may be particularly frequent in *DJ-1* variant carriers and possibly more common than in idiopathic PD [128].

7. *GBA1* gene

GBA1 gene represents the strongest genetic risk factor for the development of PD, varying between 8% and 12% across the world [129], [130]. Homozygous or compound heterozygous variants in the *GBA1* gene are responsible for Gaucher disease (GD), a lysosomal storage disorder in which the deficient activity of GCase leads to the progressive accumulation of glucosylceramide and other glycosphingolipids within lysosomes, resulting in multiorgan system disease of variable severity [131]. Interestingly, its relevance to PD was first discovered by Neudorfer and colleagues, when patients with GD and relatives were noted to develop Parkinsonian features more frequently than expected [132].

GBA1 gene and glucocerebrosidase (GCase)

The *GBA1* gene contains 11 exons spanning 7.6 kb on chromosome 1q21. The gene resides in a gene-rich region which includes 2 pseudogenes: *GBA1LP* and *MTX1P*, resulted from a duplication event which took place approximately 27–40 million years ago [133]. *GBA1LP* and *GBA1* share 96% sequence identity, whereas sequence homology reaches 98% in the region between intron 8 and the 3' untranslated region [134]. *GBA1LP* encompasses only 5 kb because it lacks intronic Alu sequences, a transposon that can relocate throughout the DNA during evolution, and a has a 55 bp deletion in exon 9 flanked by a short, inverted repeat.

The *GBA1* gene encodes for the glucocerebrosidase enzyme (GCase), which has two functional ATG initiation sites, eventually encoding for two proteins of 536 or 516 amino acids, that are processed within the endoplasmic reticulum (ER) into the mature functional enzyme, a 497 amino acids lysosomal hydrolase. It is organized into three non-continuous domains: domain I is an antiparallel

β-sheet, with two disulphide bridges which may aid proper protein folding; domain II resembles an immunoglobulin fold made up of eight β-sheets; and domain III is composed of a (β/α)8 triosephosphate isomerase (TIM) barrel and contains the active site [135]. From Golgi apparatus to lysosome, transport is mediated by a specific protein, called lysosomal membrane protein-2 [136]. Once on the lysosome, low pH results in the dissociation of LIMP-2 from GCase. Enzyme activity depends on the substrate-presenting co-factor saposin C. GCase principally degrades the glucocerebroside into ceramide and glucose, but it also cleaves glucosylsphingosines and other β-glucosides within the lysosome [134].

GBA1 gene variants and complex alleles

To date, more than 500 different disease-causing *GBA1* variants, including single base substitution, splicing-site variants, deletions, insertions, and gene–pseudogene rearrangements have been reported (Human Gene Mutation Database, HGMD). More than 100 variants have been associated with the risk of PD in the heterozygous state (Figure 5).

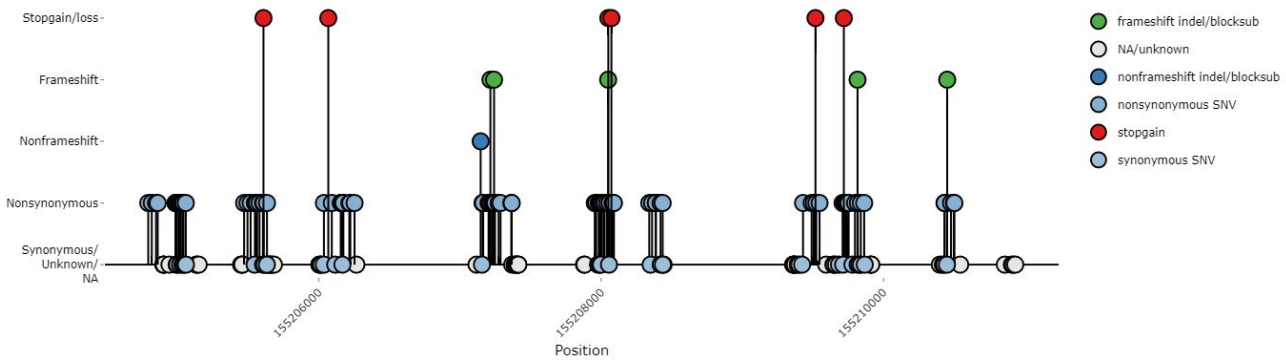

Fig. 5 *GBA1 variant base-pair distribution (https://pdgenetics.shinyapps.io/VariantBrowser/).*

The first two *GBA1* variants were described in the late 1980s [137]. These variants are the c.1226A>G (p.N370S), that cause a single nucleotide substitution leading to an aminoacidic change of asparagine at position 409 into serine, and the c.1448T> C (p.L444P) variants, which lead to an aminoacidic substitution of an arginine at position 502 into cysteine. Interestingly, some *GBA1* variants, classified

as risk variant, such as c.1093G > A (p.E326K) and c.1223C>T (p.T369M), increase the risk for developing PD, but do not cause GD in homozygous state [138], [139].

Other *GBA1* mutations are ancestry-specific and can increase the risk of PD in a determined population [140]. A recent study identified an increased incidence of the p.K198E variant in a population of PD patients from Columbia compared to controls [141]. Recently, a novel *GBA1* intronic variant (rs3115534-G) was discovered in half of PD African patients [142]. This variant has variable frequencies across African ancestry groups but is almost absent in European and Asian ancestry populations. Interestingly, the novel variant is a non-coding variant that causes splicing alteration, leading to an intron retention of intron 8, resulting in reduced protein levels and reduced glucocerebrosidase activity. This indicates the need to investigate underrepresented population to further understand the genetic architecture of PD.

Beyond missense variations, due to the high region of homology between *GBA1* and *GBA1LP,* a prevalent class of variants is caused by recombination events occurring mainly between intron 2 and exon 11 of the gene and pseudogene [143]. Indeed, more than 20 recombinant alleles (also called complex alleles) have been described, either alone or in combination with additional point variants, resulting from gene conversion, fusion, or duplication. RecNcil and Recdelta55 are the most common complex alleles reported [131]. RecNcil derives from a cross-over junction area from intron 9 to exon 10, resulting in the incorporation of a segment of *GBA1LP* that includes variants p.L444P, p.A456P, and p.V460V into the functional *GBA1* gene. On the other side, Recdelta55 comprehends a 55-bp deletion within exon 9 of the *GBA1* gene, corresponding to the deleted portion of the pseudogene. Recombinant alleles that include the 55-bp deletion within exon 9 either in association with the p.D409H alone or with the p.D409H and the RecNcil have been identified as well [144]. Also, recombinant events involving the 3′ untranslated region, introns 2, 3, and 6 of the *GBA1*, and introducing larger segments of pseudogene into the recombinant allele, have been reported. Patients with a crossover site in the 3’UTR of the *GBA1* gene or the adjacent *MTX1P1* have also been identified [145].

Effect of *GBA1* variants on GCase activity

Different *GBA1* variants could affect differentially the enzymatic activity, traffic, binding, and interaction properties of GCase. Some variants result in almost no residual activity whereas others show only reduced activity and seem to not correlate with the severity of diseases associated to *GBA1* [146]. It is therefore possible that the severity of the diseases is not only due to the enzymatic level of activity but could also be due to impaired GCase function within the lysosome, indeed some variants impair the transport of the enzyme, leading to retain Gcase in ER [145]. Also, variants that alter Gcase structure could negatively influence its function. For instance, p.N370S and p.L444P are mapped to the interacting surface of GCase with Saposin C, affecting the stability of the interaction between the two proteins and ultimately abrogating GCase functionality [147].

GBA1 variant classification and nomenclature

The *GBA1* variants are classified based on GD clinical presentation in homozygous state and are divided into four categories: severe (causing GD type II or III, neuronopathic forms), mild (causing GD-type I, nonneuropathic form), risk (associated with higher PD risk, but not reported in GD) and unknown (for which the molecular alteration is not yet known) [148]. However, the increasing complexity of emerging variants and phenotypic heterogeneity among GBA1-PD groups, renders this classification not always useful, highlighting the need to establish a new system of classification for *GBA1* gene in the context of PD.

As described above, human *GBA1* gene contains a 39-amino acid signal peptide, which is processed in the ER to form the mature β-glucocerebrosidase (GCase) enzyme, which is 497 amino acids long. Traditionally, amino acid numbering of *GBA1* gene refer to the mature protein, excluding the 39-residue signal peptide while HGVS nomenclature indicate as amino acid number 1 the first residue (Met) of the signal sequence. Here, to report *GBA1* variants related to the GD and PD, both the traditional nomenclature and the updated HSVG nomenclature have been reported.

7.1 GBA1 gene and PD

As mentioned before, the frequency of *GBA1* variants in PD ranges from 8% to 12% but it is strongly influenced by ethnicity and from the sequencing methods,. Since *GBA1* is only a risk factor for PD, some carriers will not develop the disease. Reduced penetrance of *GBA1* is not yet fully understood. Large population studies demonstrated that among *GBA1* carriers, about 9.1% will develop PD, however, the penetrance rises to 30% in patients above 80 years of age [149], [150]. Also, *GBA1* penetrance changes when comparing carriers of severe and mild or risk variants [151], [152] suggesting that other environmental and genetic modifiers are involved in *GBA1* penetrance. A recent GWAS highlighted the importance of common genetic variants, in particular *SNCA* and *CTSB* loci (rs356219 and rs1293298), as possible modifiers of risk and age at onset for *GBA1* carrier [153]. Moreover, another study investigated the contribution of rare variants in lysosomal genes, demonstrating an overall increase of deleterious variants in such genes in GBA1-PD patients compared to asymptomatic *GBA1* carriers[154].

Pathogenetic mechanism of *GBA1* variants in *GBA1-PD* patients

To date, the molecular mechanisms related to an increased PD risk in *GBA1* mutation carriers may be seen in the underlying relationship between GCase and alpha-synuclein. Three main hypotheses have been postulated: a toxic *gain of function* mechanism where misfolded GCase can directly impact its interaction with alpha-synuclein, leading to increased accumulation and aggregation [146]; a *loss-of-function* mechanism where GCase deficiency causes substrate accumulation, facilitating alpha-synuclein aggregation and toxic oligomer formation in the lysosome, eventually altering alpha-synuclein trafficking, processing, and clearance [146]. The third hypothesis suggests a bidirectional vicious neurotoxic loop where GCase deficiency promotes the formation of alpha-synuclein oligomers which in turn further reduce normal GCase activity [155].

Several possible mechanisms could explain the link between Gcase, alpha-synuclein and PD and are schematized in Figure 6. Abnormally folded GCase has been found to accumulate in the ER resulting in reduced levels of GCase in the lysosome, triggering the unfolded protein response, ER-associated degradation (ERAD) and autophagy-lysosomal alteration [156] (Fig. 6; A). Growing evidence suggests that failure of the endo-lysosomal and autophagic pathways in PD may have a pivotal role [156] . In the lysosome, the GCase plays an important contribution to these processes and in the interplay with alpha-synuclein and when its altered it could lead to lipid substrates and alpha-synuclein accumulation. Impaired degradation of alpha-syn can also lead to alpha-synuclein spreading by exosome-mediated release, allowing alpha-synuclein pathology to propagate through the other region of the brain (Fig. 6,B). Aberrant lipid homeostasis could alter membrane stability/fluidity and composition, altering the binding of alpha-synuclein, leading to subsequent neurotoxicity (Fig. 6, C). Finally, altered GCase could infer with mitochondria clearance and microglia activation. (Fig. 6, D and E).

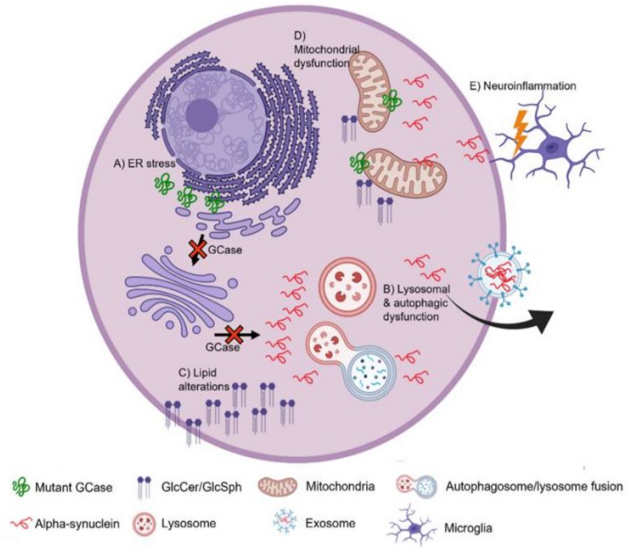

Fig. 6 *Cellular pathological mechanism induced by GCase alteration implicated in nigrostriatal neurodegeneration [156].*

GBA1-PD clinical phenotype

GBA1-PD patients are not easily recognizable from patients with idiopathic PD. Overall, at a clinical level, an association of *GBA1* variants with an earlier age of onset, more rapid progression, and cognitive functions decline was confirmed (Figure 7, A) [152].

Genotype-phenotype correlations were proposed but need to be implemented [157]. Severe *GBA1* variants were associated with younger onset, a more severe progression and a more rapid development of dysautonomia, hallucinations, cognitive impairment and dementia (5.6-fold compared to idiopathic PD). Subjects carrying complex variants had a similar phenotype, with a comparable risk of hallucinations and dementia, but also a higher frequency of delusions. Carriers of mild variants showed a milder phenotype, reaching postural instability after a longer time, less frequent delusions, and later cognitive impairment. Finally, patients carrying a risk allele had the highest age at PD onset and were the only patients showing tremor-dominant phenotype at onset and later occurrence of nonmotor fluctuations [157] (Figure 7, B).

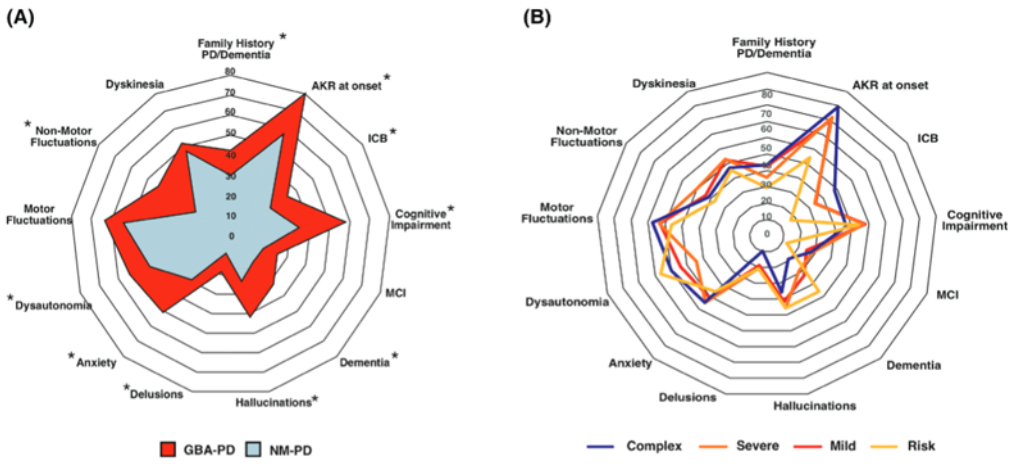

Fig. *7 (A) Comparison of frequency of motor and nonmotor symptoms GBA1-PD versus NM-PD. (B) Frequency of motor and nonmotor symptoms among GBA1-PD subgroups carrying mild, complex, severe, and risk variants [157].*

Advanced therapy: Deep brain stimulation in GBA1-PD patients

It was recently reported that DBS-STN (subthalamic nucleus) could be associated with a higher risk of non-motor complications [158] and cognitive decline [159] in GBA1-PD patients compared with idiopathic PD. Moreover, the deterioration in cognitive performance following DBS implantation in GBA1-PD patients appeared more severe also when compared with GBA1-PD patients who did not undergo DBS surgery, suggesting a possible combined effect of *GBA1* mutations and DBS intervention [160]. The use of a different target, such as the internal globus pallidum (GPi), seemed to have a minor role in determining cognitive complications [161]. However, all these observations required validation in a larger, well selected cohort.

7.3 Several strategies for molecular analysis of *GBA1*: from Sanger sequencing to NGS-based approaches

Several strategies for molecular analysis of *GBA1* gene have been proposed, ranging from Sanger sequencing to NGS-based approaches. The first (and still widely employed) approach to sequence *GBA1* is Sanger sequencing of three overlapping fragments of the gene using GBA1-specific primer pairs, one from exon 1 to 5 (2960 bp), one from exon 5 to 7 (2048 bp) and the last from exon 8 to 11 (1750 bp) (Stone et al., 2000). Due to the high homology with its pseudogene, the selective amplification of the active gene is a cumbersome task [162]. Moreover, PCR-related allele dropout (ADO) phenomena are not uncommon when amplifying the *GBA1* gene using these primers, significantly reducing the sensitivity and specificity of this approach, which, in any case, is costly and time-consuming, thus not amenable for screening large cohorts of PD patients.

Currently, short-read next-generation sequencing (sr-NGS) technology has been applied for the molecular analysis of the *GBA1* gene, both as a single gene or as part of gene panels. Despite the high-quality, efficiency, and affordability of this type of approach, sr-NGS has some main limitations in *GBA1* sequencing: conventional bioinformatic pipelines could misalign the sequencing reads of

the gene to the pseudogene reference sequence and *vice versa*, especially when complex variants are involved, leading to both false positive and false negative results [163]. Long-read NGS may represent the long-term solution for the issue of *GBA1* sequencing; however, its relatively high costs and unavailability in most diagnostic labs currently hinder its wide adoption in the clinical setting. For this reason, our project was focused on implementing an NGS workflow to validate a strategy for the identification of *GBA1*-variants only, using parallel massive sequencing, in a cheaper and less time-consuming way.

Aim of the study

PD is the second most common neurodegenerative disorder in the world after Alzheimer's disease. Several mechanisms involved in PD pathogenesis are now continuously emerging. Among the various causes, in the last two decades, the contribution of genetic factors was highlighted, accounting for around 10-15% of all PD cases. Beyond causative PD-genes, *GBA1* emerged as the major risk factor for PD. Current sequencing methods for *GBA1*, including Sanger sequencing and standard short-read NGS (sr-NGS), are hindered by the high sequence similarity between *GBA1* and its pseudogene, often leading to false positive or negative results.

The main aim of this thesis was to address the need to provide accurate, fast and cost-effective analysis of *GBA1* at large scale, by designing a novel sr-NGS-based approach, called LONG-NEXT, where both "wet" and "*in silico*" analytical steps have been developed and optimized. I demonstrated the effectiveness of this approach in selected cases, suspected of diagnostic mistakes by conventional testing (n=13) and then validated on consecutively collected PD patients already screened either by Sanger sequencing (n=101) or conventional sr-NGS (n=294).

In addition to the primary methodological work, I also took part in two other collateral projects:

- Within the framework of a study involving a large multicentric Italian PD cohort (PARKNET Study Group), investigating the prognostic impact of *GBA1* variants on long-term motor and non-motor outcomes following DBS surgery, I employed LONG-NEXT as genetic screening method for PD patients recruited at the IRCCS Mondino Foundation (n=137).
- As part of a project (RF_2023) aimed at discovering novel blood biomarkers, I contributed to measure glucocerebrosidase (GCase) activity in a cohort of 15 GBA1-PD and 15 sporadic PD patients.

Materials and methods

1. Subjects

LONG-NEXT was first tested on selected samples for which Sanger sequencing or sr-NGS performed over the past years had yielded doubtful results on *GBA1* genotype (optimization phase). For this phase, n=13 cases were selected who fulfilled either of the following criteria:

1) genotype-phenotype discrepancy (e.g., homozygous *GBA1* pathogenic variants in PD patients without GD, or wild-type genotypes in patients with clinical features or family history suggestive of *GBA1*-PD);
2) ambiguous genetic result obtained with sr-NGS (e.g., *GBA1* variants with low variant allele frequency - VAF - or coverage depth anomalies).

For the subsequent validation phase, LONG-NEXT was assessed on two cohorts of PD patients already screened for *GBA1* mutations either by Sanger sequencing using a published protocol (n=101) or by conventional sr-NGS (n=294).

LONG-NEXT was then applied to screen 137 PD patients who underwent DBS (DBS cohort of IRCCS Mondino Foundation). The DBS cohort of PD patients subjects who underwent surgery according to eligibility criteria between years 2005-2021 fulfilling the following criteria:

- absence of pathogenic/likely pathogenic variants in other major PD-related genes;
- detailed clinical data available at pre-DBS and after 1, 3 and, when available, 5 years from surgery.

For the RF_2023 project a cohort of 30 PD patients were recruited on IRCCS Mondino Foundation and after the genetic screening with LONG-NEXT was divided into 15 GBA1-PD and 15 sporadic PD patients. Detailed methodologies of these two studies (DBS study and RF_2023 project) in which I contributed are not included in this thesis, as they fall outside its scope.

Written informed consent for genetic analyses for diagnostic and research purposes was obtained from all patients.

2. DNA extraction

Genomic DNA (gDNA) was extracted from whole blood using the Maxwell® RSC Blood DNA Kit (Promega) on the Maxwell® RSC 48 instrument to provide an automated extraction of samples. The procedure is conducted following manufacturer's instructions.

Quantitative and Qualitative Evaluation of DNA

DNA samples were quantified using two different instruments: NanoDrop® ND-1000 Spectrophotometer (Thermo Fischer Scientific) and Qubit® 2.0 fluorometer (Invitrogen).

The qualitative evaluation of genomic DNA was performed running samples into agarose gel electrophoresis (0,8%) to assess the genomic integrity of them.

3. LONG-NEXT protocol: targeted-NGS of the *GBA1* gene

LONG-NEXT is a new short-read NGS-based strategy, which rely on a specific long-range PCR of a unique 6.5kb amplicon encompassing the whole *GBA1* gene and excluding *GBA1LP*. This is used as a template to create NGS libraries, which are amplified using Nextera technology (Illumina) and then run on a bench-type sequencer (e.g. MiSeq, Illumina). A tailored bioinformatic pipeline is used to mask the *GBA1LP* sequence on the reference genome (hg38) and therefore allow the correct mapping of reads to the genomic coordinates of *GBA1* gene only [164]. Therefore, the protocol steps will be described below: i) long-range PCR; ii) library preparation and sequencing; iii) tailored bioinformatic analysis.

Long-range PCR

Long-range PCR was used to optimize the amplification of *GBA1* gene in a single reaction. A fragment encompassing exons 1–11 was amplified using the GBA1_6.5kb_Forward:

TCCTAAAGTTGTCACCCATACATG and GBA1_6.5kb_Reverse: TAGTCACAGACAGCGTGTGAGC, obtaining an amplicon of 6501 bp. The GBA1_6.5kb_Forward was designed to anneal univocally to the 5'-UTR of *GBA1*, while the GBA_6.5kb_Reverse primer was designed to anneal at both the 3'-UTR of *GBA1* and *GBA1LP*, to potentially detect also gene-pseudogene rearrangements.

Long-range PCR is performed using GoTaq® Long PCR kit, following the manufacturing instruction (Promega). Briefly, the master mix is aliquoted in the tubes, which include all the PCR reagents and primer pair (Table 3), and then DNA sample is added, except for one tube (negative control) in which the DNA is not added, to detect possible contaminations. The optimal DNA concentration ranges from 60 to 150 ng/uL.

Component	**Concentration**	**Final volume**
GoTaq® Long PCR master mix (2X)	1 X	12, 5 uL
Forward primer	10 uM	1 uL
Forward primer	10 uM	1uL
DNA template	60-150ng/uL	1uL
Nuclease free water	--	-- final volume of 25uL

Table 3 *Master mix of LONG-RANGE PCR*

Once each PCRs is set up, samples are loaded into thermal cycler (BioRad) where specific thermal profile program is configured (Table 4).

Step	Temperature	Time	Number of Cycles
Initial Denaturation	94°C	2 minutes	1 cycle
Denaturation	94°C	30seconds	1 cycle
Annealing/Extension	62°C	6,5 minutes	34 cycles
Final Extension	72°C	10minutes	
Soak	4°C	Indefinite	1 cycle

Table 4 *GBA1 long 6.5kb PCR program*

Long-range PCR purification

PCR purification was performed using Beckman Coulter™ Agencourt AMPure XP purification beads following manufacturer's instructions.

Nextera XT library preparation workflow

After purification of samples, a quantification step is required, first using spectrophotometer (Nanodrop) and then fluorometer (Quibit: High sensitivity range), for checking DNA quantity and then proceed with samples dilution to obtain samples with a final concentration of 0,4 ng/uL. In fact, Nextera XT supports ultra-low DNA input of only 1 ng. The library preparation workflow is illustrated in Figure 8.

Fig.8 *Nextera XT workflow: tagmentation of DNA, amplification of fragments, purification of sequencing, normalization and pooling. (Illumina)*

Tagment DNA

During this step Nextera transposase are used to tagment PCR amplicons. Tagmentation is a process that fragments and tags DNA with adapter sequences, allowing amplification of fragments (around 300 bp) in further steps. The tagmentation of library is performed with the following protocol:

- 5ul of DNA samples (2 ng of DNA in total) and 10 ul of Tagment DNA Buffer (TD) are added to a 96-well plate;
- 5 µl Amplicon Tagment Mix (ATM) is added to each well;
- Plate is centrifuge at 280 × g at 20°C for 1 minute;
- After centrifugation, plate is placed on the preprogrammed thermal cycler with the following program: 5 minutes at 55°C and then hold at 10°C;
- When the program reaches 10°C, is necessary to immediately proceed to the successive step, adding 5 µl of Neutralize Tagment Buffer (NT) to each well, because the transposase is still active;
- Centrifuge as before and incubate at room temperature for 5'.

Amplify Libraries

This step amplifies the tagmented DNA using a limited-cycle PCR program. It is a simple PCR reaction that incorporates sequence required for sequencing cluster generation and two indexes to uniquely identify samples in a pooled library. This step involves adding index primers at the 5' and 3' ends of the fragments, to allow the recognition of the different samples when simultaneous sequencing of multiple samples takes place. In this way it is possible to proceed with the simultaneous sequencing of the amplicons of different individuals on the same flow cell. Indexes kit are provided by Illumina as pre-loaded 96-well plates (DNA/RNA UD Indexes Set A-B-C-D, Tagmentation 96 Indexes, 96 Samples) and offer predefined combinations of indexes that facilitate library preparation and subsequent data analysis. The amplification of library is performed using the following protocol:

- Add 10uL of indexes to each sample and then 15 uL of Nextera PCR Master Mix (NPM) in the plate used for the tegmentation step.
- Plate is load on the thermocycler with the program showed in Table 5.

Step	Temperature	Time	Number of Cycles
Initial Denaturation	72°C	30 minutes	1 cycle
Denaturation	95°C	30 seconds	1 cycle
Denaturation	95°C	10 seconds	
Annealing	55°C	20 seconds	12 cycles
Extension	72°C	5 minutes	
Final extension	68°C	15 minutes	1 cycles
Soak	4°C	Indefinite	1 cycle

Table 5. *NXT PCR program.*

Clean Up Libraries

This step uses bead purification to purify amplified libraries as described before using Agencourt AMPure XP purification beads.

Assess DNA Library quality and quantity.

To check library quality, Agilent 4200 TapeStation System, together with High Sensitivity D1000 reagents and ScreenTape cartridge were used, according to manufacturer's instructions (Agilent Technologies), as reported here:

- 2 µL High Sensitivity D1000 Sample Buffer and 2 µL of sample are mixed together in a 96-well sample plate (for TapeStation system, Agilent Technologies);
- The plate is vortexed using IKA vortexer and adaptor at 2000 rpm for 1 min;
- Ladder is prepared by mixing High Sensitivity D1000 Sample Buffer with High Sensitivity D1000 Ladder with a ratio of 1:1 (e.g. for 96 samples: 15uL of HS D1000 Sample Buffer and 15uL for HS D1000 Ladder);
- The ScreenTape devices, samples and ladder are placed into the device to start the run.

All the specifications of the electrophoretic run were previously detailed on the TapeStation controller software, while data output were analyzed on TapeStation Analysis software.

It is important to verify that the electropherogram obtained by libraries shows a broad size distribution of ~250–1000 bp (Figure 9).

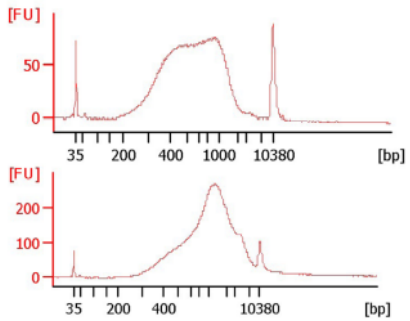

***Fig.9**. Example of Bioanalyzer trace (Illumina)*

The concentration of each library was checked via quantification with Qubit High Sensitivity as previously described.

Library normalization

After checking the quality and quantity of library, next step is the library normalization. This process normalizes the libraries, to ensure equimolar representation of samples. The normalization process was conducted with a standard protocol:

- Convert the concentration of DNA libraries obtained from ng/µl in nM, using the following formula:

$$\frac{concentration\ in\ ng/ul}{\left(660\frac{g}{mol}\right)x(mean\ leangh\ of\ library)}\ \text{x}\ 10^6$$

- To get the correct concentration for the pooled library, 4nM or 8nM in our case, the following calculation was used:

$$\frac{V(f)x\ C(f)}{\#\ x\ C(i)}$$

Where:

V (f) is the final volume of the pool,

C (f) is the final concentration of DNA within the pool (2nM),

is the number of indexes used

C (i) is the initial concentration of each sample obtained by Bioanalyzer assay

- Adjust the final volume of samples to the desired final concentration (4 or 8 nM), starting with the molarity obtained by the precedent formula and pool all together.

Library pooling and Miseq™ sample loading

This step has the goal of dilute and denature the pooled libraries.

- 5uL of 4nM (or 8nM) library and 5ul of 0.2 N NaOH are combined in a tube. Vortex briefly and then centrifuge at 280 × g for 1 minute. Incubate at RT for 5 minutes.

- 990 µl prechilled HT1 (Hybridization Buffer) was added to the tube containing the denatured library, resulting in a 1 ml of a 20 pM denatured library.
- 20 pM library was further diluted to 10pM, through mixing 300 uL of 20 pM library and 300 uL of HT1.

We proceeded with the addition of 1% PhiX library which is used for low diversity libraries as in our case. Low diversity libraries are libraries where a significant number of reads have the same sequence and lack of variation shifts the base composition because the reads are no longer random.

Once the steps described have been completed, it is possible proceed to load pooled library onto cartridge in the bench-type sequencer which, in our case, is a MiSeq™ sequencer (Illumina). Sequencing kit used are Illumina Miseq kit v2 (2 x 150 paired-end output: 4.5–5.1 Gb) or Illumina Miseq kit v2 nano (2 x 150 paired-end output: 300 Mb), depending on the number of samples processed.

We follow the setting phases provided by the company to load the library onto the instrument:

- Upload on Local Run Manager (LRM) of the MiSeq the sample sheet with the specification of the run (ID of samples, library preparation kit and index kit);
- Select Sequence on the control setting of the MiSeq (MSC), to start the guided procedure for Flow Cell, reagent cartridge and buffer loading;
- Perform a Pre-Run Check (experiment name, workflow chosen for the analysis, reads length);
- Select Start Run;
- Monitor the run on the MCS interface and verify that the run parameters Q-Score, Cluster Density, and Cluster Passing Filter are above the established threshold.

Once the run is ended, proceed with the bioinformatic analysis of the data, and perform the post-run washing for the instrument.

Optimized bioinformatic data analysis

Bioinformatic analysis (reads alignment and variant calling) was conducted following GATK4 best practices [164], but employing the hg38 reference genome masked for the *GBA1LP* pseudogene sequence through “bedtools maskfasta" command [165] allowing read alignment univocally against the *GBA1* reference sequence.

4. Sanger Sequencing and short-read NGS for *GBA1* analysis

Conventional Sanger sequencing

The GBA1 gene was amplified through three gene-specific long-range PCRs as previously described by using GoTaq® Long PCR (Promega), with some optimizations [166]. In detail, the first fragment (exons 1–5; 2972 bp) has an annealing temperature of 57 °C and extension time of 3 minutes; the second fragment (exons 5–7; 2049 bp) has annealing temperature of 58.5 °C and extension time of 2 minutes; the third fragment (exons 8–11; 1594 bp) has annealing temperature of 62 °C and extension time of 2 minutes (Supplementary Table 4) [145]. The three fragments of the whole GBA1 gene were purified by ExoSAP-IT™ enzymes (Applied Biosystems- Thermo Fisher, Waltham, Massachusetts, US). Using exon-specific internal primers (Table 6), amplicons were sequenced using the BigDye Terminator kit (BigDye Terminator V3.1, Applied Biosystems). Purified samples were loaded into the 3500 Genetic Analyzer (Applied Biosystems).

	Primers	Amplicon size (bp)
GBA_1F	5'-CCTAAAGTTGTCACCCATAC-3'	2972
GBA_1R	5'-AGCAGACCTACCCTACAGTTT-3'	
GBA_2F	5'-GACCTCAAATGATATACCTG-3'	2049
GBA_2R	5'-AGTTTGGGAGCCAGTCATTT-3'	
GBA_3F	5'-TGTGTGCAAGGTCCAGGATCAG-3'	1594
GBA_3R	5'- TAGTCACAGACAGCGTGTGAGC -3'	

Table 6. *Primer pairs used for three-fragment amplicons of GBA1 long-range PCR.*

Short-read NGS

DNA samples, on which whole-exome-sequencing (WES) analysis were performed, were sent on CeGaT GmbH (Tübingen – Germany) service company. CeGat requires specific DNA quality and quantity standard that were test before delivery of the samples. They require DNA with a concentration ≥ 10 ng/μL and a volume of at least 25 μL. which took care of the NGS sequencing.

To fulfill their request:

- We assessed DNA concentration, measuring it with a spectrophotometer (NanoDrop)
- We checked DNA integrity, performing a degradation gel electrophoresis (0.8%).

The DNA loaded in each well needs to have a concentration of 100 ng, so further calculations are made before the run.

At this point, only high-quality DNA are quantified through fluorometer (Qubit™) and diluted with nuclease-free water, according to the final concentration and volume request by the company.

The kit used by the company was the Twist Human Core + RefSeq + Mitochondrial Panel (Twist Bioscience) on the Illumina platform NovaSeq 6000, 2 x 100 bp. BWA v0.7.5 was used to align raw

sequence data to the human reference genome (GRCh37), obtaining BAM files. Then, GATK Unified Genotyper was exploited to call variants from BAM files to generate VCF files, which were annotated through the eVAI v0.7 software (EnGenome).

In other centers collaborating to this project, conventional sr-NGS was performed using distinct sr-NGS strategies (i.e. custom panel or *in house* whole-exome sequencing). Targeted enrichment approaches were either amplicon-based (119 samples) or hybrid capture (180 samples). Reads were aligned against the human reference genome (hg38) using BWA, variant calling was performed with GATK4 and variants were annotated using ANNOVAR.

Variant interpretation and classification

From VCFs, in our study, we investigated samples using a virtual panel of 52 genes, known to be causative and linked to PD and Parkinsonism, in which the analysis of *GBA1* gene was included.

For each sample, the following genes were analyzed:

ATP13A2, ATP1A3, C19orf12, CSF1R, DCTN1, DNAJC6, FBXO7, FTL, GBA1, GCH1, GRN, LRRK2, LYST, MAPT, OPA3, PANK2, PARK7, PDGFB, PINK1, PLA2G6, PRKN, PRKRA, PTRHD1, RAB39B, SLC30A10, SLC39A14, SLC6A3, SNCA, SPG11, SPR, SYNJ1, TH, TUBB4A, VPS13A, VPS35, WDR45, ARSA, CHCHD2, COASY, TAF1, ANO3, ATP6AP2, ATXN2, ATXN3, C9orf72, EIF4G1, GIGYF2, GNAL, HTRA2, HTT, IPPK, JPH3, NR4A2, SGCE, SLC41A1, SNCAIP, TBP, THAP1, TOR1A, UCHL1, ATN1_CAG, ATXN1_CAG, ATXN2_CAG, ATXN3_CAG, C9orf72_GGGGCC, HTT_CAG, JPH3_CTG, PPP2R2B_CAG, TBP_CAG

Once filtered by the genes of our interest, we prioritized variants satisfying the following criteria:

- Inheritance model (autosomal dominant, recessive and X-linked);
- Coverage > 15 reads and allele ratio > 0.25, to avoid artefacts;
- Minor allele frequency (MAF) in the general population usually <0.5-1%;

- Molecular effect: only variants altering coding sequences, affecting splicing sites, and responsible for alteration in the 5' UTR are selected. Synonymous variants, intron variants, intragenic and non-coding exon variants, were excluded.

To better investigate interesting variants, we use other databases and public literature to gather more information:

• Disease databases: primarily containing variants found in patients with disease of interest and the assessment of the variants's pathogenicity (ClinVar, OMIM, DECIPHER).

• Computational (in silico) Predictive Programs: a variety of in-silico tools, both publicly and commercially available, that can aid in the interpretation of sequence variants. The algorithms used by each tool may differ but can include determination of the effect of the sequence variant at the nucleotide and amino acid level including determination of the effect of the variant on the primary and alternative gene transcripts, other genomic elements, as well as the potential impact of the variant on the protein. The two main categories of such tools include those that predict whether a missense change is damaging to the resultant protein function or structure (e.g., Polyphen, SIFT) and those that predict if there is an effect on splicing (e.g., Human Splicing Finder).

Thereafter, American College of Medical Genetics and Genomics (ACMG) criteria were applied to classify the variants identified using variant database (e.g. Varsome), which include clinical assertions and evidence used for variant classification, according to the guidelines of ACMG criteria [167].

5. Glucocerebrosidase activity assay

The glucocerebrosidase (GCase) activity assay is a fluorometric test used to measure the enzymatic activity of glucocerebrosidase and is based on the catalytic hydrolysis of the synthetic fluorogenic substrate4-methylumbelliferyl β-d-glucopyranoside that releases the highly fluorescent 4-methylumbelliferyl (4-MU), according to previously described method [168].

We performed GCase assay on PBMCs (peripheral blood mononuclear cells, see section below) that must be extracted within 24 hours from blood drawing.

PBMCs extraction

PBMCs are extracted from whole blood following the protocol below:

- Histopaque - Ficoll (Sigma Aldrich) is removed from the refrigerator to equilibrate it to RT for approximately 30 minutes;
- 18ml of blood is layered with Histopaque – Ficoll at a 1:1 ratio in 50 mL tubes. The tube is centrifuged for 20 minutes at 800 xg;
- After centrifugation, lymphocyte rings are carefully collected using a glass pipette with a rotating motion and are transferred to a new 15 mL tube. The volume is brought up to 12 mL with 1X Phosphate-Buffered Saline (PBS). The tube is centrifuged for 15 minutes at 300 x g,
- The surnatant is collected for each sample and is transferred to a new 15 mL tube. The remaining pellet is resuspended in the initial tube with 5 mL of 1X PBS;
- Both the initial tube and the tube containing the saved supernatant from the previous step are centrifuged for 15 minutes at 300 x g;
- Supernatant from both 15 mL tubes is discarded and the pellets are combined in 2-3 mL of 1X PBS in a single 15 mL tube for cell counting;
- Lymphocytes are resuspended in an appropriate volume of 1X PBS to achieve $5x10^6$ cells per mL and centrifuged in a microcentrifuge for 10 minutes at 3000 rpm (845 x g);

- The supernatant is removed and PBMCs pellets and are than stored at -80°C as leucocyte pellet sample.

GCase assay

The protocol for GCase assay is described below:

- Leucocyte pellet samples (5×10^6 cells/each) are removed from -80°C and kept on ice.
- 200 µL CelLytic (CelLytic™ MT Cell Lysis Reagent, Sigma Aldrich) is added to each pellet to be gently resuspended;
- Resuspended pellets are kept on ice for 30 minutes on an orbital shaker. Then, pellets are centrifuged at 4°C 16.000 x g for 20 minutes;
- Supernatants are carefully removed and transferred into new tubes for both GCase assay and protein quantification (BCA assay);
- 20 µL leucocyte supernatants samples (in triplicate) and 20 µL MilliQ water (in quadruplicate) are added into a black 96-well plate (clear flat bottom, Nunc);
- 40 µL of substrate/inhibitor mix (0.15 M citrate/phosphate buffer, pH 5.9; sodium taurocholate and 1 nM 4-MUG) is added to each well (both on blanks and sample wells)
- The plate is then placed at 37°C for 3 hours;
- After 3 hours, 240 µL Glycine Buffer (0.2 M glycine-NaOH, pH 10.4) is added to each well to stop the enzymatic reaction;
- 200 µL of standard working solution (1nmol 4-Methylumbelliferone; Sigma Aldrich) is add to four wells, followed by 100 µL Glycine Buffer;
- The plate is read on fluorescent reader (CLARIOstar Plus; excitation: 355 nm; emission: 460 nm) for 15 minutes.

The activity of the enzyme is calculated as nmol of substrate per hour per microgram protein.

BCA assay

Sample protein concentrations were determined by BCA assay (Bicinchoninic Acid) with Pierce™ BCA Protein Assay Kit (Thermo Fisher) using the manufacturer's instructions.

Statistical analysis

To assess the differences between enzymatic activity of GCase in PD patients with and without *GBA1* variants, we conducted a comparative statistical analysis. In order to perform the analysis, the cohort was divided in 2 group: GBA1-PD (carrying severe, mild, risk and unknown variants) and non mutated GBA1-PD.

Normality testing

A Shapiro-Wilk normality test was performed separately for both groups to determine the type of distribution of the average enzymatic activity values.

Results

1. Optimization phase

LONG-NEXT was initially designed and optimized on the following selected cases carrying doubtful *GBA1* genotypes detected with conventional strategies (either Sanger sequencing or sr-NGS) (Tables 7 and 8).

Sample ID	Sanger results	LONG-NEXT results
PD_12934	No variant detected	c.721G>A p.(Gly241Arg) heterozygous
Me_PN13	No variant detected	c.454+96_762-121del heterozygous
20719-n	c.754T>A p.(Phe252Ile) homozygous	c.754T>A p.(Phe252Ile) heterozygous
147RPM70	c.1226A>G p.(Asn409Ser) homozygous	c.1226A>G p.(Asn409Ser) heterozygous
3333/21	c.1093G>A p.(Glu365Lys), homozygous	c.1093G>A p.(Glu365Lys) heterozygous
362VPF50	c.1223C>T p.(Thr408Met) homozygous	c.1223C>T p.(Thr408Met) heterozygous

Table 7. *Optimization phase: Sanger sequencing vs LONG-NEXT*

Sample ID	sr-NGS results	LONG-NEXT results
190826 **221690** **223755**	c.1448T>C p.(Leu483Pro) heterozygous	No variant detected
3508/22	c.1497G>C p.(Val499=) heterozygous; low coverage on exon 10-11	c.1448 T>C; p.(Leu483Pro) c.1483G>C; p.(Ala495Pro) c.1497G>C; p.(Val499=) RecNcil, heterozygous
PoliMi_15231	No variant detected, low coverage on exon 9	c.1265_1319del p.(Leu422ProfsTer4) Recombinant Δ55, heterozygous
3434/22	No variant detected	c.1448T>C; p.(Leu483Pro) heterozygous
474VDM75	No variant detected	c.475C>T; p.(Arg159Trp) heterozygous

Table 8. *Optimization phase: sr-NGS vs LONG-NEXT*

Sanger sequencing versus LONG-NEXT (n=6)

False negative cases - PD_12934 and ME_PN13

LONG-NEXT disclosed heterozygous pathogenic *GBA1* variants in two PD patients presenting clinical features and family history suggestive of *GBA1*-PD but negative at Sanger sequencing (**PD_12934** and **ME_PN13,** Table 7). One (**PD_12934**) carried the c.721G>A (p.Gly241Arg) - G202R heterozygous variant (Figure 10), while the other (**ME_PN13**) harboured a heterozygous c.454+96_762-121del (Figure 11).

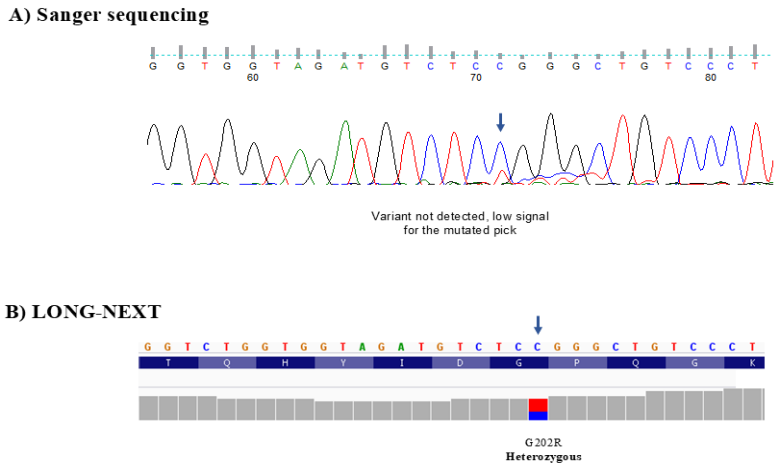

Figure 10. *A) Sanger sequencing. Electropherogram of second GBA1 fragment showing very low signal for the mutated peak, which was reported as noise background. B) LONG-NEXT. Variant p.G202R in exon 6 of GBA1 gene is correctly detected in heterozygosity.*

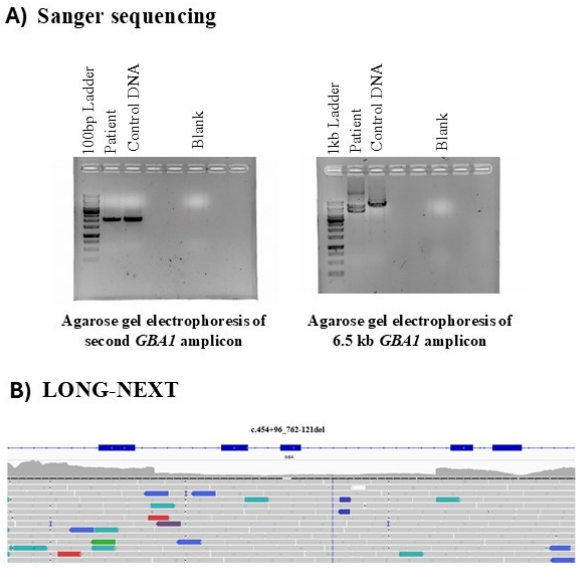

Figure 11 *A) Agarose gel electrophoresis comparison of GBA1 second amplicon (CNV not detected) and 6.5 kb GBA1 amplicon (CNV detected). B) IGV screenshot of the *.bam file showing the deletion (c.454+96_726-121del) encompassing exons 5 and 6 of GBA1, characterized by a decrease in coverage of the region of interest with well-defined deletion breakpoints.*

The identified deletion could not be identified by Sanger sequencing due to removal of the annealing site of the forward primer used for amplification of the second *GBA1* fragment, and in fact it was already detectable by visual assessment of the long-range PCR product of the whole *GBA1* gene (6.5kb) on agarose gel (Figure 11).

False zygosity cases - 20719-n.; 362VPF50; 3333/21; 147RPM70

Conversely, four PD patients without GD signs (**20719-n., 362VPF50, 3333/21, 147RPM70;** Table 7) who had previously been reported as homozygous carriers of *GBA1* variants [c.754T>A (p.Phe252Ile) – p.F213I; c.1223C>T (p.Thr408Met) - p.T369M; c.1093G>A (p.Glu365Lys) – p.E326K; c.1226A>G; (p.Asn409Ser) – p.N370S] were all correctly re-genotyped as heterozygous carriers by LONG-NEXT (Figure 12).

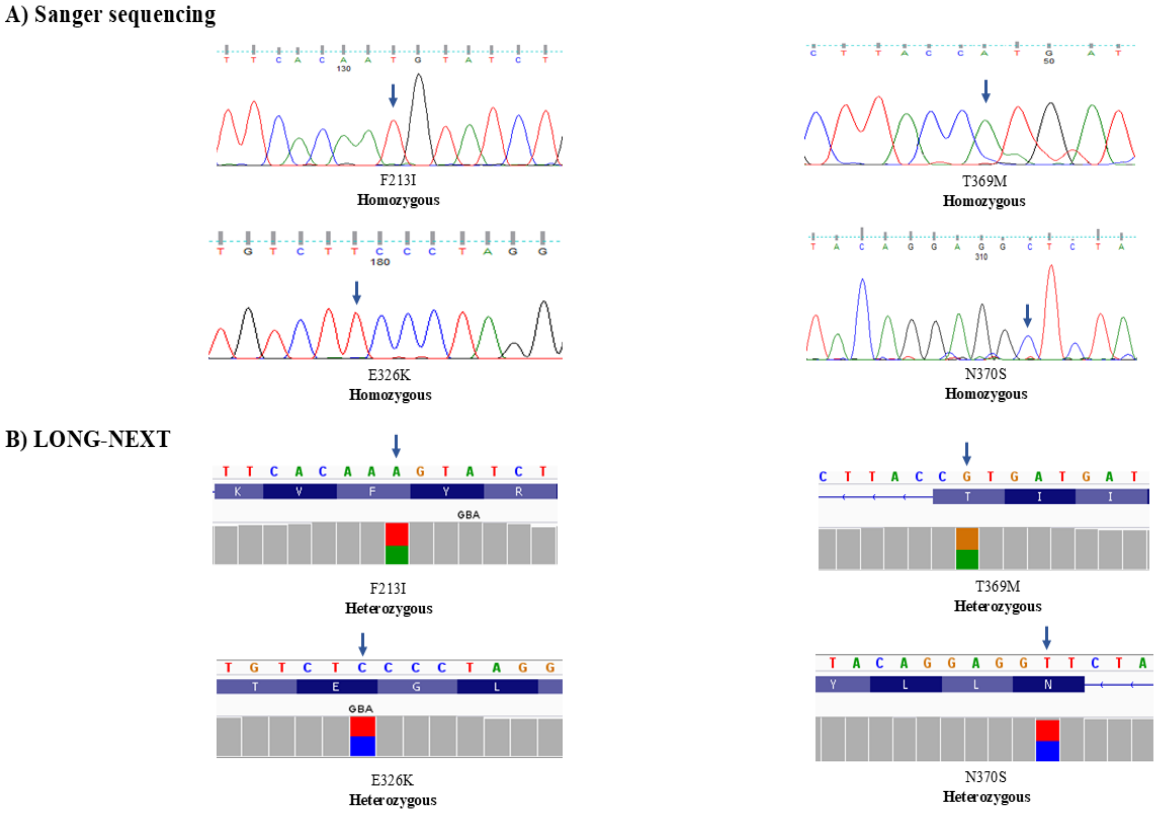

***Figure 12**. A) Sanger sequencing. Electropherograms of four patients' samples carrying the p.F213I, p.T369M, p.E326K and p.N370S variants, erroneously detected in the homozygous state by Sanger sequencing. B) LONG-NEXT. IGV screenshot of the corresponding *.bam files with p.F213I, p.T369M, p.E326K and p.N370S variants.*

The false-negative (**PD_12934** and **ME_PN13**) and false-homozygous results (**20719-n.; 362VPF50; 3333/21; 147RPM70**) were likely due to ADO events during the PCR amplification phase prior to Sanger sequencing.

Conventional sr-NGS versus LONG-NEXT (n=7)

False positive cases - 190826; 221690; 223755

Three patients (**190826, 221690, 223755;** Table 8), previously genotyped as heterozygous carriers of c.1448T>C (p.Leu483Pro) – p.L444P by sr-NGS, were found to be wild-type by LONG-NEXT (Figure 13).

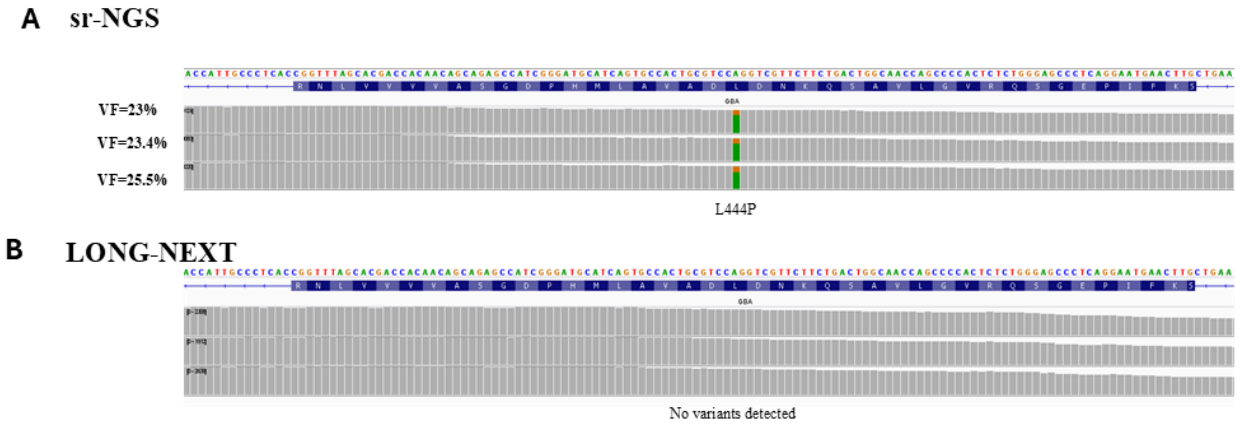

Figure 13. *IGV screenshot of three *.bam files from sr-NGS, "apparently" positive for p.L444P with unbalanced variant frequency, and from LONG-NEXT, showing absence of the variant.*

Interestingly, the VAF obtained by sr-NGS analysis was relatively low (patient 1 VAF=23%, patient 2 VAF=23.4%, patient 3 VAF=25.5%), but in all cases the variant had passed quality filters and was listed in the final annotated variant call format (*.vcf) files. Of note, c.1448T>C (p.Leu483Pro) – p.L444P is a constitutive variant of the *GBA1LP* pseudogene. Therefore, it is likely that the conventional NGS pipeline mapped the reads originating from the pseudogene on the genomic coordinates of the *GBA1* gene, erroneously calling the wild-type pseudogene sequence as a pathogenic *GBA1* genotype.

False negative cases - 3508-22; PoliMi_15231; 3434/22; 474VDM75

In another sample (**3508-22;** Table 8), the sr-NGS pipeline revealed the synonymous c.1497G>C (p.Val499=) – p.V460V variant with low VAF (26%) in exon 10. From the direct visual inspection of the *.bam file, we observed an additional missense variant c.1483G>C (p.Ala495Pro) – p.A456P with very low VAF (21%) in exon 10, which did not pass quality cutoff and was not listed in the final *.vcf file. Interestingly, the region encompassing *GBA1* exons 10 and 11 presented reduced coverage and low-quality mapping reads. This finding was suggestive of a likely misdetection of a recombinant allele. In particular, the RecNcil complex allele, originating from gene-pseudogene recombination from intron 10 to exon 11, results in the incorporation of the terminal segment of *GBA1LP* in the *GBA1* gene, including the three pseudogene variants c.1448 T>C (p.Leu483Pro) – p.L444P, c.1483G>C (p.Ala495Pro) – p.A456P and c.1497G>C (p.Val499=) – p.V460V. Re-sequencing of this case using LONG-NEXT displayed unequivocally that the patient was indeed a heterozygous carrier of the RecNcil mutation, with a balanced VAF for each variant and good quality sequencing reads (Figure 14).

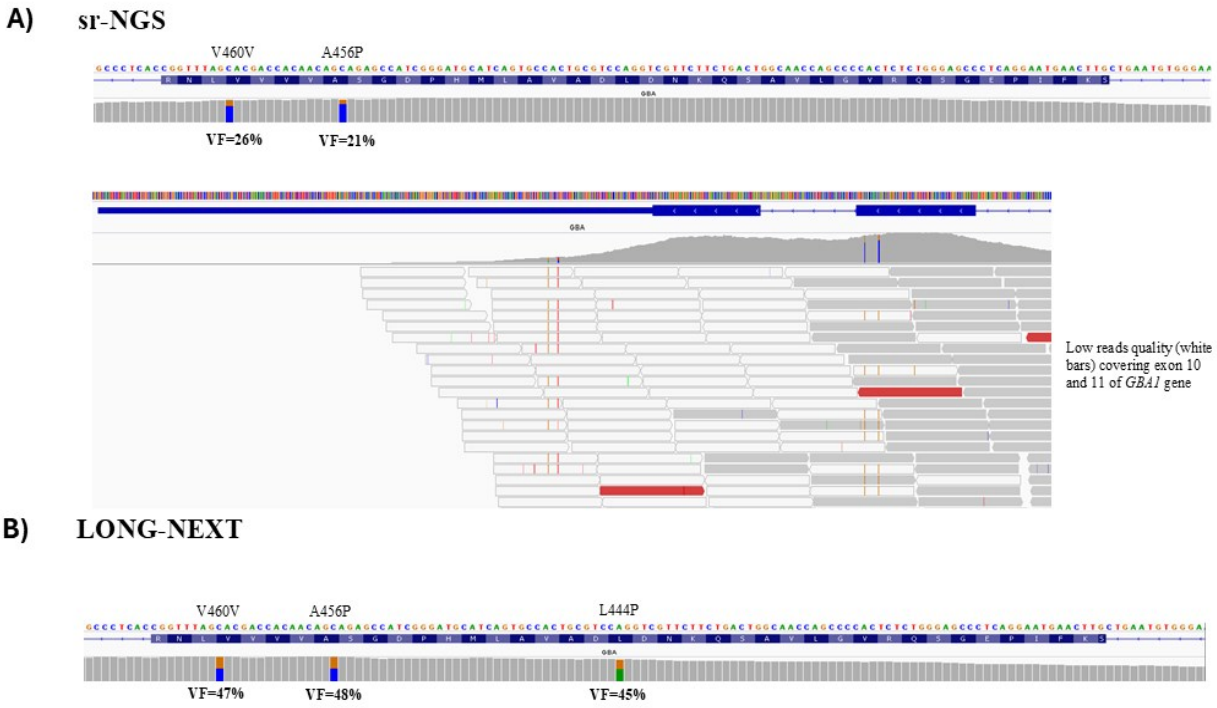

Figure 14. *IGV screenshot of *.bam file from sr-NGS, showing p.V460V and p.A456P variants with unbalanced VF (26% and 21%) and poor coverage and quality reads mapping to GBA1 exons 10 and 11 (white bars), and from LONG-NEXT correctly showing RecNcil variant.*

Another relevant example of misdetection of a *GBA1-GBA1LP* rearrangement was a sample (**PoliMi_15231;** Table 8) whose sr-NGS analysis yielded a wild-type genotype. Interestingly, the *.bam file showed a decreased coverage across exon 9 of the gene, while increased coverage was observed in the corresponding region of the pseudogene, suggesting a misalignment of gene-derived sequencing reads to the pseudogene. In line with this hypothesis, LONG-NEXT clearly showed the presence of the c.1265_1319del [p.Leu422Profs*4 (Recdelta55)] mutation (Figure 15).

A) sr-NGS

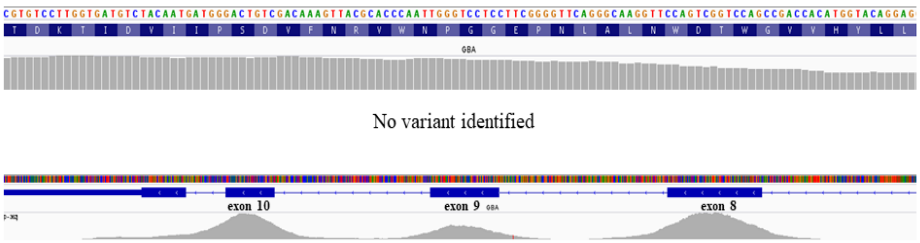

B) LONG-NEXT

Figure 15. *A) sr-NGS (hybrid capture technology). IGV screenshot of the *.bam file showing a wild-type sequence, with decreased coverage for exon 9 compared to surrounding exons. B) LONG-NEXT. IGV screenshot of the *.bam file showing the Recombinant Δ55 variant correctly identified.*

Similarly, two samples (**3434/22** and **474VDM75;** Table 8) with wild-type genotypes at sr-NGS were subsequently found to carry heterozygous single nucleotide variants (SNV) with LONG-NEXT. Also in these cases, the detected variants [c.1448T>C (p.Leu483Pro) – p.L444P and c.475C>T (p.Arg159Trp) – p.R120W] belong to the pseudogene (Figure 16). Once more, the sr-NGS approach failed to call *GBA1* variants, and notably not only complex alleles, but also pseudogene-derived SNVs falling in regions of high homology between the gene and the pseudogene, as a result of an incorrect alignment process.

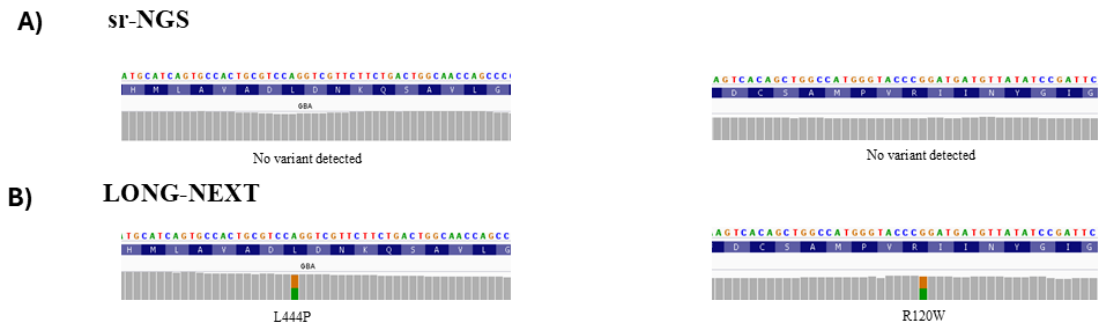

Figure 16. *A) IGV screenshot of *.bam file from sr-NGS (GBA1 exon 10 and GBA1 exon 5) showing no variants. B) IGV screenshot of *.bam files from LONG-NEXT, showing the presence of p.L444P and p.R120W, respectively.*

2. Validation phase

Prompted by these initial results, we validated LONG-NEXT comparing its diagnostic yield to either Sanger sequencing or sr-NGS in two consecutively collected cohorts of PD samples.

LONG-NEXT correctly detected all *GBA1* variants previously identified either by Sanger sequencing or sr-NGS (14/101 and 41/253, respectively).

Notably, one sample (**02353/20**; Table 9) in which Sanger detected the RecNcil complex variant (c.1448 T>C (p.Leu483Pro) – p.L444P, c.1483G>C (p.Ala495Pro) – p.A456P and c.1497G>C (p.Val499=) – p.V460V) in homozygosity was subsequently revealed to be heterozygous by LONG-NEXT (Figure 17, Table 9). Heterozygosity was then confirmed by standard NGS approach.

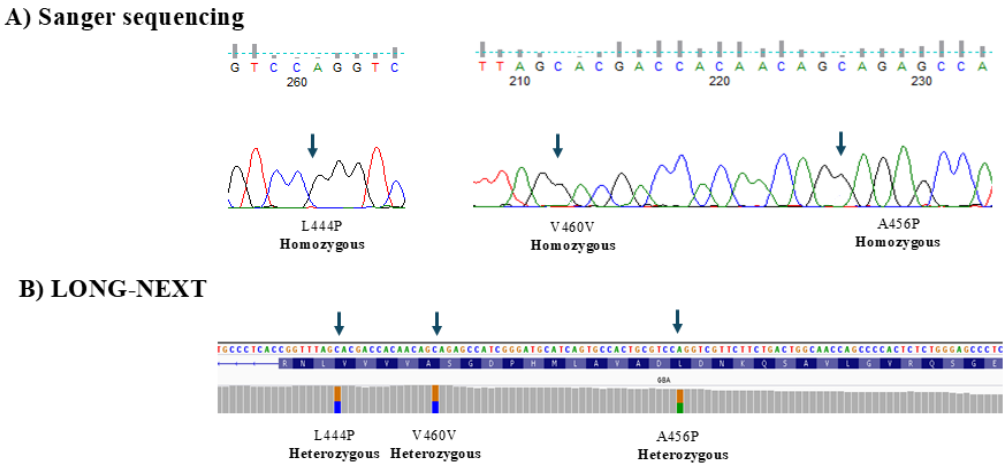

Figure 17. *A) Sanger sequencing. Electropherograms of a sample carrying the RecNcil complex allele (p.L444P – p.V460V- p.A456P), erroneously detected in the homozygous state. B) LONG-NEXT. IGV screenshot of *.bam files of RecNcil variant in the correct heterozygosity state.*

Moreover, one case (**PD-196**; Table 9) testing negative at sr-NGS with amplicon enrichment technology was subsequently found with LONG-NEXT to carry the c.1448T>C (p.Leu483Pro) – p.L444P variant, which was then validated by Sanger sequencing (Figure 18, Table 9). This provides additional evidence of sr-NGS-related false negative results caused by mismapping of reads in gene-pseudogene high homology regions.

A) sr-NGS

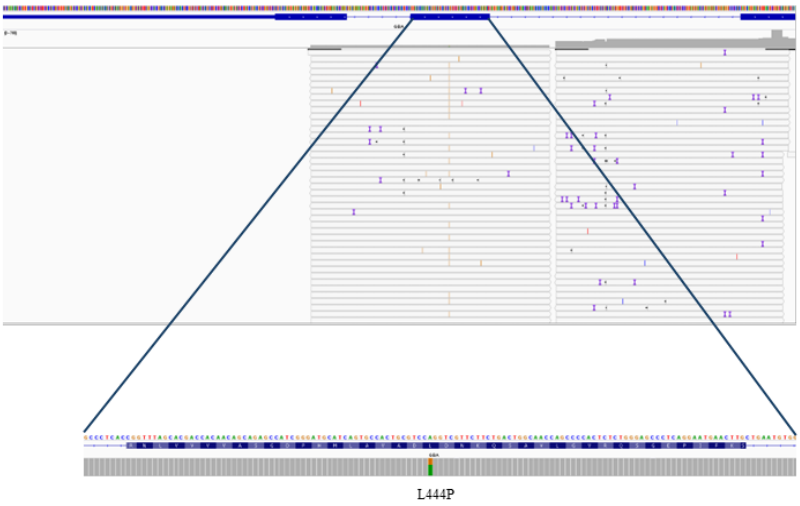

B) LONG-NEXT

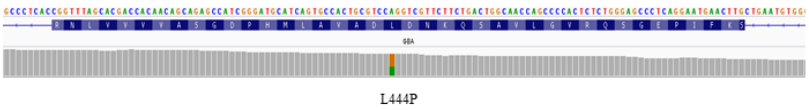

Figure 18 *A) sr-NGS (hybrid capture technology). IGV screenshot of *.bam files showing the p.L444P variant, with low quality reads (white bars) and unbalanced frequency. B) LONG-NEXT. IGV screenshot of the *.bam file showing the p.L444P variant correctly detected in heterozygosity.*

Sample ID	Sanger sequencing	sr-NGS results	LONG-NEXT results
02353/20	c.1448 T>C;p.(Leu483Pro) c.1483G>C;p.(Ala495Pro) c.1497G>C;p.(Val499=) RecNcil, homozygous	c.1448 T>C;p.(Leu483Pro) c.1483G>C;p.(Ala495Pro) c.1497G>C; p.(Val499=) RecNcil, heterozygous	c.1448 T>C; p.(Leu483Pro) c.1483G>C;p.(Ala495Pro) c.1497G>C; p.(Val499=) RecNcil, heterozygous
PD-196	c.1448T>C;p.(Leu483Pro) heterozygous	No variant detected	c.1448T>C; p.(Leu483Pro) heterozygous

Table 9. *Validation phase*

3. Multicentric Italian PD cohort genetic screening

The efficacy of the LONG-NEXT as genetic screening method was firstly tested in a study aimed at assessing the impact of *GBA1* variants on long-term motor and non-motor outcome after DBS surgery [169]. This was a multicenter retrospective, controlled, Italian cohort study involving 15 tertiary level Movement Disorder Centers contributing to the PARKNET cohort.

In particular, LONG-NEXT was applied for *GBA1* gene analysis of 137 PD patients recruited at the IRCCS Mondino Foundation. After the analysis, 41 patients resulted positive and 96 negatives. Among the positive patients, 17 were carriers of severe variants (41%), 2 of complex allele (5%), 8 of mild variants (20%), 8 of risk variants (20%) and 6 of unknown variants (15%). The results of the genetic screening for our cohort are shown in the following graph (Figure 19).

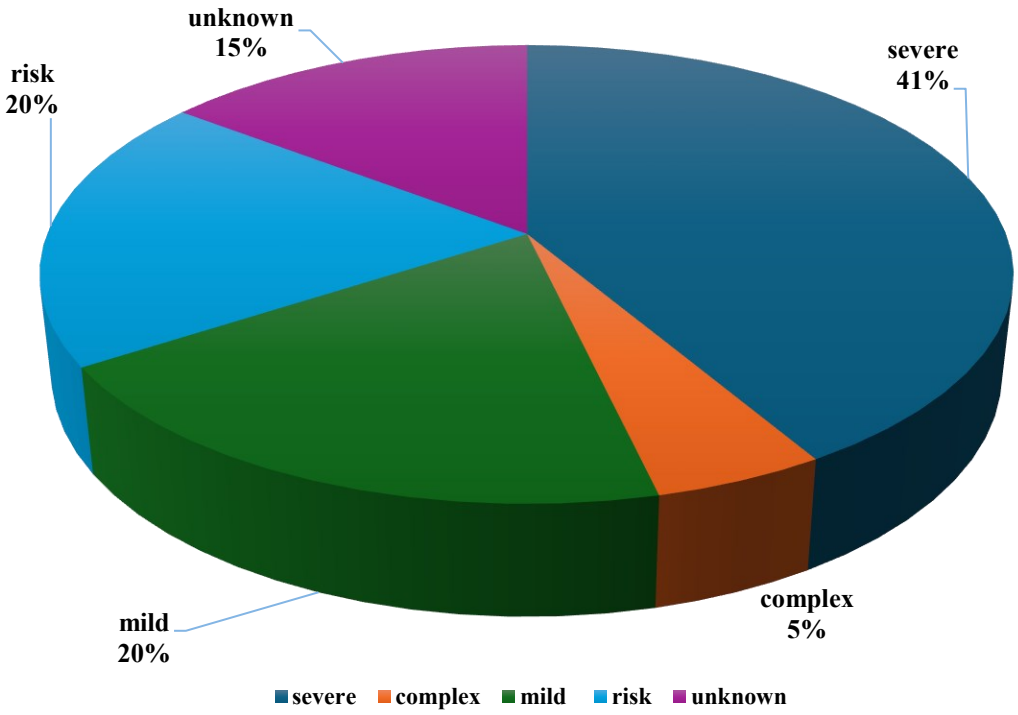

Fig.19 *GBA1 variants distribution among IRCCS Mondino cohort using LONG-NEXT.*

The remaining centres of the Italian cohort performed *GBA1* genetic testing locally, either through LONG-NEXT or alternative sequencing strategies (Sanger Sequencing, sr-NGS). Subsequently, the results were harmonized and combined into a single multicenter cohort.

A concise summary of the genetic and clinical findings of the study is provided below, as a detailed presentation of all results falls outside the scope of this thesis [169].

A total of 615 PD patients from the 15 Italian centres were recruited and the cohort was divided in two groups:

- **DBS cohort**: including 539 subjects (DBS-PD) who underwent surgery
- **nonDBS cohort**: including 76 GBA-PD subjects who fulfilled the criteria per DBS but were eventually non operated (nonDBS-GBA-PD)

After the *GBA1* gene screening, subjects in the DBS cohort were further stratified into DBS-GBA-PD (n=109), DBS-nonGBA-PD (n=430) and nonDBS-GBA-PD (n=76).

Among the DBS-GBA-PD patients, 23 (21.1%) patients carried mild variants, 26 (22.9%) risk alleles, 47 (44%) severe/complex variants and 13 (11.9%) unknown variants.

In the 76 non-operated PD subjects, 14 (18.4%) had mild variants, 23 (30.3%) risk, 30 (39.5%) severe/complex and 9 (11.8%) unknown (Fig. 20).

A detailed description of the variants identified in the whole cohort is reported in Table 10.

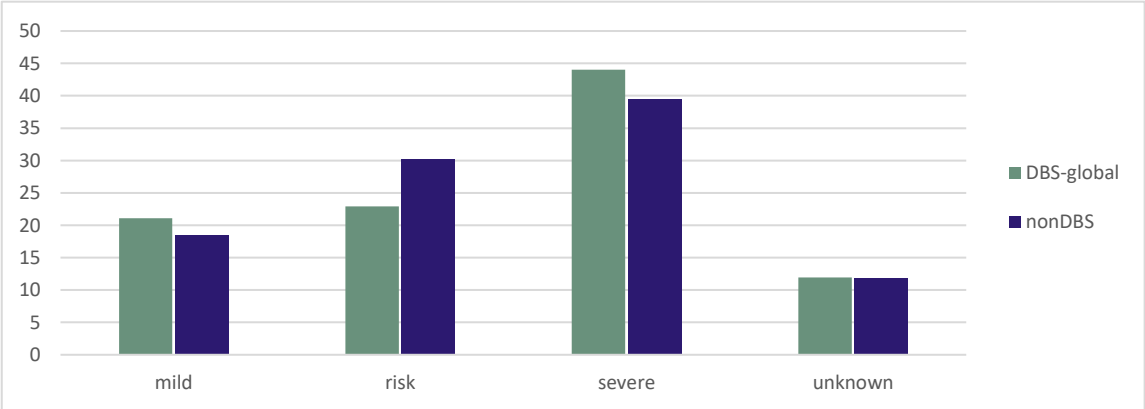

***Figure 20**. GBA1 variant classification among DBS-GBA group and non DBS-GBA group.*

Allele name	Amino acid change	Nucleotide change	Class of variant	DBS-GBA-PD (n=109)	nonDBS-GBA-PD (n=76)
H255Q	p. (His294Gln)	c.882T>G	Complex	1	-
D4098H	p. (Asp448His)	c.1342G>C			
N370S splice	p. (Asn409Ser) splice	c.1226A>G	Complex	1	-
		c.115+1G>A			
L444P	p. (Leu483Pro)	c.1448 T>C	Complex (RecNcil)	2	-
A456P	p. (Ala495Pro)	c.1483G>C			
V460V	p. (Val499=)	c.1497G>C			
R329H	p. (Arg369His)	c. 1103G>A	Mild	-	1
N370S	p. (Asn409Ser)	c.1226A>G	Mild	20	12
N370S	p. (Asn409Ser)	c.1226A>G	Mild	-	1
E326K	p. (Glu365Lys)	c.1093G>A			
G46E	p. (Gly85Glu)	c.254G>A	Mild	1	-
R48W	p.(p. (Arg87Trp)	c.259C>T	Mild	1	-
N370S	p. (Asn409Ser)	c.1226A>G			
S271G	p. (Ser310Gly)	c.928A>G	Mild	1	-
E326K	p. (Glu365Lys)	c.1093G>A	Risk	9	10
T369M	p. (Thr408Met)	c.1223C>T	Risk	1	-
E326K	p. (Glu365Lys)	c.1093G>A			
T369M	p. (Thr408Met)	c.1223C>T	Risk	13	13
E388K	p. (Glu427Lys)	c.1279G>A	Risk	3	-
L444P	p. (Leu483Pro)	c.1448T>C	Severe	1	1
E326K	p. (Glu365Lys)	c.1093G>A			
G202R	p. (Gly241Arg)	c.721G>A	Severe	4	-
P299Qfs*26	p.(Pro338GlnfsTer26)	c.1013del	Severe	1	-
Y313X	p. (Tyr352Ter)	c.1056C>A	Severe	1	1
G325R	p. (Gly364Arg)	c.1090G>A	Severe	1	-
splice	splice	c.115+1G>A	Severe	2	-
E388X	p. (Glu427Ter)	c.1279G>T	Severe	-	1
D399N	p. (Asp438Asn)	c.1312G>A	Severe	-	1
D409H	p. (Asp448His)	c.1342G>C	Severe	3	1
L444P	p. (Leu483Pro)	c.1448 T>C	Severe	19	12
R47X	p. (Arg86Ter)	c.256C>T	Severe	3	1
P99Lfs*62	p. (Pro138LeuTer62)	c.413delC	Severe	1	-
R120W	p. (Arg159Trp)	c.475C>T	Severe	1	-
R131C	p. (Arg170His)	c.509G>A	Severe	-	3
T154Qfs*68	p.(Thr193GlnfsTer68)	c.576_577delTA	Severe	-	1
R163X	p. (Arg202Ter)	c.604C>T	Severe	1	-
W184R	p. (Trp223Arg)	c.667T>A	Severe	-	2
N188S	p. (Asn227Ser)	c.681T>G	Severe	1	-
W209Gfs*6	p. (Trp248GlyfsTer6)	c.741del	Severe	1	1
F213I	p. (Phe252Il3)	c.754T>A	Severe	-	2
L (-11) Afs*18	p. (Leu29AlafsTer18)	c.84dupG	Severe	1	-
P245T	p. (Pro284Thr)	c.850C>A	Severe	-	2
H255Q	p. (His294Gln)	c.882T>G	Severe	1	1
R257X	p. (Arg296Ter)	c.886C>T	Severe	1	-
S173T	p. (Ser212Thr)	c.634T>A	Unknown	1	-

M280T	p. (Met319Thr)	c.956T>C	Unknown	1	-
T369T	p. (Thr408=)	c.1224G>A	Unknown	1	-
D380N	p. (Asp419Asn)	c.1255G>A	Unknown	1	-
L385P	p. (Leu424Pro)	c.1271T>C	Unknown	1	-
T410M	p. (Thr449Met)	c.1346C>T	Unknown	-	1
D443N M361I	p. (Asp482Asn) p. (Met400Ile)	c.1444G>A c.1200G>	Unknown	-	1
H451R	p. (His490Arg)	c.1469A>G	Unknown	-	1
G421D	p. (Gly460Asp)	c.1379G>A			
V460V	p. (Val499=)	c.1497G>C	Unknown	1	-
R463H	p. (Arg502His)	c.1505G>A	Unknown	1	-
T30I	p. (Thr69Ile)	c.206C>T	Unknown	-	1
R39C	p. (Arg78Cys)	c.232C>T	Unknown	-	1
G64D	p. (Gly103Asp)	c.308G>A	Unknown	-	1
M85V	p. (Met124Val)	c.370A>G	Unknown	1	-
M85V	p. (Met124Val)	c.370A>G	Unknown	1	-
V17V	p. (Val56=)	c.168C>T)	Unknown		
T86P	p. (Thr125Pro)	c.373A>C	Unknown	1	-
K (-27) R	p. (Lys13Arg)	c.38A>G	Unknown	1	-
S196P	p. (Ser235Pro)	c.703T>C	Unknown	-	1
-	-	c.762-18T>A	Unknown	1	-
-	-	c.762-4C>T	Unknown	1	-
-	-	c.762-18T>G	Unknown	-	1
R262C	p. (Arg301Cys)	c.901C>T	Unknown	-	1

Table 10. *GBA1 variants identified in the multicentric Italian PD cohort [169]*

Clinical data, including motor and non-motor features, were retrospectively collected before surgery and after 1, 3 and (when possible) 5 years.

At pre-DBS evaluation, the three cohort were comparable for motor, cognitive and other non-motor features.

At longitudinal assessment, both DBS groups showed sustained motor improvement, a benefit which was absent in the nonDBS-GBA1-PD cohort (Figure 21).

In both GBA-PD groups, a comparable, more marked deterioration of cognitive scores was evident compared to nonGBA-PD, regardless of DBS. After 5 years, 30% DBS-GBA-PD and 37% nonDBS-GBA-PD had dementia, compared to 12% DBS-nonGBA-PD [169].

No relevant differences were identified among carriers of different mutation types in both GBA-PD groups.

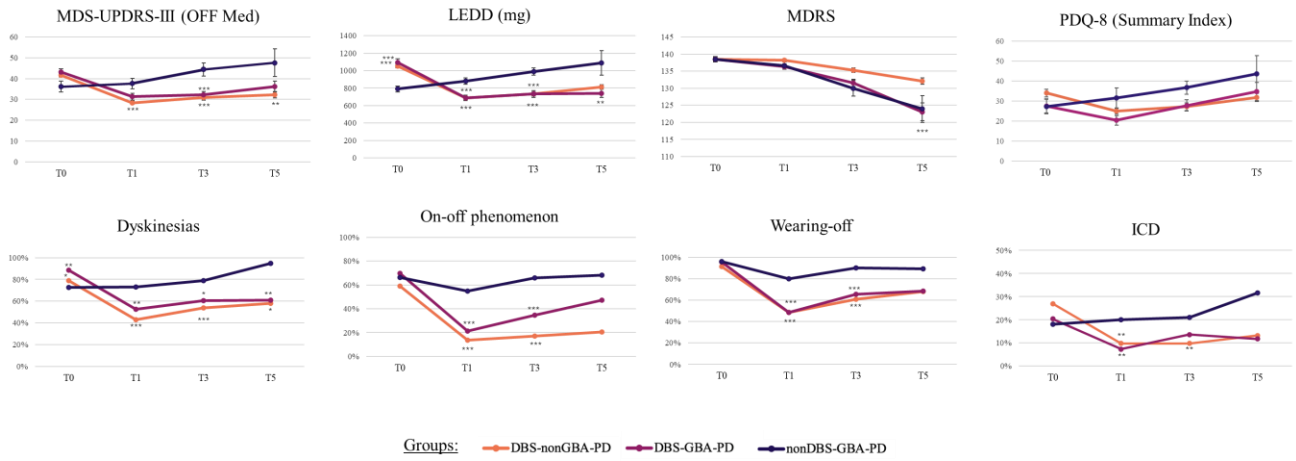

Figure 21. *Motor and non-motor characteristics of DBS-GBA-PD, DBS-GBA-PD and nonDBS-GBA-PD groups at baseline and after 1,3 and 5 year after DBS. *Significant differences [169].*

4. Glucocerebrosidase activity measurement in a PD cohort

As part of my PhD project, I also participated in a parallel study on the clinical, imaging and biochemical characterization of GBA-PD subjects. In the context of this project, I investigated the biochemical profile of different patients' groups, measuring the GCase activity using a fluorometric assay on PBMCs samples of 30 PD patients (16 males / 14 females). Half patients carried *GBA1* variants (GBA-PD), while the remaining half resulted negative (nonGBA-PD). Among GBA-PD patients, 6 carried severe variants, 3 risk, 1 mild and 5 unknown.

The specific value of GCase activity of PD patients is reported in Table 11.

Sample ID	Sex	Variant	Classification	Average GCase dosage (nmol/mg protein/h)
112PGF65	F	c.1448T>C – L444P	Severe	5,81
337BVM65	M	c.1448T>C – L444P	Severe	11,95
505ZMM64	M	c.1448T>C – L444P	Severe	9,16
971PMM72	M	c.715C>T – Q200X	Severe	7,18
940PLF89	F	c.850C>A – P245T	Severe	5,3
925VEF58	F	c.850C>A – P245T	Severe	5,95
1038GMM61	M	c.1226A>G – N370S	Mild	7,37
1027ZMF68	F	c.1223C>T – T369M	Risk	8,7
1146GDM63	M	c.1223C>T – T369M	Risk	8,79
1028ZEM66	M	c.1223C>T – T369M	Risk	9,35
690PSF88	F	c.1095G>C – E326D	Unknown	8,02
1025MAM90	M	c.626G>C – R170P	Unknown	8,56
1026MFM63	M	c.626G>C – R170P	Unknown	8,87
1005DOM64	M	c.762-18T>G	Unknown	11,82
972BAF55	F	c.956T>C – M280T	Unknown	6,9
729SRF62	F	-	-	11,26
416FMF64	F	-	-	18,06
054DBF62	F	-	-	10,74
968TAF51	F	-	-	11,9
006BEF78	F	-	-	12,78
272AMF81	F	-	-	12,41

375BAF60	F	-	-	12,31
399AFF58	F	-	-	15,08
1138DGM55	M	-	-	13,71
201BMM67	M	-	-	14,86
048LGM68	M	-	-	15,96
532CPM58	M	-	-	12
1029SPM46	M	-	-	12,78
885CCM72	M	-	-	16,5
970CPM62	M	-	-	17,63

Table 11. *Patients, sex, variant detected, variant classification and GCase activity. Each variant is reported both using HGSV nomeclature and the traditional allele name. GBA-negative PD patients present only the ID, sex and GCase activity value.*

Average values of GCase activity were calculated for each variant class (severe, mild, risk, unknown) as well as for the nonGBA-PD patients. Means ± SD were as follows: severe variants = 7,56±2,56nmol/mg protein/h; risk variants = 8,95±0,35 nmol/mg protein/h; unknown variants = 8,8±1,83 nmol/mg protein/h; nonGBA-PD = 12,27±2,86) nmol/mg protein/h. The GCase activity for the only patient carrying a mild variant was 7,37 nmol/mg protein/h (Table 12) (Fig. 22).

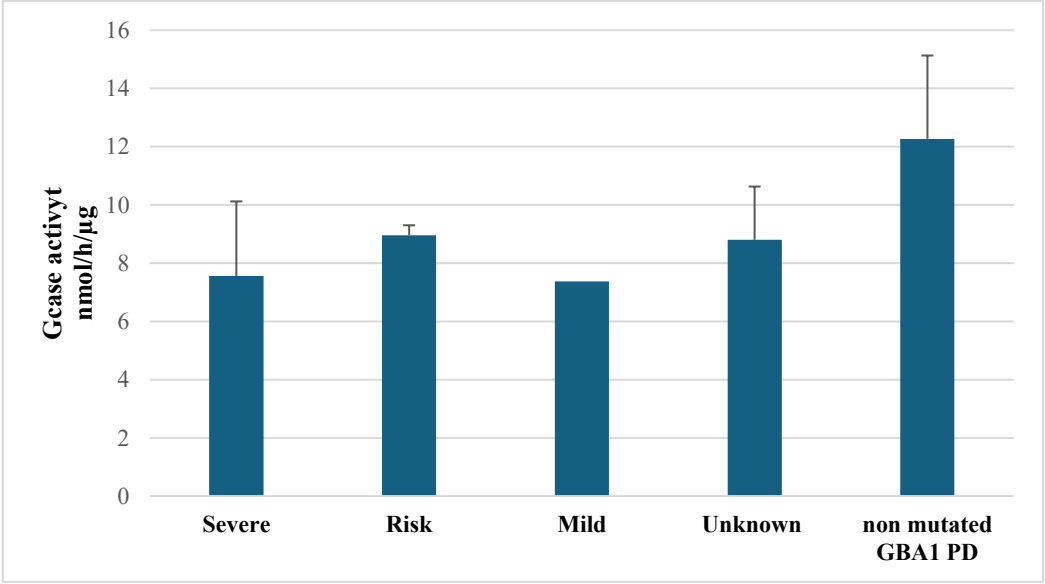

Fig. 22*. Histogram showing GCase activity levels across the four GBA1 classes (severe, risk, mild, unknown) and non-mutated GBA1-PD.*

Variant class	Average GCase activity (nmol/mg protein/h)	Std Dev	N° patients
Severe	7,56	2,56	6
Mild (single case)	7,37	-	1
Risk	8,95	0,35	3
Unknown	8,83	1,83	5
Negative	12,27	2,86	15

Table 12. *Average GCase activity levels (± standard deviation) among different GBA1 variant classes and in non-mutated GBA1-PD patients.*

The average GCase activity values changed across different variant classes. Patients carrying severe *GBA1* variants showed the lowest average activity (7,56 ± 2,56 nmol/mg protein/h), while those negative for *GBA1* variants showed the highest activity (12,27 ± 2,86 nmol/mg protein/h). The risk and unknown variant groups displayed intermediate activity levels. Among these, the risk group demonstrated the lowest variability (Std Dev = 0,35), suggesting that its average values are the most consistent and stable across patients. The severe and negative groups showed the highest standard deviations (2,56 and 2,86, respectively), suggesting greater variability in enzymatic function among these patients. The single patient classified as mild exhibited a GCase activity value of 7.37 nmol/mg protein/h, aligning more closely with the severe group.

Comparative statistical analysis showed significantly lower GCase activity in mutated compared to non-mutated subjects (Figure 23).

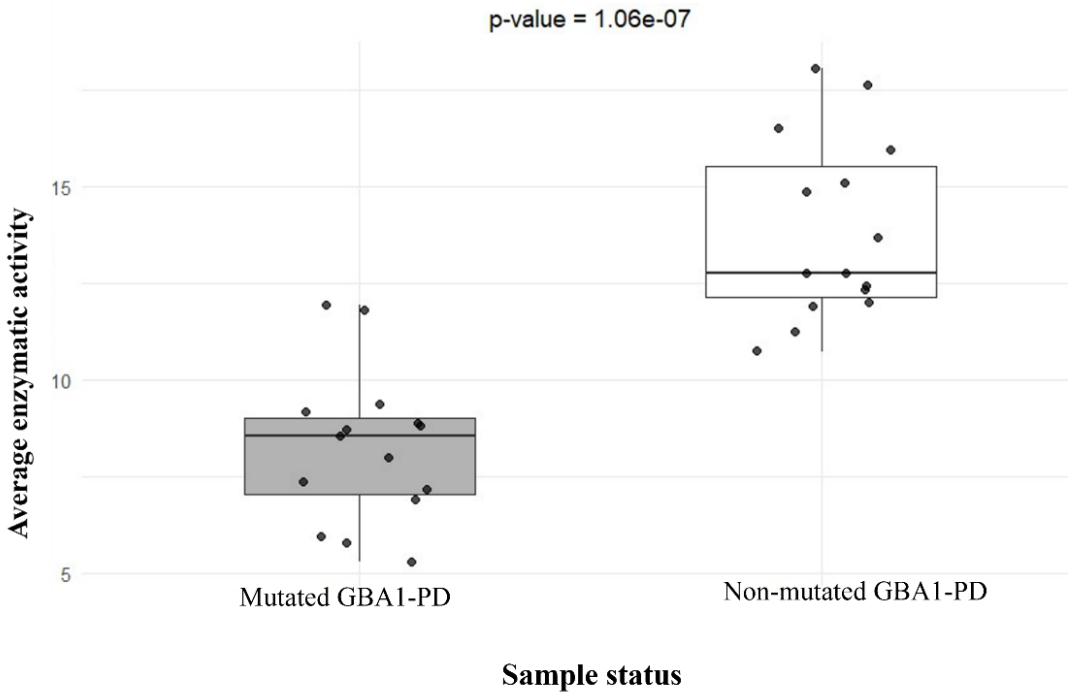

Fig.23. *Boxplots visualization of mutated and non-mutated GBA1-PD. It displays the data distributions for each group, representing the median (horizontal line inside the box), the first and third quartiles (box boundaries), and the extreme values (whiskers). The black dots represent individual observations, meaning that each dot corresponds to a patient's value.*

Discussion

Heterozygous variants in the *GBA1* gene emerged as the most relevant genetic risk factor for PD worldwide [129]. Genetic analysis with conventional methods is complicated by the presence of its pseudogene *GBAP1* that shares higher sequence homology, reaching 98% [162]. For many years, Sanger sequencing has been considered the gold standard approach to search for *GBA1* variants and the problem of sequence homology between gene and pseudogene was traditionally addressed by amplifying the *GBA1* region with three gene-specific amplicons[145]. However, this procedure is subjected to PCR-based biases, especially allele dropout (ADO) events, possibly resulting in false negatives as well as false zygosity status. Furthermore, PCR-based bias could lead to the underdetection of structural variants such as large insertions and deletions/duplications, when they fall in-between the three fragments. Lastly, this strategy is time-consuming and expensive, thus not suitable to face massive screenings. The advent of sr-NGS techniques has revolutionized genetic testing of PD patients, allowing the simultaneous analysis of many genes with reduced time and costs. Yet, the molecular analysis of the *GBA1* gene with such high-throughput technique remains challenging. Sequence homology has an impact on both library preparation step and data analysis pipeline: commercial probes for library preparation are not specific for the *GBA1* gene, resulting in unspecific probe hybridization and consequent amplification of both gene and pseudogene, eventually affecting data analysis. Alignment tools are unable to determine if generated reads derive from the gene or the pseudogene, especially in case of complex alleles derived by gene-pseudogene rearrangements, leading to decreased read depth, mapping quality and ultimately variant detection rate. The misalignment of pseudogene-derived reads against the gene causes false positive results, while the erroneous mapping of gene-derived reads against the pseudogene leads to false negative results, especially when pseudogene-derived variants are present. Recently, a specifically implemented algorithm was developed for resolving copy number variations (CNV) and complex

alleles in *GBA1* locus from short-read WGS data (i.e., Gauchian) [170]However, a recent study identified some unresolved accuracy issues of this approach as well [171]

Long-read NGS sequencing may represent the optimal solution for the long-standing problem of *GBA1* sequencing; in particular, Long-Read Sequencing, using either Oxford Nanopore or Single Molecule Real-Time (SMRT) PacBio technologies, has shown to be a promising approach to sequence complex genomic regions, although enrichment methods may be needed for the detection of *GBA1* recombinant class of variants [172]. Currently, this method is costly and limited in the diagnostic setting, narrowing its adoption for large-scale screening of PD patients [170].

For all these reasons, the main aim of this PhD project was to propose an optimized sr-NGS-based approach to expedite *GBA1* gene sequencing. This method relies on a PCR-enriched step before library preparation, followed by a tailored data analysis pipeline, by improving a strategy already proposed in the context of GD [163]. First, we optimized a unique long-range PCR encompassing the whole *GBA1* gene (6501bp). Secondly, we used the entire human genome as a reference for mapping (except for masking *GBA1LP*), greatly enhancing the compatibility of the generated files with widely used data visualization and variant interpretation tools.

By presenting several paradigmatic cases, here we have shown that LONG-NEXT can achieve a better accuracy than conventional methods. Indeed, this approach successfully identified recombinant alleles, structural variants and pseudogene-derived variants, which were missed by standard approaches such as Sanger or conventional sr-NGS. In particular, sr-NGS is more prone to mistakes in detecting RecNcil and Rec(delta55) complex alleles, because reads are preferentially aligned to the pseudogene. As for recombinant alleles, also pseudogene-derived variants, localized in highly homologous regions, may be missed. With LONG-NEXT we demonstrated to correctly identify the two most common complex alleles and gene-pseudogene derived variants, previously missed with sr-NGS. Similarly, we disclosed several negative cases, previously labelled as *GBA1*-positive, since reads belonging to the pseudogene had been erroneously aligned to *GBA1*, leading to false positive

results. We also showed the intrinsic technical limitation of Sanger sequencing due to PCR biases (i.e., ADO) by successfully solving both false negative and false zygosity status with our approach. Within the false negative group, we unravelled a gross multi-exonic deletion, completely missed by three-fragment Sanger sequencing analysis, demonstrating the capability of LONG-NEXT to detect also this type of rearrangements. Remarkably, discordant cases emerged also from the validation cohorts. We disclosed one false zygosity status in a Sanger sequenced sample, due to an ADO event, as well as a false negative result obtained with sr-NGS, that missed the pseudogene-derived variant L444P. Notably, the same L444P variant has been correctly identified by sr-NGS in additional 4 cases, demonstrating variable accuracy in detecting pseudogene-derived variants across different sr-NGS methodologies and bioinformatic pipelines. In particular, hybrid capture technologies appear generally superior to amplicon-based approaches. Moreover, lower quality filter thresholds for variant calling may increase sensitivity in detecting such variants.

LONG-NEXT method exploits all the advantages of parallel massive sequencing, being time- and cost-effective in comparison to classical Sanger sequencing but also overcoming the main limitations of standard sr-NGS.

Despite the significant advantages of LONG-NEXT in terms of reliability and speed of analysis, some limitations of this approach should be noted. The first limitation regards the possibility of ADO. While these events are less likely in comparison to Sanger sequencing approach (primers for the long-range PCR were carefully selected and only one amplicon is generated instead of three), they cannot be completely excluded. In fact, rare variants may fall in the genomic region where the primers anneal, and large complex recombinations may not be completely included in the region amplified by the long-range PCR [143]. To overcome this issue, we are improving the protocol by standardizing coverage across a given number of samples for each run, obtaining a medium read-depth score. Hence, a significant downward deviation from the standard value could suggest ADO and therefore a complex recombination event, which will need to be validated with a complementary method, such

as multiplex ligation-dependent probe amplification (MLPA). A second limitation is that the 5'UTR region is not included in the long-range PCR. This also occurs with the conventional 3-fragment *GBA1* Sanger analysis, while sr-NGS usually targets this segment, which theoretically may contain rare pathogenic variants. A long-range PCR including the 5'UTR was attempted (~12 kb, data not shown), however the rate of success of this PCR was insufficient to implement it in clinical practice and was therefore abandoned. Finally, to be a time and cost-efficient approach, the minimum number of samples per run should be ~100. Those numbers may be difficult to reach for a single genetic centre, and this might have implications on diagnostic turn-around time. In this view, the development of collaborative networks such as The National Virtual Institute for PD, a consortium of Scientific Institutes for Medical Research and Care (IRCCS) focused on PD, where few specialized hub centres can simultaneously process samples received by all spokes, could represent a solution to this challenge.

Considering current research evaluating the impact of *GBA1* variants on PD prognosis [157], clinical outcome and therapeutic choices [173] the availability of an optimized approach for large-scale *GBA1* sequencing becomes critical. LONG-NEXT has been successfully applied as rapid genetic screening tool in a cohort of PD patients (IRCCS Mondino cohort) participating in a large multicenter Italian project. The aim was to evaluate the impact of *GBA1* variants on cognitive deterioration and other non-motor features after DBS treatment. This study clearly demonstrated that DBS represents a valid therapeutic option for GBA1-PD, as it generates prolonged benefits on motor symptoms and quality of life while not modifying the occurrence of cognitive deterioration [169].

Moreover, in the final part of this PhD, I contributed to a parallel project aimed at defining the biochemical signature for GBA-PD, measuring glucocerebrosidase activity from PBMCs of PD patients with e without *GBA1* variants (and prospectively correlating such activity with clinical and imaging data). Previous works already demonstrated the utility of easily accessible PBMCs to assess various biochemical markers in GBA-PD patients (α-syn levels, GCase activity, LIMP-2, and Saposin

C levels) [174]. Preliminary results on a subcohort of 30 patients clearly confirmed the expected GCase enzymatic reduction in GBA-PD, compared to NM-PD patients. Notably, several studies reported a strong correlation between severe *GBA1* mutations and reduced GCase activity, contributing to a more aggressive phenotype [166]. To this aim, we also attempted to assess differences in GCase activity among carriers of different *GBA1* variant classes: in our small cohort, variants classified as severe and mild showed a more markedly decreased activity compared to risk and unknown variants [175]. Interestingly, the severe and non-mutated groups displayed the highest standard deviations, indicating greater fluctuations in enzymatic activity. These results are in line with previous studies, showing a correlation between the mutation class and GCase activity [176], while others failed to show relevant differences in mild versus severe variant carriers (Marano et al., 2024). The observed higher standard deviation in the severe and non-mutated groups has also been reported in other studies [177] and may point to greater heterogeneity within these categories. However, it must be pointed out that the experiments conducted in this part of the project were preliminary and included only a small sample. Enrolment for this project is now continuing to validate and extend these preliminary results, and we are considering to implement GCase dosage from a different biological matrix such as dried blood spots (DBS), since there are several difficulties in obtaining and processing PBMCs samples, especially when referred from external centres. DBS have already been largely adopted to measure GCase activity in GD screening [178] and recently they have been adopted also in PD [179]. The project will also be extended to the analysis of other blood biomarkers, such as accumulation of glucosylceramide (GlcCer) and glucosylsphingosine (GlcSph) which are substrates of GCase, and other biomarkers related to lipid metabolism (e.g., ceramide, sphingomyelin, and sphingosine) by mass spectrometry (MS), with the final aim to generate specific biochemical profiles for GBA1-PD.

Conclusions

Main aim of this thesis work was to develop, optimize and validate LONG-NEXT, a reliable, fast, and cost-effective alternative for large-scale sequencing of the *GBA1* gene. This work proved that LONG-NEXT is broadly applicable in clinical diagnostic laboratories, showing high accuracy in detecting *GBA1* variants, including those that may be missed with alternative techniques. LONG-NEXT may thus represent a strategic solution to the unmet need of genotyping *GBA1* in large cohorts of PD patients, which is becoming an essential prerequisite to offer optimized management and tailored therapies specifically targeting this common genetic subgroup. By collaborating to a large multicentric project comparing DBS outcome in GBA-PD vs nonGBA-PD, we showed that a large-scale screening of the *GBA1* gene is strategic to define genotype-based therapeutic strategies, such us DBS; the study showed that GBA-PD patients greatly benefit from DBS without demonstrating an accelerated cognitive decline compared to non-operated patients, and thus indicating that cognitive impairment is part of the natural trajectory of GBA-PD, regardless of DBS surgery. Further work on the biochemical profiling of GBA-PD patients will provide better correlates to clinical features and help stratify patients for better management and treatment.

Bibliography

[1] L. V Kalia and A. E. Lang, "Parkinson's disease," *The Lancet*, vol. 386, no. 9996, pp. 896–912, Aug. 2015, doi: 10.1016/S0140-6736(14)61393-3.

[2] R. B. Postuma *et al.*, "Identifying prodromal Parkinson's disease: Pre-Motor disorders in Parkinson's disease," *Movement Disorders*, vol. 27, no. 5, pp. 617–626, Apr. 2012, doi: 10.1002/mds.24996.

[3] J. M. Shulman, P. L. De Jager, and M. B. Feany, "Parkinson's Disease: Genetics and Pathogenesis," *Annual Review of Pathology: Mechanisms of Disease*, vol. 6, no. 1, pp. 193–222, Feb. 2011, doi: 10.1146/annurev-pathol-011110-130242.

[4] T. Pringsheim, N. Jette, A. Frolkis, and T. D. L. Steeves, "The prevalence of Parkinson's disease: A systematic review and meta-analysis," *Movement Disorders*, vol. 29, no. 13, pp. 1583–1590, Nov. 2014, doi: 10.1002/mds.25945.

[5] E. R. Dorsey, T. Sherer, M. S. Okun, and B. R. Bloem, "The Emerging Evidence of the Parkinson Pandemic," *J. Parkinsons Dis.*, vol. 8, no. s1, pp. S3–S8, Dec. 2018, doi: 10.3233/JPD-181474.

[6] G. Deuschl *et al.*, "The burden of neurological diseases in Europe: an analysis for the Global Burden of Disease Study 2017," *Lancet Public Health*, vol. 5, no. 10, pp. e551–e567, Oct. 2020, doi: 10.1016/S2468-2667(20)30190-0.

[7] M. Picillo, A. Nicoletti, V. Fetoni, B. Garavaglia, P. Barone, and M. T. Pellecchia, "The relevance of gender in Parkinson's disease: a review," *J. Neurol.*, vol. 264, no. 8, pp. 1583–1607, Aug. 2017, doi: 10.1007/s00415-016-8384-9.

[8] A. Nicoletti *et al.*, "Gender effect on non-motor symptoms in Parkinson's disease: are men more at risk?," *Parkinsonism Relat. Disord.*, vol. 35, pp. 69–74, Feb. 2017, doi: 10.1016/j.parkreldis.2016.12.008.

[9] V. Kaasinen, J. Joutsa, T. Noponen, J. Johansson, and M. Seppänen, “Effects of aging and gender on striatal and extrastriatal [123 I]FP-CIT binding in Parkinson’s disease,” *Neurobiol. Aging*, vol. 36, no. 4, pp. 1757–1763, Apr. 2015, doi: 10.1016/j.neurobiolaging.2015.01.016.

[10] A. J. Noyce *et al.*, “Meta-analysis of early nonmotor features and risk factors for Parkinson disease,” *Ann. Neurol.*, vol. 72, no. 6, pp. 893–901, Dec. 2012, doi: 10.1002/ana.23687.

[11] B. R. Bloem, M. S. Okun, and C. Klein, “Parkinson’s disease,” *The Lancet*, vol. 397, no. 10291, pp. 2284–2303, Jun. 2021, doi: 10.1016/S0140-6736(21)00218-X.

[12] M. H. Polymeropoulos *et al.*, “Mutation in the α-Synuclein Gene Identified in Families with Parkinson’s Disease,” *Science (1979).*, vol. 276, no. 5321, pp. 2045–2047, Jun. 1997, doi: 10.1126/science.276.5321.2045.

[13] C. Blauwendraat, M. A. Nalls, and A. B. Singleton, “The genetic architecture of Parkinson’s disease,” *Lancet Neurol.*, vol. 19, no. 2, pp. 170–178, Feb. 2020, doi: 10.1016/S1474-4422(19)30287-X.

[14] M. A. Nalls *et al.*, “Identification of novel risk loci, causal insights, and heritable risk for Parkinson’s disease: a meta-analysis of genome-wide association studies,” *Lancet Neurol.*, vol. 18, no. 12, pp. 1091–1102, Dec. 2019, doi: 10.1016/S1474-4422(19)30320-5.

[15] J. Jankovic, “Parkinson’s disease: clinical features and diagnosis,” *J. Neurol. Neurosurg. Psychiatry*, vol. 79, no. 4, pp. 368–376, Apr. 2008, doi: 10.1136/jnnp.2007.131045.

[16] M. A. Hely, J. G. L. Morris, W. G. J. Reid, and R. Trafficante, “Sydney multicenter study of Parkinson’s disease: Non- <scp>L</scp> -dopa–responsive problems dominate at 15 years,” *Movement Disorders*, vol. 20, no. 2, pp. 190–199, Feb. 2005, doi: 10.1002/mds.20324.

[17] M. M. Hoehn and M. D. Yahr, “Parkinsonism,” *Neurology*, vol. 17, no. 5, pp. 427–427, May 1967, doi: 10.1212/WNL.17.5.427.

[18] S. Sharma and S. Pandey, “Approach to a tremor patient,” *Ann. Indian Acad. Neurol.*, vol. 19, no. 4, p. 433, 2016, doi: 10.4103/0972-2327.194409.

[19] A. Berardelli, “Pathophysiology of bradykinesia in Parkinson’s disease,” *Brain*, vol. 124, no. 11, pp. 2131–2146, Nov. 2001, doi: 10.1093/brain/124.11.2131.

[20] M. Bologna, G. Paparella, A. Fasano, M. Hallett, and A. Berardelli, “Evolving concepts on bradykinesia,” *Brain*, vol. 143, no. 3, pp. 727–750, Mar. 2020, doi: 10.1093/brain/awz344.

[21] E. Broussolle, P. Krack, S. Thobois, J. Xie-Brustolin, P. Pollak, and C. G. Goetz, “Contribution of Jules Froment to the study of Parkinsonian rigidity,” *Movement Disorders*, vol. 22, no. 7, pp. 909–914, May 2007, doi: 10.1002/mds.21484.

[22] N. Baradaran *et al.*, “Parkinson’s Disease Rigidity: Relation to Brain Connectivity and Motor Performance,” *Front. Neurol.*, vol. 4, 2013, doi: 10.3389/fneur.2013.00067.

[23] K. M. Doherty *et al.*, “Postural deformities in Parkinson’s disease,” *Lancet Neurol.*, vol. 10, no. 6, pp. 538–549, Jun. 2011, doi: 10.1016/S1474-4422(11)70067-9.

[24] B. Palakurthi and S. P. Burugupally, “Postural Instability in Parkinson’s Disease: A Review,” *Brain Sci.*, vol. 9, no. 9, p. 239, Sep. 2019, doi: 10.3390/brainsci9090239.

[25] G. Micieli, P. Tosi, S. Marcheselli, and A. Cavallini, “Autonomic dysfunction in Parkinson’s disease,” *Neurological Sciences*, vol. 24, no. 0, pp. s32–s34, May 2003, doi: 10.1007/s100720300035.

[26] K. R. Chaudhuri and A. H. Schapira, “Non-motor symptoms of Parkinson’s disease: dopaminergic pathophysiology and treatment,” *Lancet Neurol.*, vol. 8, no. 5, pp. 464–474, May 2009, doi: 10.1016/S1474-4422(09)70068-7.

[27] C. H. Schenck, S. R. Bundlie, and M. W. Mahowald, “Delayed emergence of a parkinsonian disorder in 38% of 29 older men initially diagnosed with idiopathic rapid eye movement sleep behavior disorder,” *Neurology*, vol. 46, no. 2, pp. 388–393, Feb. 1996, doi: 10.1212/WNL.46.2.388.

[28] E. J. Olson, B. F. Boeve, and M. H. Silber, “Rapid eye movement sleep behaviour disorder: demographic, clinical and laboratory findings in 93 cases,” *Brain*, vol. 123, no. 2, pp. 331–339, Feb. 2000, doi: 10.1093/brain/123.2.331.

[29] B. R. Thanvi, S. K. Munshi, N. Vijaykumar, and T. C. N. Lo, “Neuropsychiatric non-motor aspects of Parkinson’s disease,” *Postgrad. Med. J.*, vol. 79, no. 936, pp. 561–565, Oct. 2003, doi: 10.1136/pmj.79.936.561.

[30] N. J. Diederich, G. Fénelon, G. Stebbins, and C. G. Goetz, “Hallucinations in Parkinson disease,” *Nat. Rev. Neurol.*, vol. 5, no. 6, pp. 331–342, Jun. 2009, doi: 10.1038/nrneurol.2009.62.

[31] G. Fenelon, “Hallucinations in Parkinson’s disease: Prevalence, phenomenology and risk factors,” *Brain*, vol. 123, no. 4, pp. 733–745, Apr. 2000, doi: 10.1093/brain/123.4.733.

[32] J. G. Goldman, C. G. Goetz, E. Berry-Kravis, S. Leurgans, and L. Zhou, “Genetic Polymorphisms in Parkinson Disease Subjects With and Without Hallucinations,” *Arch. Neurol.*, vol. 61, no. 8, Aug. 2004, doi: 10.1001/archneur.61.8.1280.

[33] R. L. Doty, “Olfactory dysfunction in Parkinson disease,” *Nat. Rev. Neurol.*, vol. 8, no. 6, pp. 329–339, Jun. 2012, doi: 10.1038/nrneurol.2012.80.

[34] H. Braak, K. Del Tredici, U. Rüb, R. A. I. de Vos, E. N. H. Jansen Steur, and E. Braak, “Staging of brain pathology related to sporadic Parkinson’s disease,” *Neurobiol. Aging*, vol. 24, no. 2, pp. 197–211, Mar. 2003, doi: 10.1016/S0197-4580(02)00065-9.

[35] Y.-C. Tai and C.-H. Lin, “An overview of pain in Parkinson’s disease,” *Clin. Park. Relat. Disord.*, vol. 2, pp. 1–8, 2020, doi: 10.1016/j.prdoa.2019.11.004.

[36] J. Burré, M. Sharma, and T. C. Südhof, “Cell Biology and Pathophysiology of α-Synuclein,” *Cold Spring Harb. Perspect. Med.*, vol. 8, no. 3, p. a024091, Mar. 2018, doi: 10.1101/cshperspect.a024091.

[37] B. Fauvet *et al.*, “α-Synuclein in Central Nervous System and from Erythrocytes, Mammalian Cells, and Escherichia coli Exists Predominantly as Disordered Monomer,” *Journal of Biological Chemistry*, vol. 287, no. 19, pp. 15345–15364, May 2012, doi: 10.1074/jbc.M111.318949.

[38] X. Dong-Chen, C. Yong, X. Yang, S. Chen-Yu, and P. Li-Hua, “Signaling pathways in Parkinson’s disease: molecular mechanisms and therapeutic interventions,” *Signal Transduct. Target. Ther.*, vol. 8, no. 1, p. 73, Feb. 2023, doi: 10.1038/s41392-023-01353-3.

[39] K. M. Danzer *et al.*, “Different Species of α-Synuclein Oligomers Induce Calcium Influx and Seeding,” *The Journal of Neuroscience*, vol. 27, no. 34, pp. 9220–9232, Aug. 2007, doi: 10.1523/JNEUROSCI.2617-07.2007.

[40] B.-K. Choi *et al.*, “Large α-synuclein oligomers inhibit neuronal SNARE-mediated vesicle docking,” *Proceedings of the National Academy of Sciences*, vol. 110, no. 10, pp. 4087–4092, Mar. 2013, doi: 10.1073/pnas.1218424110.

[41] L. A. Volpicelli-Daley *et al.*, “Exogenous α-Synuclein Fibrils Induce Lewy Body Pathology Leading to Synaptic Dysfunction and Neuron Death,” *Neuron*, vol. 72, no. 1, pp. 57–71, Oct. 2011, doi: 10.1016/j.neuron.2011.08.033.

[42] L. A. Volpicelli-Daley *et al.*, “Exogenous α-Synuclein Fibrils Induce Lewy Body Pathology Leading to Synaptic Dysfunction and Neuron Death,” *Neuron*, vol. 72, no. 1, pp. 57–71, Oct. 2011, doi: 10.1016/j.neuron.2011.08.033.

[43] G. Bieri, A. D. Gitler, and M. Brahic, “Internalization, axonal transport and release of fibrillar forms of alpha-synuclein,” *Neurobiol. Dis.*, vol. 109, pp. 219–225, Jan. 2018, doi: 10.1016/j.nbd.2017.03.007.

[44] A. Ciechanover and Y. T. Kwon, “Degradation of misfolded proteins in neurodegenerative diseases: therapeutic targets and strategies,” *Exp. Mol. Med.*, vol. 47, no. 3, pp. e147–e147, Mar. 2015, doi: 10.1038/emm.2014.117.

[45] G. Quinet, M. Gonzalez-Santamarta, C. Louche, and M. S. Rodriguez, “Mechanisms Regulating the UPS-ALS Crosstalk: The Role of Proteaphagy,” *Molecules*, vol. 25, no. 10, p. 2352, May 2020, doi: 10.3390/molecules25102352.

[46] O. Coux, K. Tanaka, and A. L. Goldberg, “STRUCTURE AND FUNCTIONS OF THE 20S AND 26S PROTEASOMES,” *Annu. Rev. Biochem.*, vol. 65, no. 1, pp. 801–847, Jun. 1996, doi: 10.1146/annurev.bi.65.070196.004101.

[47] K.-L. Lim and J. M. Tan, “Role of the ubiquitin proteasome system in Parkinson’s disease,” *BMC Biochem.*, vol. 8, no. Suppl 1, p. S13, 2007, doi: 10.1186/1471-2091-8-S1-S13.

[48] X. Hou, J. O. Watzlawik, F. C. Fiesel, and W. Springer, “Autophagy in Parkinson’s Disease,” *J. Mol. Biol.*, vol. 432, no. 8, pp. 2651–2672, Apr. 2020, doi: 10.1016/j.jmb.2020.01.037.

[49] S. R. Subramaniam and M.-F. Chesselet, “Mitochondrial dysfunction and oxidative stress in Parkinson’s disease,” *Prog. Neurobiol.*, vol. 106–107, pp. 17–32, Jul. 2013, doi: 10.1016/j.pneurobio.2013.04.004.

[50] W. M. Johnson, A. L. Wilson-Delfosse, and John. J. Mieyal, “Dysregulation of Glutathione Homeostasis in Neurodegenerative Diseases,” *Nutrients*, vol. 4, no. 10, pp. 1399–1440, Oct. 2012, doi: 10.3390/nu4101399.

[51] C. Guo, L. Sun, X. Chen, and D. Zhang, “Oxidative stress, mitochondrial damage and neurodegenerative diseases.,” *Neural Regen. Res.*, vol. 8, no. 21, pp. 2003–14, Jul. 2013, doi: 10.3969/j.issn.1673-5374.2013.21.009.

[52] M. T. Henrich, W. H. Oertel, D. J. Surmeier, and F. F. Geibl, “Mitochondrial dysfunction in Parkinson’s disease – a key disease hallmark with therapeutic potential,” *Mol. Neurodegener.*, vol. 18, no. 1, p. 83, Nov. 2023, doi: 10.1186/s13024-023-00676-7.

[53] A. Grünewald, K. A. Rygiel, P. D. Hepplewhite, C. M. Morris, M. Picard, and D. M. Turnbull, “Mitochondrial <scp>DNA</scp> Depletion in Respiratory Chain–Deficient <scp>P</scp> arkinson Disease Neurons,” *Ann. Neurol.*, vol. 79, no. 3, pp. 366–378, Mar. 2016, doi: 10.1002/ana.24571.

[54] M. Filosto and M. Mancuso, “Mitochondrial diseases: a nosological update,” *Acta Neurol. Scand.*, vol. 115, no. 4, pp. 211–221, Apr. 2007, doi: 10.1111/j.1600-0404.2006.00777.x.

[55] E. Koutsilieri and P. Riederer, “Excitotoxicity and new antiglutamatergic strategies in Parkinson’s disease and Alzheimer’s disease,” *Parkinsonism Relat. Disord.*, vol. 13, pp. S329–S331, 2007, doi: 10.1016/S1353-8020(08)70025-7.

[56] Z. Zhang *et al.*, “Roles of Glutamate Receptors in Parkinson’s Disease,” *Int. J. Mol. Sci.*, vol. 20, no. 18, p. 4391, Sep. 2019, doi: 10.3390/ijms20184391.

[57] M. Noda, “Possible Contribution of Microglial Glutamate Receptors to Inflammatory Response upon Neurodegenerative Diseases,” *J. Neurol. Disord.*, vol. 01, no. 03, 2013, doi: 10.4172/2329-6895.1000131.

[58] G. Arena, K. Sharma, G. Agyeah, R. Krüger, A. Grünewald, and J. C. Fitzgerald, “Neurodegeneration and Neuroinflammation in Parkinson’s Disease: a Self-Sustained Loop,” *Curr. Neurol. Neurosci. Rep.*, vol. 22, no. 8, pp. 427–440, Aug. 2022, doi: 10.1007/s11910-022-01207-5.

[59] J. A. Obeso *et al.*, “The basal ganglia in Parkinson’s disease: Current concepts and unexplained observations,” *Ann. Neurol.*, vol. 64, no. S2, pp. S30–S46, Jan. 2009, doi: 10.1002/ana.21481.

[60] H. Bernheimer, W. Birkmayer, O. Hornykiewicz, K. Jellinger, and F. Seitelberger, “Brain dopamine and the syndromes of Parkinson and Huntington Clinical, morphological and neurochemical correlations,” *J. Neurol. Sci.*, vol. 20, no. 4, pp. 415–455, Dec. 1973, doi: 10.1016/0022-510X(73)90175-5.

[61] J. K. Andersen, “What causes the build-up of ubiquitin-containing inclusions in Parkinson’s disease?,” *Mech. Ageing Dev.*, vol. 118, no. 1–2, pp. 15–22, 2000, doi: 10.1016/S0047-6374(00)00150-0.

[62] N. B. Cole and D. D. Murphy, “The cell biology of alpha-synuclein: a sticky problem?,” *Neuromolecular Med.*, vol. 1, no. 2, pp. 95–109, 2002, doi: 10.1385/NMM:1:2:95.

[63] C. B. Lücking and A. Brice, “Review Alpha-synuclein and Parkinson’s disease,” *CMLS, Cell. Mol. Life Sci*, vol. 57, pp. 1894–1908, 2000, doi: 10.1007/PL00000671.

[64] K. Wakabayashi, K. Tanji, S. Odagiri, Y. Miki, F. Mori, and H. Takahashi, “The Lewy Body in Parkinson’s Disease and Related Neurodegenerative Disorders,” *Mol. Neurobiol.*, vol. 47, no. 2, pp. 495–508, Apr. 2013, doi: 10.1007/s12035-012-8280-y.

[65] G. Bellini *et al.*, “α-Synuclein in Parkinson’s Disease: From Bench to Bedside,” *Med. Res. Rev.*, Dec. 2024, doi: 10.1002/med.22091.

[66] R. B. Postuma *et al.*, “MDS clinical diagnostic criteria for Parkinson’s disease,” *Movement Disorders*, vol. 30, no. 12, pp. 1591–1601, Oct. 2015, doi: 10.1002/mds.26424.

[67] A. J. Hughes, S. E. Daniel, L. Kilford, and A. J. Lees, “Accuracy of clinical diagnosis of idiopathic Parkinson’s disease: a clinico-pathological study of 100 cases.,” *J. Neurol. Neurosurg. Psychiatry*, vol. 55, no. 3, pp. 181–184, Mar. 1992, doi: 10.1136/jnnp.55.3.181.

[68] K. Y. Yamashita, S. Bhoopatiraju, B. D. Silverglate, and G. T. Grossberg, “Biomarkers in Parkinson’s disease: A state of the art review,” *Biomark. Neuropsychiatry*, vol. 9, p. 100074, Dec. 2023, doi: 10.1016/j.bionps.2023.100074.

[69] W. Oertel and J. B. Schulz, “Current and experimental treatments of Parkinson disease: A guide for neuroscientists,” *J. Neurochem.*, vol. 139, no. S1, pp. 325–337, Oct. 2016, doi: 10.1111/jnc.13750.

[70] M. Freitas, C. Hess, and S. Fox, “Motor Complications of Dopaminergic Medications in Parkinson’s Disease,” *Semin. Neurol.*, vol. 37, no. 02, pp. 147–157, May 2017, doi: 10.1055/s-0037-1602423.

[71] R. Tintner and J. Jankovic, “Dopamine agonists in Parkinson’s disease,” *Expert Opin. Investig. Drugs*, vol. 12, no. 11, pp. 1803–1820, Nov. 2003, doi: 10.1517/13543784.12.11.1803.

[72] H. D. Weiss and L. Marsh, “Impulse control disorders and compulsive behaviors associated with dopaminergic therapies in Parkinson disease,” *Neurol. Clin. Pract.*, vol. 2, no. 4, pp. 267–274, Dec. 2012, doi: 10.1212/CPJ.0b013e318278be9b.

[73] J. Jankovic, “Current approaches to the treatment of Parkinson’s disease,” *Neuropsychiatr. Dis. Treat.*, p. 743, Sep. 2008, doi: 10.2147/NDT.S2006.

[74] J. M. Miyasaki *et al.*, “Practice Parameter: Evaluation and treatment of depression, psychosis, and dementia in Parkinson disease (an evidence-based review): [RETIRED],” *Neurology*, vol. 66, no. 7, pp. 996–1002, Apr. 2006, doi: 10.1212/01.wnl.0000215428.46057.3d.

[75] L. L. Borek, R. Kohn, and J. H. Friedman, “Phenomenology of dreams in Parkinson’s disease,” *Movement Disorders*, vol. 22, no. 2, pp. 198–202, Jan. 2007, doi: 10.1002/mds.21255.

[76] J. K. Krauss *et al.*, “Technology of deep brain stimulation: current status and future directions,” *Nat. Rev. Neurol.*, vol. 17, no. 2, pp. 75–87, Feb. 2021, doi: 10.1038/s41582-020-00426-z.

[77] Y. Chu, R. T. Bartus, F. P. Manfredsson, C. W. Olanow, and J. H. Kordower, “Long-term post-mortem studies following neurturin gene therapy in patients with advanced Parkinson’s disease,” *Brain*, vol. 143, no. 3, pp. 960–975, Mar. 2020, doi: 10.1093/brain/awaa020.

[78] M. M. Migliore, R. Ortiz, S. Dye, R. B. Campbell, M. M. Amiji, and B. L. Waszczak, “Neurotrophic and neuroprotective efficacy of intranasal GDNF in a rat model of Parkinson’s disease,” *Neuroscience*, vol. 274, pp. 11–23, Aug. 2014, doi: 10.1016/j.neuroscience.2014.05.019.

[79] S. Mullin *et al.*, “Ambroxol for the Treatment of Patients With Parkinson Disease With and Without Glucocerebrosidase Gene Mutations,” *JAMA Neurol.*, vol. 77, no. 4, p. 427, Apr. 2020, doi: 10.1001/jamaneurol.2019.4611.

[80] S. Bandres-Ciga, M. Diez-Fairen, J. J. Kim, and A. B. Singleton, “Genetics of Parkinson’s disease: An introspection of its journey towards precision medicine,” *Neurobiol. Dis.*, vol. 137, p. 104782, Apr. 2020, doi: 10.1016/j.nbd.2020.104782.

[81] S. Lesage and A. Brice, “Parkinson’s disease: from monogenic forms to genetic susceptibility factors,” *Hum. Mol. Genet.*, vol. 18, no. R1, pp. R48–R59, Apr. 2009, doi: 10.1093/hmg/ddp012.

[82] C. Blauwendraat *et al.*, “Parkinson’s disease age at onset genome-wide association study: Defining heritability, genetic loci, and α-synuclein mechanisms,” *Movement Disorders*, vol. 34, no. 6, pp. 866–875, Jun. 2019, doi: 10.1002/mds.27659.

[83] J. O. Day and S. Mullin, “The Genetics of Parkinson’s Disease and Implications for Clinical Practice,” *Genes (Basel).*, vol. 12, no. 7, p. 1006, Jun. 2021, doi: 10.3390/genes12071006.

[84] C. Blauwendraat, M. A. Nalls, and A. B. Singleton, “The genetic architecture of Parkinson’s disease,” *Lancet Neurol.*, vol. 19, no. 2, pp. 170–178, Feb. 2020, doi: 10.1016/S1474-4422(19)30287-X.

[85] M. Quadri *et al.*, “LRP10 genetic variants in familial Parkinson’s disease and dementia with Lewy bodies: a genome-wide linkage and sequencing study,” *Lancet Neurol.*, vol. 17, no. 7, pp. 597–608, Jul. 2018, doi: 10.1016/S1474-4422(18)30179-0.

[86] D. A. Kia *et al.*, “Identification of Candidate Parkinson Disease Genes by Integrating Genome-Wide Association Study, Expression, and Epigenetic Data Sets,” *JAMA Neurol.*, vol. 78, no. 4, p. 464, Apr. 2021, doi: 10.1001/jamaneurol.2020.5257.

[87] H. Deng, K. Fan, and J. Jankovic, “The Role of *TMEM230* Gene in Parkinson’s Disease,” *J. Parkinsons Dis.*, vol. 8, no. 4, pp. 469–477, Aug. 2018, doi: 10.3233/JPD-181421.

[88] J. Follett *et al.*, “DNAJC13 p.Asn855Ser, implicated in familial parkinsonism, alters membrane dynamics of sorting nexin 1,” *Neurosci. Lett.*, vol. 706, pp. 114–122, Jul. 2019, doi: 10.1016/j.neulet.2019.04.043.

[89] J. Simón-Sánchez *et al.*, “Genome-wide association study reveals genetic risk underlying Parkinson’s disease,” *Nat. Genet.*, vol. 41, no. 12, pp. 1308–1312, Dec. 2009, doi: 10.1038/ng.487.

[90] M. A. Nalls *et al.*, “Large-scale meta-analysis of genome-wide association data identifies six new risk loci for Parkinson’s disease,” *Nat. Genet.*, vol. 46, no. 9, pp. 989–993, Sep. 2014, doi: 10.1038/ng.3043.

[91] M. Bisaglia, S. Mammi, and L. Bubacco, “Structural insights on physiological functions and pathological effects of ±-synuclein,” *The FASEB Journal*, vol. 23, no. 2, pp. 329–340, Feb. 2009, doi: 10.1096/fj.08-119784.

[92] M. G. Spillantini, M. L. Schmidt, V. M.-Y. Lee, J. Q. Trojanowski, R. Jakes, and M. Goedert, “α-Synuclein in Lewy bodies,” *Nature*, vol. 388, no. 6645, pp. 839–840, Aug. 1997, doi: 10.1038/42166.

[93] R. Krüger *et al.*, “AlaSOPro mutation in the gene encoding α-synuclein in Parkinson’s disease,” *Nat. Genet.*, vol. 18, no. 2, pp. 106–108, Feb. 1998, doi: 10.1038/ng0298-106.

[94] J. J. Zarranz *et al.*, “The new mutation, E46K, of α-synuclein causes parkinson and Lewy body dementia,” *Ann. Neurol.*, vol. 55, no. 2, pp. 164–173, Feb. 2004, doi: 10.1002/ana.10795.

[95] S. Lesage *et al.*, “G51D α-synuclein mutation causes a novel Parkinsonian–pyramidal syndrome,” *Ann. Neurol.*, vol. 73, no. 4, pp. 459–471, Apr. 2013, doi: 10.1002/ana.23894.

[96] P. Ibáñez *et al.*, “Causal relation between α-synuclein locus duplication as a cause of familial Parkinson’s disease,” *The Lancet*, vol. 364, no. 9440, pp. 1169–1171, Sep. 2004, doi: 10.1016/S0140-6736(04)17104-3.

[97] A. Di Fonzo *et al.*, “A frequent LRRK2 gene mutation associated with autosomal dominant Parkinson’s disease,” *The Lancet*, vol. 365, no. 9457, pp. 412–415, Jan. 2005, doi: 10.1016/S0140-6736(05)17829-5.

[98] W. C. Nichols *et al.*, “Genetic screening for a single common LRRK2 mutation in familial Parkinson’s disease,” *The Lancet*, vol. 365, no. 9457, pp. 410–412, Jan. 2005, doi: 10.1016/S0140-6736(05)17828-3.

[99] U. Kumari and E. K. Tan, “LRRK2 in Parkinson’s disease: genetic and clinical studies from patients,” *FEBS J.*, vol. 276, no. 22, pp. 6455–6463, Nov. 2009, doi: 10.1111/j.1742-4658.2009.07344.x.

[100] B. D. Lee *et al.*, “Inhibitors of leucine-rich repeat kinase-2 protect against models of Parkinson’s disease,” *Nat. Med.*, vol. 16, no. 9, pp. 998–1000, Sep. 2010, doi: 10.1038/nm.2199.

[101] A. Zimprich *et al.*, “A Mutation in VPS35, Encoding a Subunit of the Retromer Complex, Causes Late-Onset Parkinson Disease,” *The American Journal of Human Genetics*, vol. 89, no. 1, pp. 168–175, Jul. 2011, doi: 10.1016/j.ajhg.2011.06.008.

[102] K. Bono, C. Hara-Miyauchi, S. Sumi, H. Oka, Y. Iguchi, and H. J. Okano, “Endosomal dysfunction in iPSC-derived neural cells from Parkinson’s disease patients with VPS35 D620N,” *Mol. Brain*, vol. 13, no. 1, p. 137, Dec. 2020, doi: 10.1186/s13041-020-00675-5.

[103] Z. Hanss *et al.*, “Mitochondrial and Clearance Impairment in p. <scp>D620N VPS35</scp> Patient-Derived Neurons,” *Movement Disorders*, vol. 36, no. 3, pp. 704–715, Mar. 2021, doi: 10.1002/mds.28365.

[104] T. M. Dawson and V. L. Dawson, “The role of parkin in familial and sporadic Parkinson’s disease,” *Movement Disorders*, vol. 25, no. S1, Jan. 2010, doi: 10.1002/mds.22798.

[105] A. M. Pickrell *et al.*, “Endogenous Parkin Preserves Dopaminergic Substantia Nigral Neurons following Mitochondrial DNA Mutagenic Stress,” *Neuron*, vol. 87, no. 2, pp. 371–381, Jul. 2015, doi: 10.1016/j.neuron.2015.06.034.

[106] D. N. Hauser, C. T. Primiani, and M. R. Cookson, “The Effects of Variants in the Parkin, PINK1, and DJ-1 Genes along with Evidence for their Pathogenicity,” *Curr. Protein Pept. Sci.*, vol. 18, no. 7, pp. 702–714, May 2017, doi: 10.2174/1389203717666160311121954.

[107] N. Abbas *et al.*, “A Wide Variety of Mutations in the Parkin Gene Are Responsible for Autosomal Recessive Parkinsonism in Europe,” *Hum. Mol. Genet.*, vol. 8, no. 4, pp. 567–574, Apr. 1999, doi: 10.1093/hmg/8.4.567.

[108] W. Yi *et al.*, “The landscape of Parkin variants reveals pathogenic mechanisms and therapeutic targets in Parkinson’s disease,” *Hum. Mol. Genet.*, vol. 28, no. 17, pp. 2811–2825, Sep. 2019, doi: 10.1093/hmg/ddz080.

[109] S. Michiorri *et al.*, “The Parkinson-associated protein PINK1 interacts with Beclin1 and promotes autophagy,” *Cell Death Differ.*, vol. 17, no. 6, pp. 962–974, Jun. 2010, doi: 10.1038/cdd.2009.200.

[110] K. Okatsu *et al.*, “PINK1 autophosphorylation upon membrane potential dissipation is essential for Parkin recruitment to damaged mitochondria,” *Nat. Commun.*, vol. 3, no. 1, p. 1016, Aug. 2012, doi: 10.1038/ncomms2016.

[111] G. Arena and E. M. Valente, “PINK1 in the limelight: multiple functions of an eclectic protein in human health and disease,” *J. Pathol.*, vol. 241, no. 2, pp. 251–263, Jan. 2017, doi: 10.1002/path.4815.

[112] A. Voigt, L. A. Berlemann, and K. F. Winklhofer, “The mitochondrial kinase <scp>PINK</scp> 1: functions beyond mitophagy,” *J. Neurochem.*, vol. 139, no. S1, pp. 232–239, Oct. 2016, doi: 10.1111/jnc.13655.

[113] S. M. Jin and R. J. Youle, “The accumulation of misfolded proteins in the mitochondrial matrix is sensed by PINK1 to induce PARK2/Parkin-mediated mitophagy of polarized

mitochondria," *Autophagy*, vol. 9, no. 11, pp. 1750–1757, Nov. 2013, doi: 10.4161/auto.26122.

[114] F. Koyano *et al.*, "Ubiquitin is phosphorylated by PINK1 to activate parkin," *Nature*, vol. 510, no. 7503, pp. 162–166, Jun. 2014, doi: 10.1038/nature13392.

[115] M. Lazarou *et al.*, "The ubiquitin kinase PINK1 recruits autophagy receptors to induce mitophagy," *Nature*, vol. 524, no. 7565, pp. 309–314, Aug. 2015, doi: 10.1038/nature14893.

[116] E. M. Valente *et al.*, "Hereditary Early-Onset Parkinson's Disease Caused by Mutations in *PINK1*," *Science (1979).*, vol. 304, no. 5674, pp. 1158–1160, May 2004, doi: 10.1126/science.1096284.

[117] R. Marongiu *et al.*, "*PINK1* heterozygous rare variants: prevalence, significance and phenotypic spectrum," *Hum. Mutat.*, vol. 29, no. 4, pp. 565–565, Apr. 2008, doi: 10.1002/humu.20719.

[118] G. D. Mellick *et al.*, "Screening PARK genes for mutations in early-onset Parkinson's disease patients from Queensland, Australia," *Parkinsonism Relat. Disord.*, vol. 15, no. 2, pp. 105–109, Feb. 2009, doi: 10.1016/j.parkreldis.2007.11.016.

[119] A. Puschmann *et al.*, "Heterozygous PINK1 p.G411S increases risk of Parkinson's disease via a dominant-negative mechanism," *Brain*, vol. 140, no. 1, pp. 98–117, Jan. 2017, doi: 10.1093/brain/aww261.

[120] R. M. Canet-Avilés *et al.*, "The Parkinson's disease protein DJ-1 is neuroprotective due to cysteine-sulfinic acid-driven mitochondrial localization," *Proceedings of the National Academy of Sciences*, vol. 101, no. 24, pp. 9103–9108, Jun. 2004, doi: 10.1073/pnas.0402959101.

[121] E. Junn, W. H. Jang, X. Zhao, B. S. Jeong, and M. M. Mouradian, "Mitochondrial localization of DJ-1 leads to enhanced neuroprotection," *J. Neurosci. Res.*, vol. 87, no. 1, pp. 123–129, Jan. 2009, doi: 10.1002/jnr.21831.

[122] N. Lev, D. Ickowicz, E. Melamed, and D. Offen, "Oxidative insults induce DJ-1 upregulation and redistribution: Implications for neuroprotection," *Neurotoxicology*, vol. 29, no. 3, pp. 397–405, May 2008, doi: 10.1016/j.neuro.2008.01.007.

[123] C.-Y. Xu *et al.*, "DJ-1 Inhibits α-Synuclein Aggregation by Regulating Chaperone-Mediated Autophagy," *Front. Aging Neurosci.*, vol. 9, Sep. 2017, doi: 10.3389/fnagi.2017.00308.

[124] V. Bonifati *et al.*, "Mutations in the *DJ-1* Gene Associated with Autosomal Recessive Early-Onset Parkinsonism," *Science (1979).*, vol. 299, no. 5604, pp. 256–259, Jan. 2003, doi: 10.1126/science.1077209.

[125] C. Klein and A. Westenberger, "Genetics of Parkinson's disease.," *Cold Spring Harb. Perspect. Med.*, vol. 2, no. 1, p. a008888, Jan. 2012, doi: 10.1101/cshperspect.a008888.

[126] J. E. Ahlskog, "Parkin and PINK1 parkinsonism may represent nigral mitochondrial cytopathies distinct from Lewy body Parkinson's disease," *Parkinsonism Relat. Disord.*, vol. 15, no. 10, pp. 721–727, Dec. 2009, doi: 10.1016/j.parkreldis.2009.09.010.

[127] E. Sidransky *et al.*, "Multicenter analysis of glucocerebrosidase mutations in Parkinson's disease.," *N. Engl. J. Med.*, vol. 361, no. 17, pp. 1651–61, Oct. 2009, doi: 10.1056/NEJMoa0901281.

[128] M. Avenali, F. Blandini, and S. Cerri, "Glucocerebrosidase Defects as a Major Risk Factor for Parkinson's Disease," *Front. Aging Neurosci.*, vol. 12, Apr. 2020, doi: 10.3389/fnagi.2020.00097.

[129] K. S. Hruska, M. E. LaMarca, C. R. Scott, and E. Sidransky, “Gaucher disease: mutation and polymorphism spectrum in the glucocerebrosidase gene (GBA),” *Hum. Mutat.*, vol. 29, no. 5, pp. 567–583, May 2008, doi: 10.1002/humu.20676.

[130] O. Neudorfer *et al.*, “Occurrence of Parkinson’s syndrome in type 1 Gaucher disease,” *QJM*, vol. 89, no. 9, pp. 691–694, Sep. 1996, doi: 10.1093/qjmed/89.9.691.

[131] M. M. Miyamoto, B. F. Koop, J. L. Slightom, M. Goodman, and M. R. Tennant, “Molecular systematics of higher primates: genealogical relations and classification.,” *Proc. Natl. Acad. Sci. U. S. A.*, vol. 85, no. 20, pp. 7627–31, Oct. 1988, doi: 10.1073/pnas.85.20.7627.

[132] A. Migdalska-Richards and A. H. V. Schapira, “The relationship between glucocerebrosidase mutations and Parkinson disease,” *J. Neurochem.*, vol. 139, no. S1, pp. 77–90, Oct. 2016, doi: 10.1111/jnc.13385.

[133] H. Dvir *et al.*, “X-ray structure of human acid-β-glucosidase, the defective enzyme in Gaucher disease,” *EMBO Rep.*, vol. 4, no. 7, pp. 704–709, Jul. 2003, doi: 10.1038/sj.embor.embor873.

[134] D. Reczek *et al.*, “LIMP-2 is a receptor for lysosomal mannose-6-phosphate-independent targeting of beta-glucocerebrosidase.,” *Cell*, vol. 131, no. 4, pp. 770–83, Nov. 2007, doi: 10.1016/j.cell.2007.10.018.

[135] S. Tsuji, P. V Choudary, B. M. Martin, S. Winfield, J. A. Barranger, and E. I. Ginns, “Nucleotide sequence of cDNA containing the complete coding sequence for human lysosomal glucocerebrosidase.,” *Journal of Biological Chemistry*, vol. 261, no. 1, pp. 50–53, Jan. 1986, doi: 10.1016/S0021-9258(17)42428-8.

[136] Y. Huang, L. Deng, Y. Zhong, and M. Yi, “The Association between E326K of *GBA* and the Risk of Parkinson’s Disease,” *Parkinsons Dis.*, vol. 2018, pp. 1–6, 2018, doi: 10.1155/2018/1048084.

[137] V. Mallett *et al.*, "*GBA* p.T369M substitution in Parkinson disease: Polymorphism or association? A meta-analysis," *Neurol. Genet.*, vol. 2, no. 5, Oct. 2016, doi: 10.1212/NXG.0000000000000104.

[138] Y. Zhang *et al.*, "Integrated Genetic Analysis of Racial Differences of Common GBA Variants in Parkinson's Disease: A Meta-Analysis," *Front. Mol. Neurosci.*, vol. 11, Feb. 2018, doi: 10.3389/fnmol.2018.00043.

[139] C. Velez-Pardo *et al.*, "The distribution and risk effect of GBA variants in a large cohort of PD patients from Colombia and Peru," *Parkinsonism Relat. Disord.*, vol. 63, pp. 204–208, Jun. 2019, doi: 10.1016/j.parkreldis.2019.01.030.

[140] P. Álvarez Jerez *et al.*, "African ancestry neurodegeneration risk variant disrupts an intronic branchpoint in GBA1," *Nat. Struct. Mol. Biol.*, vol. 31, no. 12, pp. 1955–1963, Dec. 2024, doi: 10.1038/s41594-024-01423-2.

[141] A. Velayati, M. A. Knight, B. K. Stubblefield, E. Sidransky, and N. Tayebi, "Identification of recombinant alleles using quantitative real-time PCR implications for Gaucher disease.," *J. Mol. Diagn.*, vol. 13, no. 4, pp. 401–5, Jul. 2011, doi: 10.1016/j.jmoldx.2011.02.005.

[142] A. J. Sarria, P. Giraldo, J. I. Perez-Calvo, and M. Pocov□, "Detection of three rare (G377S, T134P and 1451delAC), and two novel mutations (G195W and Rec[1263del55;1342G>C] in Spanish Gaucher disease patients," *Hum. Mutat.*, vol. 14, no. 1, pp. 88–88, 1999, doi: 10.1002/(SICI)1098-1004(1999)14:1<88::AID-HUMU16>3.0.CO;2-E.

[143] D. L. Stone, N. Tayebi, E. Orvisky, B. Stubblefield, V. Madike, and E. Sidransky, "Glucocerebrosidase gene mutations in patients with type 2 Gaucher disease.," *Hum. Mutat.*, vol. 15, no. 2, pp. 181–8, 2000, doi: 10.1002/(SICI)1098-1004(200002)15:2<181::AID-HUMU7>3.0.CO;2-S.

[144] E. Sidransky and G. Lopez, “The link between the GBA gene and parkinsonism,” *Lancet Neurol.*, vol. 11, no. 11, pp. 986–998, Nov. 2012, doi: 10.1016/S1474-4422(12)70190-4.

[145] S. Atrian, E. López-Viñas, P. Gómez-Puertas, A. Chabás, L. Vilageliu, and D. Grinberg, “An evolutionary and structure-based docking model for glucocerebrosidase–saposin C and glucocerebrosidase–substrate interactions—Relevance for Gaucher disease,” *Proteins: Structure, Function, and Bioinformatics*, vol. 70, no. 3, pp. 882–891, Feb. 2008, doi: 10.1002/prot.21554.

[146] S. C. Parlar, F. P. Grenn, J. J. Kim, C. Baluwendraat, and Z. Gan-Or, “Classification of <scp> *GBA1* </scp> Variants in Parkinson’s Disease: The <scp> *GBA1* -PD </scp> Browser,” *Movement Disorders*, vol. 38, no. 3, pp. 489–495, Mar. 2023, doi: 10.1002/mds.29314.

[147] M. Anheim *et al.*, “Penetrance of Parkinson disease in glucocerebrosidase gene mutation carriers,” *Neurology*, vol. 78, no. 6, pp. 417–420, Feb. 2012, doi: 10.1212/WNL.0b013e318245f476.

[148] A. Skrahin *et al.*, “GBA1-Associated Parkinson’s Disease Is a Distinct Entity,” *Int. J. Mol. Sci.*, vol. 25, no. 13, p. 7102, Jun. 2024, doi: 10.3390/ijms25137102.

[149] L. Straniero *et al.*, “The SPID-GBA study,” *Neurol. Genet.*, vol. 6, no. 6, Dec. 2020, doi: 10.1212/NXG.0000000000000523.

[150] Z. Gan-Or *et al.*, “Differential effects of severe vs mild GBA mutations on Parkinson disease.,” *Neurology*, vol. 84, no. 9, pp. 880–7, Mar. 2015, doi: 10.1212/WNL.0000000000001315.

[151] C. Blauwendraat, M. A. Nalls, and A. B. Singleton, “The genetic architecture of Parkinson’s disease,” *Lancet Neurol.*, vol. 19, no. 2, pp. 170–178, Feb. 2020, doi: 10.1016/S1474-4422(19)30287-X.

[152] L. Straniero *et al.*, “Role of Lysosomal Gene Variants in Modulating <scp> *GBA* </scp> -Associated Parkinson’s Disease Risk,” *Movement Disorders*, vol. 37, no. 6, pp. 1202–1210, Jun. 2022, doi: 10.1002/mds.28987.

[153] J. R. Mazzulli *et al.*, “Gaucher Disease Glucocerebrosidase and α-Synuclein Form a Bidirectional Pathogenic Loop in Synucleinopathies,” *Cell*, vol. 146, no. 1, pp. 37–52, Jul. 2011, doi: 10.1016/j.cell.2011.06.001.

[154] L. Smith and A. H. V. Schapira, “GBA Variants and Parkinson Disease: Mechanisms and Treatments,” *Cells*, vol. 11, no. 8, p. 1261, Apr. 2022, doi: 10.3390/cells11081261.

[155] S. Petrucci *et al.*, “GBA-Related Parkinson’s Disease: Dissection of Genotype-Phenotype Correlates in a Large Italian Cohort.,” *Mov. Disord.*, vol. 35, no. 11, pp. 2106–2111, Nov. 2020, doi: 10.1002/mds.28195.

[156] V. Lythe *et al.*, “*GBA* -Associated Parkinson’s Disease: Progression in a Deep Brain Stimulation Cohort,” *J. Parkinsons Dis.*, vol. 7, no. 4, pp. 635–644, Aug. 2017, doi: 10.3233/JPD-171172.

[157] G. Mangone *et al.*, “Early cognitive decline after bilateral subthalamic deep brain stimulation in Parkinson’s disease patients with GBA mutations,” *Parkinsonism Relat. Disord.*, vol. 76, pp. 56–62, Jul. 2020, doi: 10.1016/j.parkreldis.2020.04.002.

[158] G. Pal *et al.*, “Parkinson Disease and Subthalamic Nucleus Deep Brain Stimulation: Cognitive Effects in <scp> *GBA* </scp> Mutation Carriers,” *Ann. Neurol.*, vol. 91, no. 3, pp. 424–435, Mar. 2022, doi: 10.1002/ana.26302.

[159] W. K. W. Fung, M. Cohn, A. E. Lang, and A. Fasano, “Precision Vs. Personalized <scp>DBS</scp> for <scp> *GBA* </scp> -Related Parkinson Disease,” *Ann. Neurol.*, vol. 92, no. 5, pp. 906–908, Nov. 2022, doi: 10.1002/ana.26499.

[160] N. Tayebi *et al.*, “Reciprocal and nonreciprocal recombination at the glucocerebrosidase gene region: implications for complexity in Gaucher disease.,” *Am. J. Hum. Genet.*, vol. 72, no. 3, pp. 519–34, Mar. 2003, doi: 10.1086/367850.

[161] S. Zampieri, S. Cattarossi, B. Bembi, and A. Dardis, “GBA Analysis in Next-Generation Era: Pitfalls, Challenges, and Possible Solutions.,” *J. Mol. Diagn.*, vol. 19, no. 5, pp. 733–741, Sep. 2017, doi: 10.1016/j.jmoldx.2017.05.005.

[162] G. A. Van der Auwera *et al.*, “From FastQ data to high confidence variant calls: the Genome Analysis Toolkit best practices pipeline.,” *Curr. Protoc. Bioinformatics*, vol. 43, no. 1110, pp. 11.10.1-11.10.33, 2013, doi: 10.1002/0471250953.bi1110s43.

[163] A. R. Quinlan and I. M. Hall, “BEDTools: a flexible suite of utilities for comparing genomic features.,” *Bioinformatics*, vol. 26, no. 6, pp. 841–2, Mar. 2010, doi: 10.1093/bioinformatics/btq033.

[164] E. Sidransky *et al.*, “Multicenter Analysis of Glucocerebrosidase Mutations in Parkinson’s Disease,” *New England Journal of Medicine*, vol. 361, no. 17, pp. 1651–1661, Oct. 2009, doi: 10.1056/NEJMoa0901281.

[165] N. Papagiannakis *et al.*, “Lysosomal alterations in peripheral blood mononuclear cells of Parkinson’s disease patients,” *Movement Disorders*, vol. 30, no. 13, pp. 1830–1834, Nov. 2015, doi: 10.1002/mds.26433.

[166] M. Avenali *et al.*, “Long-term motor and cognitive outcome of Deep Brain Stimulation in GBA-PD: the Italian PARKNET study,” Dec. 28, 2024. doi: 10.1101/2024.12.23.24319546.

[167] M. Toffoli *et al.*, “Comprehensive short and long read sequencing analysis for the Gaucher and Parkinson’s disease-associated GBA gene.,” *Commun. Biol.*, vol. 5, no. 1, p. 670, Jul. 2022, doi: 10.1038/s42003-022-03610-7.

[168] N. Tayebi, J. Lichtenberg, E. Hertz, and E. Sidransky, “Is Gauchian genotyping of GBA1 variants reliable?,” *medRxiv*, Oct. 2023, doi: 10.1101/2023.10.26.23297627.

[169] M. Leija-Salazar *et al.*, “Evaluation of the detection of GBA missense mutations and other variants using the Oxford Nanopore MinION.,” *Mol. Genet. Genomic Med.*, vol. 7, no. 3, p. e564, Mar. 2019, doi: 10.1002/mgg3.564.

[170] M. Avenali *et al.*, “Are patients with GBA-Parkinson disease good candidates for deep brain stimulation? A longitudinal multicentric study on a large Italian cohort.,” *J. Neurol. Neurosurg. Psychiatry*, Oct. 2023, doi: 10.1136/jnnp-2023-332387.

[171] M. Avenali *et al.*, “Profiling the Biochemical Signature of GBA-Related Parkinson’s Disease in Peripheral Blood Mononuclear Cells,” *Movement Disorders*, vol. 36, no. 5, pp. 1267–1272, May 2021, doi: 10.1002/mds.28496.

[172] E. Menozzi and A. H. V. Schapira, “Exploring the Genotype–Phenotype Correlation in GBA-Parkinson Disease: Clinical Aspects, Biomarkers, and Potential Modifiers,” *Front. Neurol.*, vol. 12, Jun. 2021, doi: 10.3389/fneur.2021.694764.

[173] Y. E. Huh, T. Usnich, C. R. Scherzer, C. Klein, and S. J. Chung, “GBA1 Variants and Parkinson’s Disease: Paving the Way for Targeted Therapy.,” *J. Mov. Disord.*, vol. 16, no. 3, pp. 261–278, Sep. 2023, doi: 10.14802/jmd.23023.

[174] Z. Gan-Or *et al.*, “Differential effects of severe vs mild *GBA* mutations on Parkinson disease,” *Neurology*, vol. 84, no. 9, pp. 880–887, Mar. 2015, doi: 10.1212/WNL.0000000000001315.

[175] X. K. Zhang *et al.*, “Multiplex Enzyme Assay Screening of Dried Blood Spots for Lysosomal Storage Disorders by Using Tandem Mass Spectrometry,” *Clin. Chem.*, vol. 54, no. 10, pp. 1725–1728, Oct. 2008, doi: 10.1373/clinchem.2008.104711.

[176] M. Marano *et al.*, “Increased glucosylsphingosine levels and Gaucher disease in GBA1-associated Parkinson’s disease,” *Parkinsonism Relat. Disord.*, vol. 124, p. 107023, Jul. 2024, doi: 10.1016/j.parkreldis.2024.107023.

List of papers published during the PhD

Cuconato G, Palmieri I, Percetti M, Pagliarani S, Tenace S, Morelli MJ, Zapparoli E, Avenali M, Carelli V, Dentelli P, Fiorentino A, Gaudio A, Ledda C, Mandich P, Marino S, Martone T, Minardi R, Origone P, Ormanbekova D, Pasini B, Scarabotto A, Sorbera C, Trevisan L; PARKNET Study Group; Di Fonzo A, Valente EM, Monfrini E. *LONG-NEXT: A new accurate and efficient NGS-based method for GBA1 analysis in Parkinson disease*. Parkinsonism Relat Disord. 2025 May;134:107780. doi: 10.1016/j.parkreldis.2025.107780. Epub 2025 Mar 14. PMID: 40157138.

Risi B, Imarisio A, **Cuconato G**, Padovani A, Valente EM, Filosto M. *Mitochondrial DNA (mtDNA) as fluid biomarker in neurodegenerative disorders: A systematic review*. Eur J Neurol. 2025 Jan;32(1):e70014. doi: 10.1111/ene.70014. PMID: 39831374; PMCID: PMC11744304.

Colucci F, Avenali M, De Micco R, Fusar Poli M, Cerri S, Stanziano M, Bacila A, **Cuconato G,** Franco V, Franciotta D, Ghezzi C, Gastaldi M, Elia AE, Romito L, Devigili G, Leta V, Garavaglia B, Golfrè Andreasi N, Cazzaniga F, Reale C, Galandra C, Germani G, Mitrotti P, Ongari G, Palmieri I, Picascia M, Pichiecchio A, Verri M, Esposito F, Cirillo M, Di Nardo F, Aloisio S, Siciliano M, Prioni S, Amami P, Piacentini S, Bruzzone MG, Grisoli M, Moda F, Eleopra R, Tessitore A, Valente EM, Cilia R. *Ambroxol as a disease-modifying treatment to reduce the risk of cognitive impairment in GBA-associated Parkinson's disease: a multicentre, randomised, double-blind, placebo-controlled, phase II trial. The AMBITIOUS study protocol*. BMJ Neurol Open. 2023 Nov 24;5(2):e000535. doi: 10.1136/bmjno-2023-000535. PMID: 38027469; PMCID: PMC10679992.

Di Fonzo A, Percetti M, Monfrini E, Palmieri I, Albanese A, Avenali M, Bartoletti-Stella A, Blandini F, Brescia G, Calandra-Buonaura G, Campopiano R, Capellari S, Colangelo I, Comi GP, **Cuconato G,** Ferese R, Galandra C, Gambardella S, Garavaglia B, Gaudio A, Giardina E, Invernizzi F, Mandich P, Mineri R, Panteghini C, Reale C, Trevisan L, Zampatti S, Cortelli P,

Valente EM; PARKNET study group. *Harmonizing Genetic Testing for Parkinson's Disease: Results of the PARKNET Multicentric Study*. Mov Disord. 2023 Dec;38(12):2241-2248. doi: 10.1002/mds.29617. Epub 2023 Sep 26. PMID: 37750340.

Avenali M, Zangaglia R, **Cuconato G**, Palmieri I, Albanese A, Artusi CA, Bozzali M, Calandra-Buonaura G, Cavallieri F, Cilia R, Cocco A, Cogiamanian F, Colucci F, Cortelli P, Di Fonzo A, Eleopra R, Giannini G, Imarisio A, Imbalzano G, Ledda C, Lopiano L, Malaguti MC, Mameli F, Minardi R, Mitrotti P, Monfrini E, Spagnolo F, Tassorelli C, Valentino F, Valzania F, Pacchetti C, Valente EM; PARKNET Study Group. *Are patients with GBA-Parkinson disease good candidates for deep brain stimulation? A longitudinal multicentric study on a large Italian cohort.* J Neurol Neurosurg Psychiatry. 2024 Mar 13;95(4):309-315. doi: 10.1136/jnnp-2023-332387. PMID: 37879897; PMCID: PMC10958298.

Caminiti SP, Avenali M, Galli A, Malito R, **Cuconato G**, Galandra C, Calabrese R, Pilotto A, Padovani A, Blandini F, Perani D, Tassorelli C, Valente EM. *Male sex accelerates cognitive decline in GBA1 Parkinson's disease*. NPJ Parkinsons Dis. 2025 Mar 4;11(1):41. doi: 10.1038/s41531-025-00883-7. PMID: 40038314; PMCID: PMC11880540.

List of congress abstract

"*A newly implemented NGS-based methods to detect GBA1 variants in patients with Parkinson's disease*." II Annual Meeting RIN 2022 (rete IRCCS delle neuroscienze e della neuroriabilitazione). **Poster presentation**

"*A TIME- AND COST-EFFECTIVE PROTOCOL FOR GBA1 SEQUENCING AND ITS APPLICATION IN A LARGE COHORT OF ITALIAN PARKINSON'S DISEASE PATIENTS WITH DEEP BRAIN STIMULATION*." European Society of Human Genetics (ESHG) 2022-2023. **Poster presentation**

"*A TIME- AND COST-EFFECTIVE PROTOCOL FOR GBA1 SEQUENCING AND ITS APPLICATION IN A LARGE COHORT OF ITALIAN PARKINSON'S DISEASE PATIENTS WITH DEEP BRAIN STIMULATION*." Società di Genetica Umana (SIGU) 2023. **Oral presentation**

"*A time and cost-effective protocol for GBA1 sequencing and its application in the Italian PARKNET cohort: a longitudinal study investigating the cognitive trajectory of GBA Brain Stimulation*." Società di Genetica Umana (SIGU) 2024. **Poster presentation**

Websites

1. PD genetics (https://pdgenetics.shinyapps.io/VariantBrowser)

2. Human Gene Mutation Database (HGMD®) (https://www.hgmd.cf.ac.uk/ac/index.php)

3. ClinVar (http://www.ncbi.nlm.nih.gov/clinvar/)

4. OMIM (https://www.omim.org/)

5. DECIPHER (https://www.deciphergenomics.org/)

6. Human Splicing Finder (https://genomnis.com/hsf)

7. Varsome (https://varsome.com/)

8. eVAI -EnGenome (https://evai.engenome.com/)

9. ANNOVAR (https://annovar.openbioinformatics.org/en/latest/)

10. BWA (https://github.com/lh3/BWA)

11. PolyPhen (https://genetics.bwh.harvard.edu/pph2/)